Year : 2021

Drug withdrawal driven cellular and synaptic adaptations in lateral habenula circuits

Clerke Joseph Alexander

Clerke Joseph Alexander, 2021, Drug withdrawal driven cellular and synaptic adaptations in lateral habenula circuits

Originally published at : Thesis, University of Lausanne

Posted at the University of Lausanne Open Archive http://serval.unil.ch
Document URN : urn:nbn:ch:serval-BIB_A924A68AA8978

UNIL | Université de Lausanne
Faculté de biologie et de médecine

Département des Neurosciences Fondamentales

Drug withdrawal driven cellular and synaptic adaptations in Lateral Habenula circuits

Thèse de doctorat en Neurosciences

présentée à la

Faculté de biologie et de médecine
de l'Université de Lausanne

par

Joseph Alexander Clerke

Master en Neuroscience, Université de Glasgow, Écosse

Jury

Prof. Dr. Ron Stoop, Président
Prof. Dr. Manuel Mameli, Directeur de thèse
Prof. Dr. Kelly Tan, Experte
Dr. François Georges, Expert

Thèse n° 319

Lausanne, October 2021

Programme doctoral interuniversitaire en Neurosciences des Universités de Lausanne et Genève

LEMANIC NEURO SCIENCE DOCTORAL SCHOOL

UNIL | Université de Lausanne

UNIVERSITÉ DE GENÈVE

UNIL | Université de Lausanne

UNIVERSITÉ DE GENÈVE

Programme doctoral interuniversitaire en Neurosciences des Universités de Lausanne et Genève

Imprimatur

Vu le rapport présenté par le jury d'examen, composé de

Président·e	Monsieur	Prof.	Ron	**Stoop**
Directeur·trice de thèse	Monsieur	Prof.	Manuel	**Mameli**
Expert·e·s	Madame	Prof.	Kelly	**Tan**
	Monsieur	Dr	François	**Georges**

le Conseil de Faculté autorise l'impression de la thèse de

Monsieur Joseph A. Clerke

Neuroscience Msci (Masters In Science), University of Glasgow, Scotland

intitulée

Drug withdrawal driven cellular and synaptic adaptations in Lateral Habenula circuits

Date de l'examen: 14 octobre 2021
Date d'émission de l'Imprimatur: Lausanne, le 19 octobre 2021

pour Le Doyen
de la Faculté de Biologie et de Médecine

Prof. Niko GELDNER
Directeur de l'Ecole Doctorale

Acknowledgements

For me to get to this stage, the help and support of many amazing people has played a massive role. This is particularly the case considering the trials we all experienced in last 18 months of the Covid pandemic – months which were made bearable and surmountable by the support around me.

First and foremost, I would like to thank **Manuel**. He is a supervisor in the truest sense of the word – he is there, supervising you every step of the way. On day one it was him showing me the ropes on an electrophysiology rig that may as well have been a spaceship for all I knew. From then on, he has always been available such that problems are dealt with swiftly. When he pushed me, it helped me to discover that my limits are beyond what I thought possible before. His passion for neuroscience is infectious. He has built and nurtured this lab to be the way it is – exciting, driven, supportive and respectful. This lab now truly feels like another family. Perhaps the most important thing of all for me is how much he has cared about, and acted on, my development. This applies to my development as a researcher – such as my technical attributes, my ability to conceive and design projects, how I present data and face feedback, how I organise my time and how I work with my colleagues. It also applies to my health, my personal development and future outlook, beyond my time in his lab. This he has done in many ways, from practical support amidst some messy accommodation situations, through to the guidance he provided throughout my hunt for my next venture in life.

Concerning the rest of the lab, **Arnaud** has over time become akin to a 2nd supervisor for me. His incredible patience and willingness to pass down his considerable knowledge and expertise has been crucial to my training as an electrophysiologist. **Salvatore** has provided calmness and wisdom at so many points when I have need it. My friendship with **Mauro** has experienced both great joy and solidarity through tough times, as was the case particularly during periods of lockdown. **Alvaro** has been central to me acknowledging my own successes, and seeing past self-doubt whilst remaining humble. Of more recent lab members, **Sarah** has been a source of many fun times both in the lab and outside, already in the short time she has spent here – the same of which can be said of **Lea** during her time in the lab. During my early days in the lab **Massimo**, aside from being hilariously sacrilegious, was always at hand to share his encyclopaedic technical knowledge. Collectively, the lab have all provided so much discussion of research to help me fill the library in my head and realise more deeply my own interests. Outside the lab, the parties we have had will remain as somewhat blurry yet treasured memories.

Outside our lab, I would like to thank the **DNF**, for having me in this great department, and **Claudia** for her direction of it, as well as for providing me with office space among her own lab in the past month whilst this thesis has been written. I would like to specifically thank a couple other members of this department. **Lila** has rapidly become one of my closest friends and her emotional support through the trials of writing the thesis and searching for a job has been amazing. On a more practical side, **Lara** helped me more times than I care to mention concerning histology, microscopy and image analysis.

Finally, I would like to thank my family. Without their support I would never have got here in the first place. Knowing they will be by my side, even if not physically, wherever I go in life, gives me both warmth and strength.

Abstract

Drug addiction is a chronic relapsing disorder which blights the lives of millions worldwide. A central component of the addictive cycle is the emergence of an aversive withdrawal state, which starts developing during abstinence from all drugs of abuse. In general, this withdrawal state is characterised by acute physical symptoms and persistent psychological symptoms, many of which are reminiscent of depression. The withdrawal state undermines attempts to abstain from drug use, as it is frequently cited as a major contributing factor for relapse to drug intake. The majority of neuroscience research to date has focussed its resources on elucidating the neurobiology underlying the motivational drive to continually seek the euphoric high experienced during drug intake. Comparatively less is known regarding the neural substrates of withdrawal, and of the drive to terminate such an aversive experience. It is clear that to establish a fuller picture of the neural adaptations occurring during addiction in order to support development of more effective therapy, we must uncover the substrates of drug withdrawal.

One key brain node implicated in mediating the aversive state emerging in withdrawal is the epithalamic lateral habenula (LHb). LHb neurons encode aversive external stimuli through their increase in neuronal activity. Additionally, adaptations in the LHb underlie the development of depressive-like symptoms following exposure to stress and during drug withdrawal. Through its output projections, the LHb exerts control over the activity of neurons located in the ventral tegmental area (VTA) and dorsal raphe nucleus (DRN) respectively. Both these nuclei fundamentally regulate motivated behaviours and their maladaptation underlie aspects of drug addiction. Whilst several studies have demonstrated the link between LHb adaptations and the aversive state emerging during drug withdrawal, less is known concerning the downstream repercussions of such adaptations. In particular, whether drug withdrawal could influence segregated populations of LHb neurons that provide direct innervation to the VTA and DRN is currently unclear. Like the LHb, both the VTA and DRN exhibit functional diversity that is in part, due to segregated output-specific projections. This thesis aims to unravel this complex circuitry to provide a clearer, and further developed picture, of how drug withdrawal-driven adaptations in LHb circuits may contribute to the aversive state.

To this end I present in this thesis manuscript two studies examining how withdrawal from different drugs drives independent forms of synaptic plasticity in output-specific LHb circuits using a combination of electrophysiological, anatomical and behavioural techniques. We find that morphine withdrawal drives a postsynaptic depression of excitatory transmission in DRN-projecting neurons – a circuit we show to regulate social behaviour. This plasticity is mediated by an elevation of inflammatory cytokines and collectively these adaptations underlie social deficits emerging in morphine withdrawal. Concerning the LHb projection to the VTA, we first provide a precise anatomical characterisation of this projection and its targets in the VTA. We observe that cocaine withdrawal drives opposing plasticity of glutamate release probability from LHb axons on to VTA neurons projecting to the medial Prefrontal Cortex (mPFC) and Nucleus Accumbens (NAc), adaptations that are not visible when globally examining total LHb innervation of the VTA. These VTA circuits are considered to represent functionally distinct populations that principally regulate processing of aversion and reward respectively.

In light of these results I propose a framework of how adaptations in the LHb may contribute to the aversive state emerging during drug withdrawal. The observation that drug withdrawal drives precise forms of LHb circuit plasticity represents an overall nuanced adaptation of this important brain nucleus' regulation of downstream targets. These plastic processes may represent a substrate for the control the LHb has over many aspects of motivated behaviour that can be hijacked during addiction. Altogether these studies expand our knowledge of the neural-circuit basis of drug withdrawal.

Résumé

L'addiction aux drogues d'abus est un trouble chronique récurrent qui affecte la vie de millions de personnes dans le monde. Un élément central du cycle de la dépendance aux drogues est l'apparition d'un état de manque aversif. En général, cet état de manque se caractérise par des symptômes physiques aigus et psychologiques persistants, dont beaucoup rappellent la dépression. L'état de manque participent aux échecs de tentative de sevrage, car c'est un facteur majeur de rechute dans la consommation de drogues. La majorité des recherches en neurosciences se sont focalisées sur l'élucidation de la neurobiologie qui sous-tend la motivation à rechercher l'euphorie lors de la prise de drogue, mais on en sait relativement peu sur les substrats neuronaux du sevrage. Pour obtenir une image plus complète des adaptations neuronales qui se produisent au cours de la dépendance, nous devons découvrir les substrats du sevrage afin de soutenir le développement d'une thérapie plus efficace.

L'un des structures neuronales impliqués dans la médiation d'un état aversive induit par les drogues est la latérale habenula (LHb). Les neurones de la LHb encodent les stimuli aversifs en augmentant leurs activités neuronales. Après une exposition au stress ou pendant le sevrage d'une drogue, les adaptations de la LHb sont à l'origine des symptômes de type dépressif. De par ces projections, la LHb exerce un contrôle de l'activité des neurones de l'aire tegmentale ventrale (VTA) et du raphé dorsal (DRN). Ces deux noyaux régulent les comportements motivés tandis que leurs dysfonctionnements sous-tendent certains aspects de la toxicomanie. Alors que plusieurs études ont démontré le lien entre les adaptations de la VTA, du DRN et l'état aversif du sevrage, on en sait moins sur les répercussions en aval de ces adaptations. En particulier, on ne sait pas encore si le sevrage de la drogue peut influencer des populations distinctes de neurones de la LHb qui projettent sur la VTA et le DRN. Comme la LHb, la VTA et le DRN présentent une diversité fonctionnelle qui est en partie due à leurs projections spécifiques sur des noyaux distincts. Cette thèse a pour but de disséquer ces circuits complexes afin de fournir une image plus claire et développée de la manière dont les adaptations des circuits de la LHb, induites par le sevrage, contribuent à l'état aversif.

Je présente dans ce manuscrit de thèse deux études examinant comment le sevrage de différentes drogues entraîne des formes de plasticité synaptique dans les circuits de spécifiques des efférences de la LHb en utilisant une combinaison de techniques électrophysiologiques, anatomiques et comportementales. Nous avons constaté que le sevrage de la morphine entraîne une dépression post-synaptique de la transmission excitatrice des neurones qui projettent sur le raphé qui en retour régule le comportement social. Cette plasticité est médiée par une élévation des cytokines inflammatoires et, collectivement, ces adaptations sous-tendent les déficits sociaux qui apparaissent lors du sevrage de la morphine. Concernant les projections de la LHb vers la VTA, nous avons décrits dans un premier temps les connexions spécifiques au sein de la VTA. Nous avons observé que le sevrage de la cocaïne entraîne un effet opposé sur la probabilité de libération du glutamate sur les neurones de la VTA qui projettent vers le cortex préfrontal médian (mPFC) et le noyau Accumbens (NAc). Ces sous-circuits de la VTA représentent des populations fonctionnellement distinctes qui régulent principalement le traitement de l'aversion et de la récompense respectivement.

En dernière partie, je propose un cadre pour expliquer comment ces adaptations de la LHb peuvent contribuer à l'état d'aversion qui émerge pendant le sevrage des drogues. L'observation selon laquelle le sevrage de la drogue entraîne des formes précises de plasticité du circuit de la LHb, représente une adaptation nuancée globale de la régulation des cibles en aval de cet important noyau cérébral. Ces processus plastiques peuvent représenter un substrat pour le contrôle que la LHb exerce sur de nombreux aspects de comportement motivé qui peuvent être détournés lors la dépendance. Dans l'ensemble, ces études élargissent nos connaissances sur les circuits neuronaux à la base du sevrage des drogues.

List of abbreviations

AMPAR	α-amino-3-hydroxy-5-methyl-isoxazole propionic acid receptor
BDNF	Brain Derived Neurotrophic Factor
BLA	Basolateral Amygdala
BNST	Bed Nucleus of the Stria Terminalis
CeA	Central Amygdala
cLH	Congenital Learned Helplessness
CLi	Caudal Linear nucleus
CNS	Central Nervous System
CP-AMPAR	Calcium-permeable AMPAR
CPP	Conditioned Place Preference
CRF	Corticotropin-Releasing Factor
CS	Conditioned Stimulus
DA	Dopamine
DAT	Dopamine Transporter
DBS	Deep Brain Stimulation
DLS	Dorsolateral Striatum
DRN	Dorsal Raphe Nucleus
DST	Dorsal Striatum
eCBs	Endocannabinoids
EPN	Entopeduncular Nucleus
EPSC	Excitatory Postsynaptic Current
GABA	γ-aminobutyric acid
HSV	Herpes Simplex Virus
i.p.	Intraperitoneal
IF	Interfascicular Nucleus
IPN	Interpenduncular Nucleus
LDTg	Laterodorsal Tegmental Nucleus
LH	Lateral Hypothalamus
LHb	Lateral Habenula
LPO	Lateral Preoptic Area
LTD	Long-term Depression
LTP	Long-term Potentiation
MDMA	(±)3,4-methylenedioxymethamphetamine
mGluRII	Type II Metabotropic Glutamate Receptor
MOR	μ-opioid receptor
mPFC	Medial Prefrontal Cortex
MPLA	Monophosphoryl lipid A
MRN	Median Raphe Nucleus
MS	Medial Septum
MSN	Medium Spiny Neuron
NAc	Nucleus Accumbens
NAcLS	NAc Lateral Shell
NAcMS	NAc Medial Shell
NE	Norepinephrine
NMDA	N-methyl-D-aspartic acid
NPY	Neuropeptide Y
OFC	Orbitofrontal Cortex
p38 MAPK	p38 mitogen-activated protein kinases
PBP	Parabrachial Pigmented Nucleus

PI3K	Phosphoinositide 3-kinase
PN	Paranigral Nucleus
PP1	Protein Phosphatase 1
PPR	Paired Pulse Ratio
PR	Progressive Ratio
RMTg	Rostromedial Tegmental Nucleus
RPE	Reward Prediction Error
SNc	Substantia Nigra Pars Compacta
TH	Tyrosine Hydroxylase
THC	Δ9-tetrahydrocannabinol
TLR4	Toll-like Receptor 4
TNFα	Tumour Necrosis Factor alpha
TrkB	Tropomyosin receptor kinase B
VGAT	Vesicular GABA Transporter
VP	Ventral Pallidum
VTA	Ventral Tegmental Area

List of contents

List of figures

List of Boxes

Chapter 1. Introduction

Drug addiction is a chronic relapsing disease that affects an estimated 35 million people worldwide (United Nations Office on Drugs and Labor, 2021). When including alcohol addiction alongside addiction to other illicit substances, addiction accounts for over 5% of global disease burden as measured using Disability-adjusted Life Years (Global Burden of Disease, 2018). Humans have consumed, and become addicted to psychoactive drugs for centuries. The ability of potent drugs to bring entire nations to its knees is visible throughout modern history. The steady escalation of opium use in China throughout the 17th century eventually culminated in two brutal wars after shaping domestic-economic relations such was its omnipresence in Chinese society (Hanes & Sanello, 2002). More recently, the burgeoning popularity of cocaine in the USA during the 1980s left in its wake a trail of corruption, assassinations and terrorism, particularly in Colombia where its production and subsequent export fuelled the empires of brutal drug cartels (Garcés et al 2005). Within the USA itself, widespread controversial prescription practices of opioid painkillers in the early 2000s are argued to have generated an opioid addiction epidemic that continues to ravage the country today (DeWeerdt, 2019). Drug addiction is a disease that steadily acquires an iron grip over the lives of those affected, particularly prevalent in its targeting of the most vulnerable groups within society (Lloyd, 1998). Despite the abundance of negative consequences arising from continued use of drugs – such as physical, social, financial and legal problems (Lüscher et al., 2020) – the grip of addiction causes many users to relapse even when they strongly desire to abstain. Effective treatment of drug addiction remains limited in spite of the pressing need to tackle this societal burden.

A particular feature common in dependence to all addictive substances, although with varying individual profiles, is the emergence of an aversive withdrawal state when use is abruptly discontinued (Koob, 2011). Withdrawal can elicit a broad range of physical and persistent psychological symptoms. For many, this aversive state proves unbearable and the possible release from this state by relapsing ultimately proves too strong a driving force (Koob, 2011). It has become clear over decades of clinical research that treating drug addiction requires careful management of both the acute and protracted periods of withdrawal to prevent relapse (Simpson et al., 1999). Many users will experience this cycle of withdrawal and relapse numerous times, underlining the power it has against efforts to abstain from drug use (McLellan et al., 2000).

Fundamental to efforts to alleviate this immense health issue, is research into the neurobiological processes that regulate it. Whilst intensive research resources have been dedicated to the neurobiological processes underlying positive reinforcement of drugs use - those associated with the high experienced immediately following drug use - comparatively less is known concerning the neural systems and circuits at play during withdrawal. Recent research has highlighted the epithalamic lateral habenula (LHb) as a key node for the development of drug withdrawal-driven aversive states (Meye et al., 2017). The LHb is widely recognised as a hub for aversion. LHb neurons transiently encode aversive stimuli and their predictors (Matsumoto & Hikosaka, 2007; 2009) whilst adaptations in LHb activity and plasticity are fundamental for the emergence of aversive states including depression (Hu et al., 2020; Nuno-Perez et al., 2018; Yang et al., 2018) and drug withdrawal (Meye et al., 2017). LHb's role in addictive processes is perhaps unsurprising given its efferent projections to and control over the activity of monoaminergic centres including the ventral tegmental area (VTA) and dorsal raphe nucleus (DRN) (Bernard & Veh, 2012; Herkenham & Nauta, 1979; Matsumoto & Hikosaka, 2007; Omolchenko et al., 2009). These two nuclei, the primary sources of dopamine (DA) and serotonin in the brain, have been shown over decades of research to be perhaps the most important regulators of mood, motivation and reward (Wise, 2004; Young & Leyton, 2002). In particular, dysregulation of VTA DA circuits is a prominent feature of all drugs of abuse (Lüscher, 2016). These pieces of complementary evidence posit the LHb as a critical regulator of withdrawal, yet how withdrawal-driven adaptations in the LHb manifest in downstream

structures, or indeed whether distinct synaptic adaptations occur at these synapses remains unknown.

As an introduction to my thesis work I will first provide an overview of the stages of addiction from recreational to compulsive use before outlining the distinct components of drug taking behaviour occurring in the lives of addicted individuals. After describing the specific withdrawal syndromes emerging from drugs of different classes I will focus on the neural systems hijacked by drug addiction: First I will convey some of the numerous competing and overlapping visions of how drug addiction shapes neural systems regulating the desire to obtain rewards before moving to discuss pathways known to play a role in the withdrawal state, as well as pathways which participate in aversive processing and present potential candidates for further study in this context. Finally, I will provide a basic overview of LHb anatomy and function before delving into why this brain nucleus is considered so important to the emergence of the withdrawal-driven aversive state and what questions remain concerning adaptations in LHb circuits during drug withdrawal, which the two papers serve to answer. The first article examines how withdrawal from morphine shapes LHb plasticity in specific circuits to impact social behaviour (Valentinova et al., 2019), whilst the second reveals how LHb projections undergo divergent plastic adaptations selectively targeting output-specific circuits of the VTA during cocaine withdrawal (Clerke et al., 2021a).

1.1 Drug addiction: from positive to negative reinforcement

Pioneering experiments by B.F. Skinner presented the concept of reinforcement learning to the world (Skinner, 1938; 1984). He posited that responses or behaviours leading to the acquisition of a reward will be strengthened by this reward and thus repeated (positive reinforcement). Equally, behaviours which serve to terminate a negative experience will also be strengthened (negative reinforcement) (Skinner, 2014). These two forces play fundamental roles in addiction. It is widely accepted that the initial stages of addiction leverage our natural tendency to continually seek what is rewarding, positive reinforcement. However, as drug use takes an increasingly strong hold over life, a desperate desire to be relieved of the negative experience of withdrawal becomes the predominant factor (Koob, 2011; Piazza & Deroche-Gamonet, 2013). Below I will describe the stages that span this progression from recreational use, to escalation and eventual loss of control over use (Piazza & Deroche-Gamonet, 2013)

1.1.1 The stages of drug addiction

The transition to full-blown drug addiction can occur across a variety of different timescales and be instigated by numerous distinct factors yet generally contains three well-defined stages. (Piazza & Deroche-Gamonet, 2013). Initial, recreational use can occur for a variety of reasons, such as experimenting with party drugs, curiosity for the unknown, and pressure from peers. In this first phase drug use is sporadic, controlled and goal-directed. The act of taking drugs is to achieve a state of euphoria otherwise unreachable. However, importantly, drug use does not yet usurp the user's ability to feel and drive towards natural rewards. In a second stage drug use is escalated. In a second stage the user is motivated to take higher doses of the drug over limited periods of time (binges). At this point a great portion of their life is dedicated to acquiring and using drugs and its relative significance and value in the life of the user is elevated respective to natural rewards. However, here the user still remains largely integrated in society. The great majority of drug users manage to restrict drug use to the first or second stage stipulated above, however for some (generally around 15-20% but variable by drug), a final transition to compulsive use occurs (Anthony et al.,1994). This final stage arrives when drug use is no longer under any control and becomes the principle behaviour of the user. Here, avoidance of withdrawal syndromes represents the greatest driving force for continued

use than seeking a high. The continued use despite myriad negative consequences ultimately results in social breakdown (Piazza & Deroche-Gamonet, 2013).

Drug taking behaviour during each of these phases follows a characteristic pattern of binge/intoxication, followed by withdrawal/negative affect and eventual preoccupation/anticipation, where the user is mentally consumed by thoughts of the next drug use which will ultimately follow (Figure 1). As addiction progresses from recreational to loss of control, the relative importance attributed to these elements of drug taking play shifts (Piazza & Deroche-Gamonet, 2013). The cyclical relationship between these stages of drug taking behaviour ultimately results in a self-sustaining collection of driving forces to promote drug use that make it incredibly difficult to escape addiction (Koob & Le Moal, 1997).

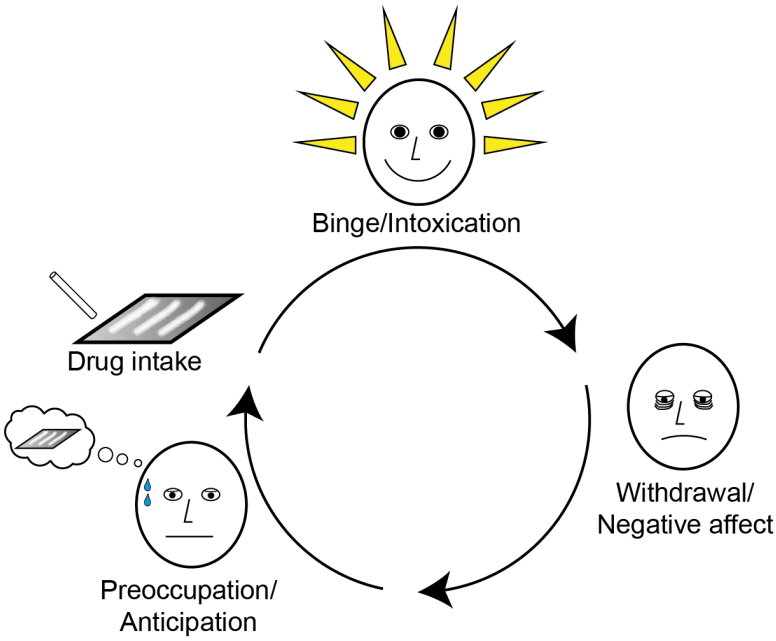

Figure 1. The cycle of drug taking behaviour. Following acute drug intake, users enter the binge/intoxication phase where they are driven to consume more to amplify and maintain the euphoria of the high. After acute effects wear off users experience a withdrawal/negative affect phase characterised by both physical and psychological symptoms that instead promote a negative reinforcement of drug use - to escape this syndrome. Even after acute withdrawal dissipates, drugs of abuse retain a stronghold over cognitive processes such that users enter a state of preoccupation/anticipation concerning the next drug use.

1.1.2 The stages of drug taking behaviour

1.1.2.1 Binge/Intoxication

While there are distinctions of individual drug effects, acute intake of all addictive substances results in euphoria. Drugs are often taken intensely in a concentrated period of time (binges) that can last from hours to days. Bingeing is particularly visible in alcohol and cocaine use, with numerous users concentrating use to more socially accepted times such as weekends. The short-lived effects of cocaine also drive repetitive consumption throughout a session (Gawin, 1991). As drug addiction progresses consumption of progressively larger amounts result in a tolerance, thus dampening the reward received and driving even greater use (Piazza & Deroche-Gamonet, 2013). The extremely rewarding high created by these agents provides the source of positive reinforcement of drug taking, the prominent driving force in the early stages of addiction formation (Koob & Le Moal, 1997).

1.1.2.2 Withdrawal/Negative affect

After the high subsides a withdrawal state emerges. This can involve a multitude of aversive symptoms elicited by the absence of the drug from the system. These can be physical in nature (eg. nausea, tremors, sleep disturbances) and/or psychological (eg. Depressive-like symptoms, irritability, anxiety) (West & Gossop, 1994). This aversive state becomes a source of negative reinforcement of drug use, as addicts know that relapse will terminate withdrawal symptoms. As drug use escalates the severity of withdrawal similarly increases and thus

becomes a stronger source of reinforcement as users progress to later stages of addiction (Koob & Le Moal, 1997).

1.1.2.3 Preoccupation/Anticipation

The combination of the high achieved by taking the drug, in excess of natural rewards, with the aversive state emerging during withdrawal, results in intense craving to consume drugs. This results in much time spent thinking about future drug use, of deciding whether to consume drugs, planning and executing the acquisition of drugs, and the ritualistic preparing of the drug. As result, even when outside the intense highs and lows of binge and withdrawal respectively – the behavioural repertoire is narrowed and the user remains locked in a state that ultimately promotes further drug use, restarting the cycle (Koob, 2010; Koob & Le Moal, 1997). This altered view of what activities in life deserve focus and attention, combined with the intense negative reinforcement of withdrawal can ultimately overpower concerns the user may have of negative effects associated with further use. As such, despite the damaging impacts on various aspects of life, many continue to take drugs.

1.1.3 Withdrawal fuels and maintains the addictive cycle

Much research focus of recent decades has been invested in the neurobiological processes underlying the positive reinforcement of drug use, created by the intense euphoria during the binge/intoxication stage, as well as sensitivity to craving-inducing cues and altered decision making associated with the anticipation/preoccupation stage. Comparatively less is known regarding the brain processes involved in withdrawal (Clerke et al., 2021b).

The aversive state elicited following withdrawal from all addictive substances has been shown as a critical component of addiction cycle. Studies examining relapse rates of abstinent users seeking treatment find that extent of withdrawal symptoms, or anticipated relief from them are a significant factor towards relapse in virtually all drugs including cocaine (Paliwal et al., 2008), opioids (Pergolizzi et al., 2020), alcohol (Becker, 2008), cannabis (Budney et al., 2008) and tobacco (Robinson et al., 2019).

Thus, the withdrawal state represents a critical link maintaining the addictive cycle by promoting relapse thus undermining attempts at recovery from addiction. Many drug users report continued use of drugs despite a desire to stop due to fear of withdrawal, particularly in opioid addiction (Pergolizzi et al., 2020). As a result, withdrawal can be seen to not only maintain addiction, but to fuel the cycle by ensuring addicts prolong use to avoid withdrawal symptoms.

1.2 Withdrawal syndromes from various drug classes

Whilst withdrawal from all addictive substances results in an aversive state that can contribute to relapse, withdrawal from different drug classes vary in their temporal pattern, often as a result of distinct symptom and pharmacokinetic profiles (for example cocaine has a very short half-life compared to heroin and thus onset of withdrawal is faster) (West & Gossop, 1994). Symptoms generally reflect a state of direct opposition in characteristics to the high felt following intake.

1.2.1 Psychostimulants

Initial studies examining cocaine use following its popularisation across the US in the late 1970s, stated that cocaine produced no withdrawal syndrome, likely in lieu of the fact cocaine withdrawal lacks the physical manifestations of other commonly abused drugs such as opioids and alcohol (Ginspoon & Bakalar, 1980). However, prevailing years saw the number of inpatients

presenting with cocaine dependence escalate dramatically. Closer examination of these patients resulted in the description of a now widely accepted definition of a withdrawal state from cocaine (Gawin & Kleber, 1988). A similar timeline and pathology has been described for withdrawal from other psychostimulant drugs such as methamphetamine (McGregor et al., 2005).

Withdrawal from cocaine and other psychostimulants occurs in a series of phases (Gawin & Kleber, 1988; West and Gossop, 1994). In the immediate minutes to hours following abstinence, users experience a “crash” phase which can last from hours to a few days following last use depending on the duration and severity of use. This phase is time limited and initially involves extreme drug craving, symptoms reminiscent of depression, anxiety and irritability. This is followed by exhaustion that overrides and supplants further craving in the short term. This stage reflects a recovery from excessive stimulation of the central nervous system (CNS). This phase is likened to the hangover of alcohol whilst the withdrawal syndrome that follows after is more persistent (Gawin & Kleber, 1988).

The withdrawal syndrome from psychostimulants re-emerges gradually several days after cessation of heavy, uncontrolled binge use as a series of psychological symptoms. Principle among these are anhedonia, amotivation and boredom (Gawin & Kleber, 1988; West and Gossop, 1994). Although perhaps more subtle than the intense physical withdrawal from CNS depressants such as opioids and alcohol, psychostimulant withdrawal depressive symptoms can remain for weeks and in some cases months. Many psychostimulant users during this period relapse, often citing relief of withdrawal symptoms coupled with exposure to cues as the reason (Brecht et al., 2000; Paliwal et al., 2008). The withdrawal state is also known as a period where users are highly susceptible to develop clinical depression as a secondary disorder in which case the depressive symptoms intensify rather than abate over time (Gawin & Kleber, 1988).

The withdrawal from psychostimulants evolves as time since last use increases. During later periods anhedonia and other depressive symptoms diminish yet intermittent cravings emerge in response to cued memories of psychostimulant euphoria. Thus, users are still susceptible to relapse even after long periods of abstinence (Gawin & Kleber, 1988).

Altogether withdrawal from regular use of psychostimulants results in an initial intense “hangover” followed by a lengthy psychological syndrome which principally evokes symptoms reminiscent of depression. Whilst only an estimated 17% of cocaine users go on to become dependent (Anthony et al., 1994), for those that do transition to addiction this withdrawal pathology acts as a key driver for relapse (Paliwal et al., 2008).

1.2.2 Opioids

Opioid withdrawal is well known to be a horrendous ordeal for addicts. The onset of withdrawal symptoms appears within 8-24 hours of last use (yet up to 36 hours for long acting prescription opioids) (West & Gossop, 1994). Unlike psychostimulant withdrawal, a large proportion of opioid withdrawal symptoms are intense physical maladies. Withdrawal symptoms tend to peak after around 2 days of abstinence – intense flu-like symptoms including fever, vomiting and diarrhoea emerge, alongside insomnia, rapid breathing and heart rate as well as intense drug-craving (West & Gossop, 1994). During this period users are particularly vulnerable to relapse as a means to relieve the withdrawal state. Drug cravings gradually abate in both intensity and frequency and by 1-2 weeks of abstinence are much less pronounced unless brought on by cues (Pergolizzi et al., 2020).

Concurrent with these physical symptoms are several psychological disturbances. These tend to outlast the physical symptoms and include anxiety, depressive symptoms and social deficits such as decreased sociality and increased aggression/irritability (Bakken et al., 2007;

Powell & Taylor, 1991). Other persistent symptoms include restlessness and sleep disturbances. During a longer post-acute withdrawal syndrome these symptoms will generally come and go and gradually decrease in intensity over time (Pergolizzi et al., 2020).

Due to the intense physical nature of opiate withdrawal, the process of coming is often managed gradually using slow and long-acting substitute therapies such as methadone which prevent the emergence of severe withdrawal states and allow the user to gradually reduce the dose (Pergolizzi et al., 2020). However, the use of such agents, although widespread, also carries significant abuse potential (Whelan & Remski, 2012) as it targets the same opioid receptors as more commonly abused drugs such as heroin. We currently find ourselves amidst an ongoing opioid crisis which is widely considered to have emerged through lax prescribing of prescription opioids to treat pain conditions (DeWeerdt et al., 2019). As such, the need to understand distinct psychophysical components and mechanisms underlying this vicious withdrawal state has never been greater.

1.2.3 Alcohol

In spite of its widespread acceptance as part of everyday culture in many societies – in stark contrast to other drugs of abuse – alcoholism is the most prevalent addiction globally. Its use is attributable to 2.8 million deaths worldwide each year (Global Burden of Disease, 2018). Its withdrawal syndrome is considered short yet in many cases very intense.

Early alcohol withdrawal symptoms emerge 6-12 hours following the last drink and are initially milder in nature such as mild anxiety, tremors, headache and stomach disturbances. Each of these symptoms dramatically increase in intensity as more hours pass and are accompanied by disturbances in heart rate, increased blood pressure, hyperthermia and confusion (Foy et al., 1997; West & Gossop, 1994). In latter stages of withdrawal (after 24-48 hours) many of these symptoms will level off or begin to diminish. However, in heavy drinkers withdrawal is further prolonged and intensified in the second and third day. Here users experience Delirium Tremens – a collection of symptoms involving visual/auditory hallucinations, delusions and seizures (Foy et al., 1997; West & Gossop, 1994).

Similarly, to other drugs of abuse, mood disturbances such as anhedonia can persist for longer periods of time. Additionally, in some cases insomnia can also carry beyond the acute phase of withdrawal (Brower & Perron, 2010).

1.2.4 Other drug classes

Whilst the above drug classes represent a largest proportion of addicts seeking/requiring treatment to overcome the obstacle of the withdrawal state, all addictive drugs by their nature result in a withdrawal state of some kind during abstinence, particularly following heavy use. Some others who's use is prevalent include the most commonly abused widely illegal drug – cannabis, and sedatives such as benzodiazepines.

Cannabis withdrawal produces myriad psychological disturbances, particularly depressed mood, inability to focus, irritability as well as somatic symptoms that mirror the acute effects of the drug such as insomnia, depressed appetite and headaches (West & Gossop, 1994).

The withdrawal syndrome in benzodiazepine abstinence by comparison is severe, particularly following heavy use. Many symptoms the sedative was initially taken/prescribed for re-emerge in a stronger form such as insomnia, anxiety and panic attacks, seizures and muscle spasms. Further to this, users may experience irritability, psychotic disturbances, nausea and heart palpitations, thus both psychological and physical manifestations of benzodiazepine

withdrawal are considered intense. The withdrawal period generally lasts between 10-14 days but can be prolonged in severe cases (West & Gossop, 1994).

It is clear that withdrawal from all drugs of abuse drive an aversive state that typically involves a strong psychological component. Additionally, withdrawal from several drug classes elicits powerful physical symptoms. Given the critical role of withdrawal in maintaining addiction, it is essential we understand the neurobiological substrates of drug withdrawal, particularly the cellular, circuit and synaptic functions that are hijacked during this period. This will help us to tailor interventions to more precisely target these substrates and with it, bring about better treatment outcomes. Below I will discuss advances in our understanding of neurobiological adaptations pertaining to specific features of drug addiction including withdrawal.

Box 1: Rodent Models used to study drug addiction (Figure 2)

By modelling precise components of drug addiction pathology, animal models have proved crucial in furthering our understanding of the underlying neurobiology.

Operator-administered

Several aspects of drug-mediated behavioural and neurobiological adaptations relevant to understanding the pathology of addictive disorders can be modelled by intraperitoneal (i.p.) injections of drugs to rodents.

(i) Locomotor Sensitisation

Particularly used as an indicator of early drug mediated persistent adaptations, increased locomotion is visible after the first injections of many drugs of abuse such as cocaine and morphine. Repeated doses result in further increases in locomotion until a ceiling is reached (normally after 3-5 days). This increase in locomotion remains "sensitised" thereafter such that even after periods of abstinence, a single injection of the drug can elicit the same elevated locomotion (Valjent et al., 2010).

(ii) Drug-induced Conditioned Place Preference

By pairing repeated drug injections with a particular compartment of a Conditioned Place Preference (CPP) apparatus (rodents are enclosed in the compartment) and saline injections in the opposite, rodents will reliably develop a conditioned preference for the drug paired side when allowed to freely explore the two compartments on a later test day (drug free) (McKendrick & Graziane, 2020). This task has been used as an indirect surrogate of drug-seeking behaviours assessed in self-administration paradigms although the validity of this interpretation in controversial. Regardless, contextual-environmental cue processing, pavlovian learning and motivation are all assessed by CPP testing and each represent brain functions dysregulated by addiction (McKendrick & Graziane, 2020).

(iii) Withdrawal Aversive State

Key psychological and physical symptoms of withdrawal, as well as associated neurobiological adaptations, can be reliably elicited by providing rodents with daily i.p. injections of the drug before a period of forced abstinence. For opioid withdrawal the emergence of aversive symptoms can be precipitated by antagonism of the same receptors targeted by abused opioid drugs. Psychological manifestations of withdrawal can be measured by further behavioural testing (eg. for depressive/anxiety-like phenotypes) or via home cage observation of somatic symptoms such as wet dog shakes in morphine withdrawal (Clerke et al., 2021b; Meye et al., 2017)

Self-administration

To understand several key components of addiction it is necessary to train animals to self-administer drugs. This is usually achieved by pairing intravenous delivery of a small dose of the drug with the pressing of a lever in an operant behavioural chamber, making drug administration an outcome of an instrumental behaviour that is learned and repetitively reinforced. Whilst this paradigm can be used and modified to examine many distinct features of drug addiction the principle ones include:

Box 1 continued.

(i) Motivation

Drug delivery is generally given following a 'progressive-ratio' (PR) of a number of lever presses. The number of presses required for drug delivery can be steadily increased across sessions to determine the 'break-point' at which rodents will no longer press for drug delivery. The greater FR number of the break-point, the more effort a rodent will devote to access the drug, thus indicating increased motivation for the drug (Hodos, 1961).

(iv) Compulsion

Coupling drug delivery with a form of punishment (typically electric shocks) will prevent further drug-seeking in a subset of mice susceptible to this intervention, whereas others will continue to seek the drug regardless of the shocks that they will receive. This models a key component of addiction, continued use despite negative consequences, considered by many to be indicative of compulsive drug use (Deroche-Gamonet et al., 2004; Pascoli et al 2015, 2018).

(v) Relapse

Drug seeking behaviour can be rapidly reinstated at later time points by various means in spite of prior extinction (Mantsch et al., 2016; Stewart & De Wit, 1987). Once drug-seeking responding is established, extinction of the association between lever pressing and drug occurs gradually, following removal of the contingent drug delivery. Reinstatement of drug-seeking can be initiate by exposure to cues previously coupled with drug delivery, by stress or by delivery of a challenge dose of the drug itself. This is in part due to long-lived memories of the intense reward associated with drug use as well as protracted withdrawal symptoms. This paradigm models the process of relapse.

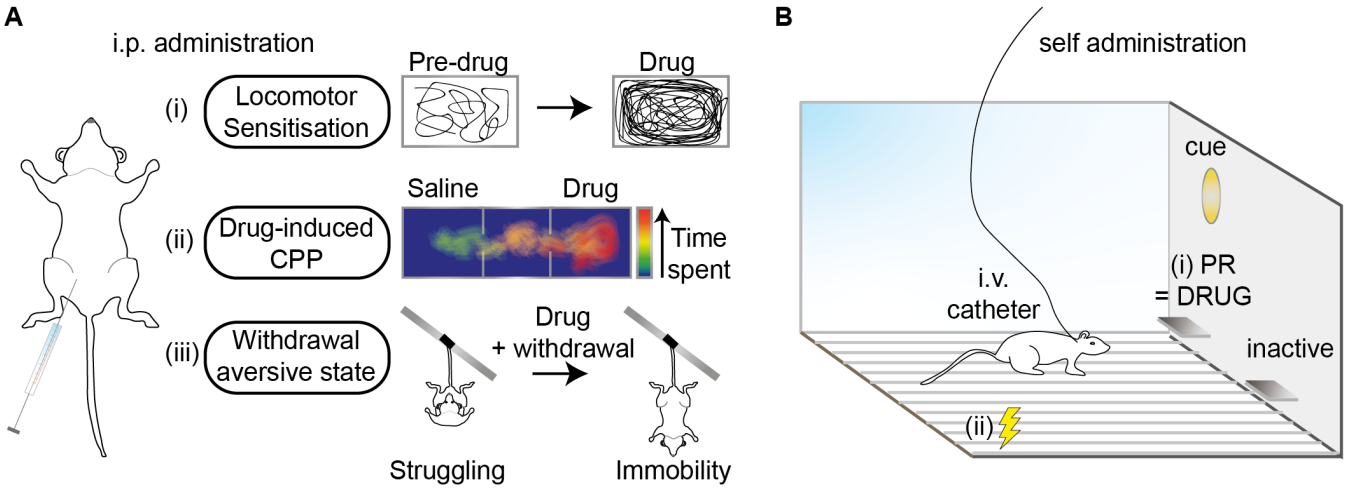

Figure 2. Rodent models used to study drug addiction. A. Self-administration paradigms in which drug delivery through an intravenous catheter is coupled to lever pressing following cue presentation can be used to infer the (i) motivation to consume the dug based on the PR break-point i.e. the maximal number of lever presses a rodent will perform to receive a single drug infusion. Additionally (ii) compulsion can be observed in mice that continue to lever press despite drug delivery being coupled with electric shocks via the chamber floor. **B.** (i) Locomotor sensitisation over repeated i.p.injections of a drug is used as an early indication of drug-adaptive behaviours. (ii) i.p. injections, when paired to a compartment of a place preference box can result in a CPP which can be seen as a proxy for drug-seeking. (iii) Following withdrawal from repeated i.p. drug injections, rodents exhibit depressive-like behaviours as can be seen using classical tests such as the tail suspension test shown here.

1.3 Brain systems hijacked by drug addiction

Many competing theories of the behavioural underpinnings of addiction and the neurobiological adaptations serving them have been posited over recent decades. These neurobiological adaptations have largely been elucidated using a variety of preclinical animal models of specific components of drug addiction (Box 1). In order to provide a framework for understanding the neurobiology of drug-withdrawal, here I will provide an overview, although not exhaustive, of some of the key adaptations contributing towards addictive behaviour.

1.3.1 Adaptations in reward pathways

In the early stages of addiction, users are driven to seek and consume drugs of abuse because of their intense rewarding properties (Koob, 2011; Piazza & Deroche-Gamonet, 2013). Circuits that regulate drive to seek natural rewards, as well as the hedonic experience that arises following consumption of that reward, are pharmacologically manipulated by drugs of abuse. Over time functional adaptations in these circuits account for key components of drug addiction, such as attributing greater value to drug rewards over natural ones (Kalivas & Volkow, 2005), sensitising locomotor responses to drugs (Lüscher, 2016), impairing top-down cognitive control of decision making and the formation of habits (Everitt & Robbins, 2016). Ultimately these adaptations collectively contribute to compulsive use of drugs where users are insensitive to the appearance of negative consequences that for natural rewards would disincentivize further consumption (Lüscher et al., 2020).

1.3.1.1 Aberrant drug-driven DA release distorts reward processing

Seminal work by Wolfram Shultz in the 1990s illustrated the role of DA neurons in reward learning (Shultz et al., 1997). It demonstrated that a majority of DA neurons encode a reward prediction error (RPE) signal, whereby their activity transferred from the receipt of a reward to the conditioned stimulus predicting it over time. Thus, over repeated trials, once reward delivery becomes expected, DA neuron activity was not altered during delivery, only by the conditioned stimulus (CS) predicting it (Shultz et al., 1997). These RPE encoding DA neurons, located in the VTA principally project to the nucleus accumbens (NAc) where DA acts on receptors on Medium Spiny Neurons (MSNs). This RPE signalling guides reward learning processes that ultimately dictate how we live our lives. DA transmission provides the motivation for actions leading to rewards, as well as those promoting avoidance of aversive situations. In this way it is considered a powerful teaching signal that guides, and reinforces much of our behaviour. The reinforcing nature of DA has been further demonstrated by experiments showing that mice are highly motivated to continually press a lever resulting in selective stimulation of DA neurons (Pascoli et al., 2015).

All drugs of abuse exert their primary euphoric effects by increasing the levels of DA release in the NAc. This is achieved through various pharmacological mechanisms depending on the drug of abuse (Nestler, 2005) (Figure 3). Psychostimulants block the activity of the dopamine transporter (DAT) which clears excess DA from the synaptic cleft. Nicotine acts by directly exciting DA neurons through its activation of nicotinic acetylcholine receptors in the VTA. Opioid drugs, Benzodiazepines and alcohol act to inhibit midbrain γ-aminobutyric acid (GABA) inhibitory neurons, meanwhile Δ9-tetrahydrocannabinol (THC) the main psychoactive component of cannabis suppresses the release of GABA (Bloomfield et al., 2016; Tan et al., 2010). Both these actions result in a release of inhibitory tone on DA neurons and thus increase their activity (Nestler, 2005). The importance of this surge in DA in driving drug-seeking is clear from studies showing that prior heroin administration occludes reinforcement of DA self-stimulation (Corre et al 2018).

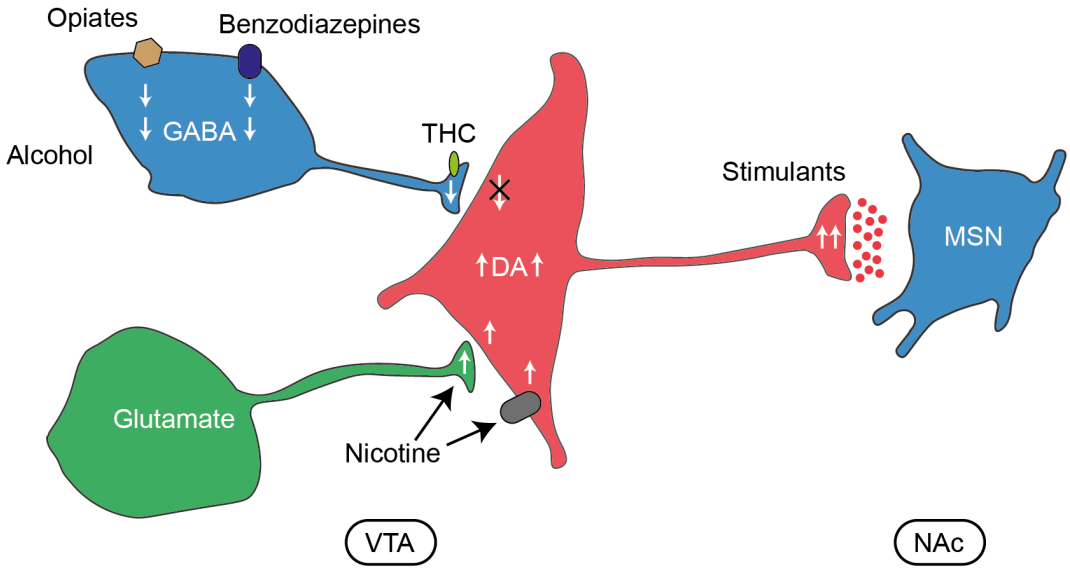

Figure 3. All drugs of abuse drive DA release in the NAc through diverse mechanisms. Opioids, Benzodiazepines both act to hyperpolarize VTA GABA neurons thus reducing their activity. Meanwhile, Alcohol has complex actions that are not fully understood but are proposed to similarly impair VTA GABA transmission on the VTA DA neurons. Similarly THC supresses GABA release on to VTA DA neurons. These effects on VTA GABA disinhibit VTA DA neurons projecting to the NAc. In contrast, Nicotine directly depolarizes VTA DA neurons and also increases glutamate release from excitatory axon terminals, both which act to amplify VTA DA transmission. Finally Psychostimulants acting on DA transporters increase the amount of DA released at synaptic terminals in the NAc which increases activation of DA receptors on NAc MSNs. Adapted from [Nestler, 2005: Is there a common molecular pathway for addiction]

Unlike natural rewards, where DA release is scaled back, and will ultimately not be altered by rewards once they become fully predictable, these addictive substances will reliably result in increased DA release every time (Di Chiara, 1999). By distorting DA transmission from its typical RPE activity, drugs of abuse result in an overvaluation of drug cues, relative to those encoding natural rewards (Keiflin & Janak, 2015). Further support for this aberrant DA teaching signal in promoting addiction is that a subset of mice will continue to self-stimulate DA neurons despite the introduction of concurrent foot-shocks, modelling compulsive use despite negative consequences, a key tenet of late-stage addiction (Pascoli et al., 2015). Whilst all drug users experience a high mediated by DA, most do not progress from the first stage of addiction outlined above (Anthony et al., 1994; Piazza & Deroche-Gamonet, 2013). Seminal experiments that further served to implicate DA transmission as central to drug-reinforcement showed that this variability depended, at least in part, on the inherent susceptibility of an individual's DA circuits to be sensitised by drugs. It was shown that individual variability in responding (High vs Low responding) for amphetamines can be predicted based on basal activity of mesolimbic DA (derived from DA turnover) (Piazza et al., 1991) as well as the extent of stress-induced increases in NAc DA levels (Rougé-Pont et al., 1993) (For an overview assessing individual vulnerability to addiction see Piazza & Deroche-Gamonet, 2013).

1.3.1.2 Ventral to dorsal striatal transition underlies habit formation

Another component contributing to the compulsive drug use in addiction is the formation of habits. Following excessive repetition, certain actions will become habitual. Instead of considering the relative value of an outcome associated with a particular action (goal-directed behaviour) we respond automatically to a learned stimulus that is associated with a given outcome, regardless of motivational drive for that outcome.

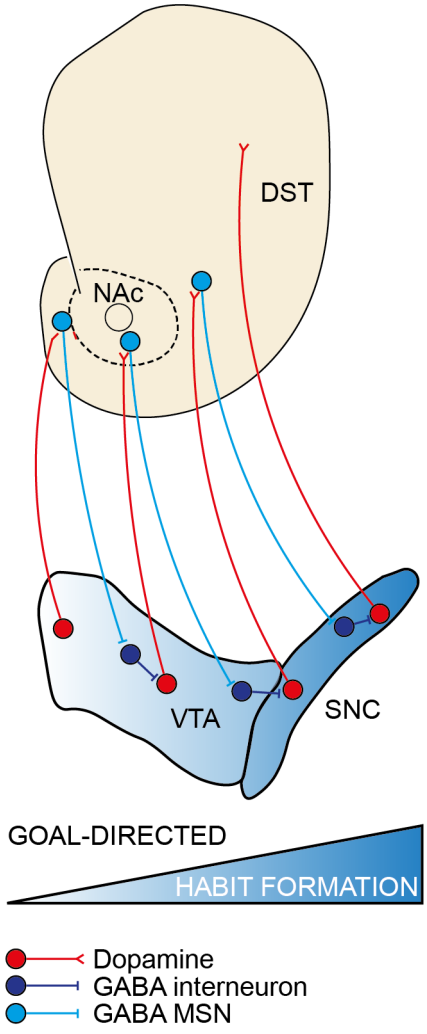

Figure 4. Mediolateral progression of mesostriatal connections underlies habit formation. Medially located VTA DA projections target MSNs in the NAc medial shell which in turn inhibit VTA GABA neurons thus releasing more lateral DA neurons. This series repeats in a spiral of mesostriatal connections ultimately ending in SNc projections to the DST. Whilst VTA-NAc DA projections are considered vital for goal-directed actions, repetition of reward seeking results in habitual behaviour which is more tightly regulated by SNc-DST. This progression of control over reward seeking behaviour is considered to be a feature of well-documented habit formation during drug addiction.

Theoretical models concerning habit formation emerged following initial experiments investigating habitual sucrose consumption (Yin et al., 2004; 2005). They posit that while goal directed actions are driven by DA release in more ventral and medial portions of the striatum (such as the NAc), emergence of habit formation occurs via DA projections to more dorsal and lateral portions of the striatum (Everitt & Robbins, 2016). The recruitment of more lateral mesostriatal circuits occurs in a sequential pattern of spiralling connections. VTA DA neurons target inhibitory D1 receptor containing MSNs (D1-MSNs) in the medial shell of the NAc (NAcMS), which in turn project back to more lateral portions of the VTA, here they inhibit local interneurons thus disinhibiting laterally located VTA DA neurons which target more lateral portions of the NAc. This sequence is repeated, and progresses laterally until substantia nigra pars compacta (SNc) DA projections target MSNs located in the dorsolateral striatum (DLS) (Figure 4) (Haber et al., 2000; Ikemoto, 2007).

Habit formation is visible in addiction. Upon encountering drug-cues, addicts in late-stage addiction will often instantly act to consume drugs in a process devoid of deliberation and often seemingly against their own best wishes. Following the model described above, whilst infusions of D1 receptor antagonists impact acquisition of cocaine seeking (Robledo et al., 1992), once responding is well established, DA receptor blockade in the DLS, but not in the NAc, disrupt cocaine seeking (Vanderschuren et al., 2005). Furthermore, DLS inactivation shifts habitual alcohol and cocaine responding - insensitive to reward devaluation - back to goal-directed (Corbit et al., 2012; Zapata et al., 2010). Finally, human neuroimaging experiments have shown that presentation of drug-cues to recreational users of alcohol resulted in increased activity in ventral striatum whilst showing the same cues to alcoholics increased activity in the dorsal striatum (DST) (Vollstädt-Klein et al., 2010).

Altogether, evidence suggests that while early reinforcement of drug responding is dependent on goal-orientated behaviour, in later stages habitual responding plays a key role in driving drug-seeking. Habits are a commonplace feature of life and typically are not necessarily pathological as they are often still sensitive to regulation by negative feedback (Lüscher et al., 2020). However, it is thought that stronger than usual habit formation is established in addiction through excessive cue-driven DA release in the DLS resulting in pervasive habits contributing to compulsive use, particularly in later stages of drug addiction.

1.3.1.3 Synaptic plasticity in the mesolimbic dopamine system

Drug-driven elevation of DA release in the NAc critically regulates the ensuing synaptic plasticity – adaptations of synaptic strength - of excitatory and inhibitory transmission within the mesolimbic system which mediate persistent adaptations arising at distinct timepoints of drug addiction (Lüscher & Janak, 2021). Most of the initial work in this regard has focussed on adaptations driven by cocaine (Figure 5) however many of the observed plastic events occur similarly between different drugs of abuse. Above I have discussed the effect of drug intake, and drug-cue presentation, on transient DA release. Here, instead, I will discuss the persistent adaptations of synaptic strength in circuits which actively control the mesolimbic system, and how it shapes key components of addiction behaviour such as drug-cue associations and reward-seeking.

Rats subjected to only one i.p. injection cocaine exhibit an increase in synaptic strength in the VTA within hours (Ungless et al., 2001). This potentiation of excitatory glutamatergic transmission in VTA DA neurons is dependent on local, dendritic released DA acting on D1 receptors. This plasticity is expressed postsynaptically, resulting from a switch in the distribution of α-amino-3-hydroxy-5-methyl-isoxazole propionic acid receptor (AMPAR) subunits. Following cocaine exposure there is an insertion of GluA2 subunit lacking AMPARs which are permeable to calcium (Bellone & Lüscher, 2006). Due to faster inactivation kinetics and larger conductance of this receptor relative to GluA2 containing AMPARs, shifts in the balance of AMPAR membrane expression towards GluA2 lacking receptors result in a potentiation of excitatory transmission (Clem & Huganir, 2010). This plasticity was also shown to be dependent on activation of N-methyl-D-aspartic acid (NMDA) glutamate receptors (Ungless et al., 2001). NMDA-dependant AMPA plasticity, a well-established phenomenon, typically requires GluA1 subunits (Shi et al., 2001). Predictably, this plasticity does not occur in mice lacking the GluA1 subunit (Dong et al., 2004, Engblom et al., 2008). Interestingly, these mice still develop locomotor sensitization to repetitive cocaine injections. However, unlike wild-type controls they do not develop locomotor responses to cocaine paired contexts (Dong et al., 2004) and do not extinguish drug-seeking once cocaine delivery is removed (Engblom et al., 2008). These findings suggest this plasticity underlies attribution of motivational salience to cocaine-associated cues and persistence of drug-seeking behaviour (Figure 5).

This rapid yet transient plasticity in the VTA becomes persistent following repeated cocaine injections, after which the excitatory synapses remain potentiated long into withdrawal (Mameli et al., 2009). Critically, blocking this persistent plasticity significantly attenuates cue-induced reinstatement of cocaine-seeking during protracted withdrawal. The stabilisation of this plasticity in turn shapes glutamatergic plasticity in NAc MSNs. Following repeated, yet not a single cocaine injection, there is a depression of overall glutamatergic synaptic strength on to NAc MSNs, which is reversed during withdrawal, resulting in a potentiation that is similarly mediated by the insertion of GluA2-lacking calcium permeable AMPARs (CP-AMPARs). Blocking the induction of persistent cocaine plasticity in the VTA prevented both the initial depression and subsequent potentiation in the NAc (Mameli et al., 2009). The insertion of CP-AMPARs in the NAc during protracted cocaine withdrawal has been shown to regulate the phenomenon termed “incubation of cocaine craving”. Modelling a key facet of cocaine addiction – relapse after prolonged abstinence - cue-induced cocaine seeking increases over the first months of withdrawal from chronic self-administration (Conrad et al., 2008; Mameli et al., 2009). Interestingly, the direction of change in excitatory synaptic strength is not only dependent on temporal factors but also is not uniform throughout distinct afferent inputs to the NAc. At time points corresponding to protracted withdrawal from cocaine, excitatory synaptic strength of medial prefrontal cortex (mPFC) input to the NAc is diminished (Pascoli et al., 2014; Thomas et al., 2001) whilst input from the ventral hippocampus is potentiated (Pascoli et al., 2014). Reversal of these contrasting forms of cocaine-driven excitatory postsynaptic adaptations in inputs to NAc

DA D1 receptor expressing MSNs (D1-MSNs) abolished cue-induced reinstatement of cocaine seeking further implicating the role of synaptic plasticity in the mesolimbic system for this process (Pascoli et al., 2014). Like the early plasticity occurring in the VTA, cocaine-driven potentiation of glutamatergic plasticity in the NAc also requires D1 receptors (Pascoli et al., 2011) (Figure 5).

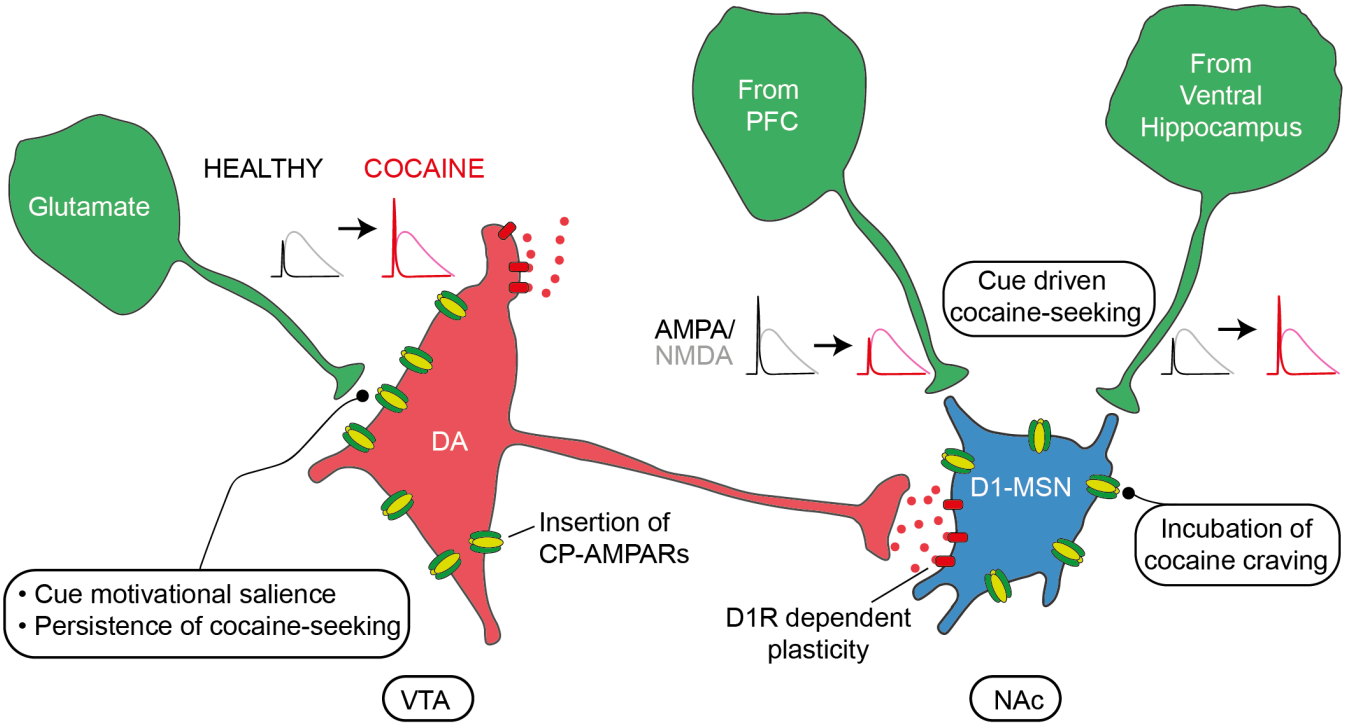

Figure 5. Cocaine-driven synaptic plasticity in the mesolimbic system. An increase in glutamatergic synaptic strength on to VTA DA neurons is visible after only one i.p. injection of cocaine in rats - as evidences by an increase in the AMPA:NMDA ratio. This potentiation is mediated by insertion of CP-AMPARs and regulates attribution of motivational salience to cocaine-associated cues, as well as perseverance of cocaine seeking. Repeated injections of cocaine render this plasticity persistent and drive changes downstream in the NAc. Similarly there is an insertion of CP-AMPARs which regulates the incubation of cocaine craving, whilst cocaine drives opposing changes in synaptic strength of inputs from the mPFC and Ventral Hippocampus which collectively regulate cocaine-seeking. Critically, these alterations in synaptic strength, both in the VTA and NAc, rely on intact DA signalling at D1 receptors.

Altogether, it can be seen that cocaine drives DA receptor dependent plastic adaptations in inputs to the mesolimbic system which critically regulate further cocaine seeking. These data support the DA hypothesis of drug addiction, whereby excessive DA release in response to drugs of abuse shapes persistent plasticity that underlies the emergence of addictive behaviour. Whilst the majority of work examining drug driven plasticity in this circuit have investigated cocaine, similar plasticity in the NAc has been described following heroin exposure (Hearing et al., 2016), whilst the insertion of calcium permeable AMPARs in VTA DA neurons is present following exposure to all drugs of abuse tested so far (Lüscher, 2016).

1.3.1.4 Cortico-striatal dysregulation

Interestingly, whilst D1 receptor dependant synaptic plasticity in the NAc critically underlies drug-adaptive behaviours, DA receptor activation in the NAc is not required for mice undergoing stress- or cocaine-induced reinstatement of cocaine seeking. Instead, blocking DA receptors in the mPFC abolishes cocaine-and stress-induced reinstatement, whilst local mPFC application of exogenous DA alone elicits reinstatement of drug seeking (McFarland et al., 2004; McFarland & Kalivas, 2001). Furthermore, silencing the mPFC during stress or drug primed reinstatement of cocaine seeking abolishes the associated increase in glutamate released in the

core subregion of the NAc (McFarland et al., 2004). Altogether, it appears that during reinstatement of drug-seeking, DA increases in the mPFC may activate NAc projecting mPFC glutamate neurons to drive seeking behaviour (Figure 6).

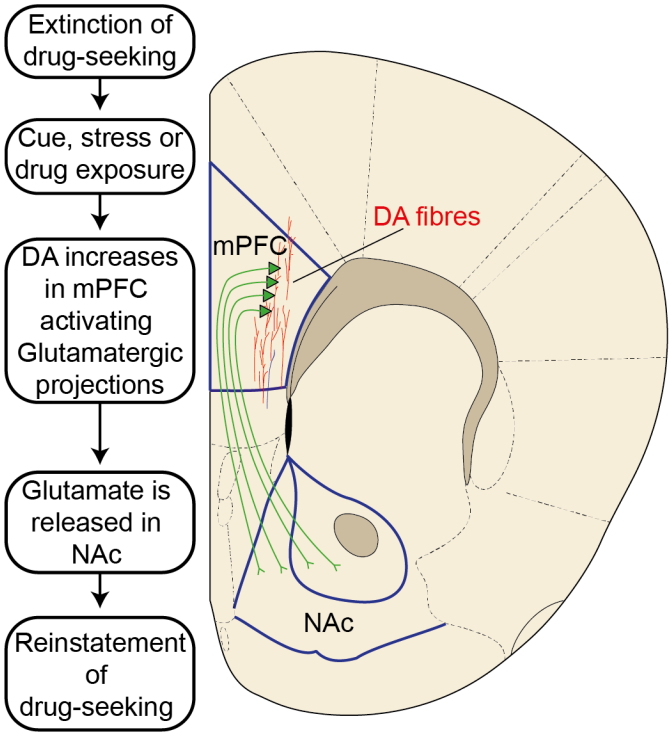

Figure 6. mPFC projections to the NAc: The final common pathway for drug seeking. Reinstatement of drug-seeking in self-administration paradigms models relapse processes that critically underpin drug addiction. A series of experiments have demonstrated that reinstatement induced by stress, a drug cue or the drug itself drive DA release in the mPFC and glutamate release in the NAc. Local application of DA or glutamate antagonists in the respective regions reliably prevents the reinstatement of drug-seeking. Thus, it can be viewed that DA driven mPFC-NAc projections represent a common pathway for all forms of reinstatement of previously extinguished drug-seeking.

This profound involvement of mPFC in reinstatement models occurs amidst a broader backdrop of numerous human neuroimaging studies in patients demonstrating mPFC dysfunction in addicts. mPFC activity was shown to increase in response to drug cues (Wexler et al., 2001), and the extent of activation of the mPFC by a dose of the psychostimulant methylphenidate correlated with self-reported cocaine craving (Volkow et al., 1999). Interestingly, at baseline, in a resting state, there is rather a decreased metabolic activity in the mPFC of drug users (Goldstein & Volkow, 2002), and the region is found to be hypoactive in addicts during decision making tasks, likely underlying cognitive deficits in this area (Kaufman et al, 2003) and in response to sexually evocative cues (Garavan et al., 2000), suggesting that this hypoactivity could contribute to the prioritisation of drug rewards over natural rewards. Hypoactivity of the mPFC in addicts has also been long-hypothesised to impair cognitive control of behaviour leading to compulsive use. In mice who compulsively consume cocaine despite receiving contingent foot-shocks mPFC neurons were shown to have diminished excitability (Chen et al., 2013). Optogenetically activating or inhibiting these cells bidirectionally modified the compulsive drug behaviour.

Overall, preclinical data using rodent models of addiction and human neuroimaging data heavily implicate dysfunction in a circuit originating in VTA DA projections to mPFC neurons, which in turn project to NAc. This pathway has been termed ‘the final common pathway’ for initiation of drug-seeking (Figure 6). Blocking any point within this circuit abolishes drug seeking behaviour. Aberrant activity in this circuit may mediate central features of drug addiction such as impaired decision making and inhibitory regulation of behaviour, as well as heightened motivation for drug seeking.

Whilst aberrant prefrontal-NAc circuits clearly play a role in drug addiction, this is not the only corticostriatal pathway underlying the transition to addiction. A central phenomenon of addiction is continued use despite negative consequences, illustrating the compulsive nature of drug addiction. Interestingly, whilst drugs of abuse exert powerful effects in the mesolimbic system of all users, only a small percentage (variable depending on drug) fully transition to compulsive use (Anthony et al., 1994). A set of ground-breaking experiments by Pascoli and colleagues (2018) demonstrated that plasticity in glutamatergic projections from the Orbitofrontal Cortex (OFC) to the DST critically regulate this process. Whilst all mice will reliably self-stimulate

DA neurons, only a subset will continue to persevere when their activation is coupled with a foot-shock. Interestingly, in mice that display this behaviour OFC activity increases immediately prior to self-stimulation and continues to rise during the reward/punishment combined delivery. On the contrary, in mice that renounce self-stimulation once punishments are introduced, this activity decreases during the same window of time (Pascoli et al., 2018). OFC neurons have been shown to encode relative values of action/outcome associations, thus suggesting that for compulsive mice, the value of DA stimulation overpowers the aversive nature of the foot-shock. Further experiments showed that synaptic strength of OFC projections to the DST mediated this transition to compulsive reward seeking (Pascoli et al., 2018). These results indicate that a gain of function in corticostriatal transmission is responsible for compulsive use, mirroring the loss of function present in research showing prefrontal hypoactivity as fundamental to compulsive use (Chen et al., 2011). This suggests that these distinct corticostriatal circuits regulate separate maladaptive behaviours in addiction, relative valuation of drug reward vs negative consequences for OFC-to-DST, and impaired decision making/behavioural inhibition for mPFC-to-NAc.

In summary, aberrant activity of, and adaptations within, pathways regulating the positive reinforcement of drugs of abuse contribute greatly to the emergence of drug addiction. The natural release of DA to guide reward learning is directly manipulated by drugs of abuse, thus distorting this vital function. Powerful habit formation due to adaptations in DA transmission in the DLS combined with impaired executive control impair the ability of users to summon the concerted effort required to abstain. Additionally, circuits impinging on the mesolimbic system undergo persistent synaptic plasticity to promote intense motivation for drugs. This aberrant motivational value is also manifested in dysregulation of corticostriatal circuits which ultimately hold direct control over the decision to seek drugs. The majority of the studies I have described, and indeed the main focus of drug addiction neuroscience research, has been on cocaine addiction. Many of the adaptations listed above likely also apply to other drugs given the common recruitment of mesolimbic DA throughout all drugs (Lüscher, 2016), however future studies will need to probe whether the same mechanisms do indeed apply. These adaptations collectively explain much of the urge to feel the intense euphoria resulting from acute drug intake. However, they fail to account for another critical driving force behind continued drug use – drug withdrawal.

1.3.2 Adaptations in pathways regulating aversive states

Whilst the establishment of addiction primarily relies on distortions of positive reinforcement, due to tolerance over time the reward elicited from drugs of abuse diminishes and users must consume more drugs to experience the same rewarding effect. The other side of this phenomenon is the emergence of an increasingly aversive withdrawal state. Whilst the neurobiological substrates involved in the binge/intoxication stage, as well as preoccupation/anticipation stage (both of which largely pertain to positive reinforcement of drug taking) have been extensively studied, comparatively less is known regarding the circuits regulating the aversive state in withdrawal. In later stages of addiction, the withdrawal state becomes the principal driving force maintaining use of drugs – thus switching from positive reinforcement to negative reinforcement (Koob, 2011). The severe withdrawal state also critically undermines attempts to come off drugs. During this process, several different circuits which are engaged in normal processing of aversion are recruited and undergo persistent adaptations.

1.3.2.1 Heterogeneity in the midbrain: implications for aversion encoding and drug withdrawal

Predominant theories regarding the function of VTA circuits have portrayed a vision of DA projections from the VTA encoding reward and motivational drive, with excitatory inputs to these VTA DA neurons facilitating this rewarding signal and inhibitory inputs acting to diminish it. It is clear that this model does accurately depict the activity of some VTA circuits (Shultz et al., 1997).

However, a greater appreciation of the considerable complexity and heterogeneity of the VTA, in terms of its neurochemical composition, circuit architecture and functional roles, is revealing that this model is incomplete (Morales & Margolis, 2017) (Figure 7).

With the advent of sophisticated viral tools to delineate output-specific sub-circuits, appreciation of organisation of behavioural function following projection patterns has steadily grown and is now widely accepted. However, reports challenging views that all DA neurons encode reward, and that this may be due to output-specific sub-circuits dates back to the 1980s. A sophisticated study using antidromic stimulation of various VTA output structures showed that a majority of putative VTA DA neurons (classified based on in-vivo electrophysiological properties) projecting to the mPFC were excited by noxious tail pinch, whereas the vast majority of NAc and Septum projecting DA neurons were unaffected by this stimulus (Mantz et al., 1989). Furthermore, a population of neurochemically confirmed DA neurons are also excited by foot-shock (Brischoux et al., 2009). In agreement with these data, noxious tail pinch increases DA levels in the mPFC, as measured by microdialysis (Di Chiara et al., 1999). Interestingly, this effect is potentiated in the Chronic Mild Stress model of depression, suggesting a sensitisation in aversive states that may underlie excessive aversive processing (Di Chiara et al., 1999). Whether this could also occur during drug withdrawal induced depressive states remains unknown.

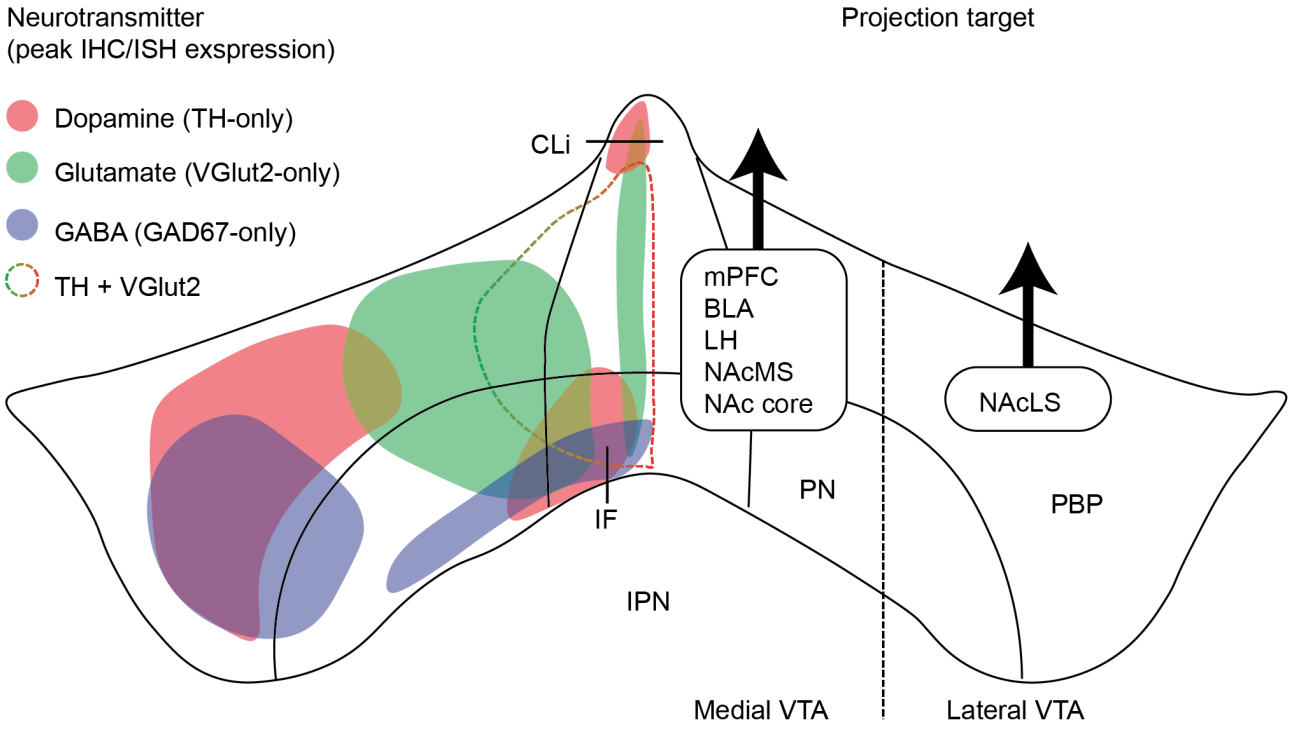

Figure 7. Cellular and functional heterogeneity in the VTA. The VTA contains several neurochemical cell types (left) who's distribution throughout the VTA varies. DA neurons (red) are found throughout the VTA but are most densely distributed in lateral parts of the parabrachial pigmented nucleus (PBP), within the interfascicular nucleus (IF) and in the dorsal tip of the caudal linear nucleus (CLi). GABA neurons (blue) also occupy the lateral PBP and are most visibile in the IF and Paranigral nucleus (PN) lying close to the border with the interpenduncular nucleus (IPN) which is ventral to the VTA. glutamate neurons (green) are almost exclusively found medially within the VTA with many close to the midline whilst glutamate/DA co-releasing neurons (dashed line) also lie within this zone. Distinct VTA populations can also be catagorised based on projection target (right). Projection neurons in the lateral portion of the VTA preferentially target the lateral shell of the nucleus accumbens (NAcLS) and DA neurons of this region represent classic RPE encoding described by Shultz and colleagues (1997). More medially located projection neurons have a wide range of downstream targets including the medial prefrontal cortex (mPFC), basolateral amygdala (BLA),lLateral hypothalamus (LH), as well as the core and the medial shell of the nucleus accumbens (NAcMS). Data points towards segregation of precise behavioural functions of these output-specific cell types, for instance mPFC projecting neurons are widely considered to encode aversive stimuli.

A series of studies examining physiological characteristics and experience-dependant plasticity in output-specific VTA populations helped to further unpick this complexity (Lammel et al., 2014). It was shown by retrogradely labelling output-specific VTA neurons that typical electrophysiological properties used to characterise VTA DA neurons in acute slice preparations reliably described a subset of neurons projecting to the lateral shell of the NAc (NAcLS), which were preferentially distributed in the lateral portion, meanwhile more medial located VTA neurons instead targeted structures including the mPFC and BLA and possessed a considerably different electrophysiological profile (Lammel et al., 2008). Recently differences in basal electrophysiological characteristics of output-specific populations have also been described in-vivo (Farassat et al., 2019). These output-specific populations also show considerable differences in experience dependent plasticity. In accordance with early findings of Ungless et al (2001), a single injection of cocaine potentiated AMPA mediated transmission in NAc projecting neurons, yet did not affect postsynaptic strength in mPFC projecting cells. On the contrary, excitatory strength on to mPFC neurons increased following an aversive stimulus (formalin injection in the hindpaw) which instead minimally affected excitatory synapses on to NAcLS projecting cells and had no effect on NAcMS projecting cells (Lammel et al., 2011). Interestingly, NAcLS and mPFC projecting VTA DA cells receive excitatory input from distinct structures. NAcLS projectors are innervated by the laterodorsal tegmental nucleus (LDTg), whereas mPFC projectors are targeted by the LHb. Optogenetically stimulating these afferent inputs in the VTA drove opposite effects, conditioned place preference following LDTg axon stimulation and conditioned place aversion following LHb axon stimulation. Both these behavioural effects were subsequently abolished by infusion of DA receptor antagonists in the implicated downstream targets of NAcLS and mPFC respectively, directly implicating these projections in mediating the opposing behavioural effects of their inputs (Lammel et al., 2012). Altogether, considerable complementary evidence implicates VTA DA projections to the mPFC in aversive processing. Given DA in the mPFC critically regulates the process of reinstatement of drug seeking (McFarland et al., 2004; McFarland & Kalivas, 2001), it is plausible that this circuit is strengthened in drug withdrawal, and could mediate the overall aversive state as well as susceptibility to stimuli inducing relapse during withdrawal, such as stress.

Whilst all drugs of abuse reliably drive DA increases in the NAc, it has been shown that for cocaine at least a heterogenous array of VTA neuronal firing responses in-vivo occur following acute administration. Interestingly, cells which were excited by foot-shock were also excited by cocaine (Mejias-Aponte et al., 2015). How this distribution of responses may be altered by cocaine withdrawal remains unknown. Considerable proportions of both DA and non-DA neurons were excited or inhibited by cocaine, demonstrating that non-DA VTA neurons likely actively participate in the response to drugs in ways that go beyond purely regulating DA transmission (Mejias-Aponte et al., 2015). Indeed, the VTA contains both GABA and glutamate neurons, and both cell types have been shown to regulate motivational and aversive behaviours. Some estimates of proportions suggested that DA neurons account for roughly 70% of all VTA neurons, with the majority otherwise and only a very small contribution from glutamate neurons around 3% (Nair-Roberts et al., 2008) however recent studies of VTA projection neurons challenge this, suggesting the proportion of glutamate neurons has been underestimated (Breton et al., 2019). Whilst containing an equally broad array of projection targets as DA projection neurons (Breton et al., 2019), few studies to date have interrogated the role of non-DA projections to structures other than the NAc. Optogenetic stimulation of VTA GABA neurons locally drives aversion due to inhibition of reward encoding DA neurons (Tan et al., 2012). Meanwhile, VTA GABAergic projections preferentially target Acetylcholine interneurons (ChIns) in the NAc, pausing their activity. This process critically underlies associative learning processes dysregulated in addiction (Brown et al., 2012). Interestingly during cocaine withdrawal, VTA GABA to NAc transmission is enhanced (Ishikawa et al., 2013). Stimulation of VTA glutamate cell bodies is rewarding (Wang et al., 2015b) whilst stimulation of VTA glutamatergic axons in the NAc has given contrasting results of aversion (Qi et al., 2016) and reward (Yoo et al., 2016)

which are like accounted for by varying stimulation protocols. Additionally, a population of VTA neurons projecting to the NAc among other outputs co-releases DA and glutamate. Recent work demonstrated that the reinforcing nature of this pathway (mice will self-stimulate) is not dependent on the co-released DA (Zell et al., 2020). A collection of work employing transgenic mouse lines to unpick this co-transmission has proposed a role in flexibly shifting strategies to obtain rewards, a process dysregulated in addiction (Bimpisidis & Wallén-Mackenzie, 2019). Finally, VTA GABA and glutamate projection neurons receive input from many of the same limbic regions as VTA DA projection neurons (Beier et al., 2015; 2019). Clear evidence thus suggests a role for non-DA VTA, both locally and in projecting neurons, in motivation and aversion. How these circuits may be recruited in aversive states, such as during withdrawal from drugs of abuse, remains unknown.

1.3.2.2 Neuropeptides in the extended amygdala

The above section describes an aversive system within VTA circuits, opposing the more commonly studied rewarding circuits. Aversion encoding regions more functionally separated from the midbrain are also believed to be recruited in drug withdrawal. Fluctuations in the levels of the neuropeptides corticotropin-releasing factor (CRF) and neuropeptide Y (NPY) during withdrawal mirror those elicited by acute and chronic stressors. These alterations take place in a collection of nuclei termed extended amygdala, comprising the bed nucleus of the stria terminalis (BNST), the central amygdala (CeA) and the posterior shell of the NAc (Logrip et al., 2011) and are hypothesized to generate a form of 'anti-reward' (Koob, 2008; Koob & Le Moal, 1997).

CRF critically regulates the activity of stress hormones including corticosterone in the hypothalamic-pituitary-adrenal axis who's activity accounts for much of the body's physiological stress response (Guillemin et al., 1959). In addition to its endocrine regulatory role, CRF also has direct, neuromodulatory actions in the central nervous system with numerous limbic regions containing CRF receptors (Pilcher & Joseph, 1984).

Extracellular CRF levels increase in the extended amygdala during withdrawal from cocaine, opioids, ethanol, nicotine and THC) (Koob, 2011). Studies employing either systemic or CeA infusions of selective CRF receptor antagonists in rodents have successfully abolished or attenuated aversive features of withdrawal from multiple different drugs of abuse (For a review see Logrip et al., 2011) suggesting a role for CRF in mediating aspects of withdrawal, however, evidence of cellular/synaptic mechanisms at play remain limited. One candidate mechanism lies in the relationship between CRF and NPY, which is thought to be reciprocal yet opposing (Heilig et al., 1994). Both neuropeptides are enriched in the BNST, which is heavily implicated in the pathogenesis of alcohol addiction (Silberman & Winder, 2013). In the BNST, NPY acting on Y1 receptors potentiates inhibitory transmission on to CRF neurons, and long-term alterations in NPY transmission in the BNST were shown to regulate binge-ethanol drinking in mice (Pleil et al., 2015). In line with this, CRF/GABA neurons of the BNST projecting to the VTA have been shown to promote binge ethanol drinking (Rinker et al., 2017).

In summary, several distinct yet overlapping systems are known to be hijacked during addiction and act in concert to produce the behavioural pathology. In addition, particular neural circuits known to be active in aversive processing could also be recruited during withdrawal. With the advent of new viral strategies to dissect the roles of specific circuits, our understanding of drug-withdrawal driven adaptations can be expanded to provide a more rounded view of addiction neurobiology where the contribution of withdrawal is fully appreciated not only from a clinical standpoint, but from a neurobiological standpoint also. To this end my thesis focuses on synaptic adaptations occurring in LHb circuits during drug withdrawal.

1.4 The lateral habenula: a hub for aversive states

My thesis aims to unravel drug-withdrawal driven cellular and synaptic adaptions in LHb circuits. Recent decades have witnessed a steadily growing appreciation of the importance of the LHb as a key node for processing of aversive stimuli and emergence of aversive states. Here I will provide a brief description of LHb anatomy, connectivity and principle functions before detailing its contribution to disease and in particular drug withdrawal.

1.4.1 LHb function and anatomy

The LHb, located dorsal to the thalamus and ventral to the dentate gyrus in rodents, is a phylogenetically old, evolutionarily conserved brain nucleus, present in all vertebrate species (Bianco and Wilson, 2009). Early studies examining the behavioural functions of LHb by lesioning the nucleus demonstrated its important to an array of functions critical to survival including behavioural components of pain, stress, reward, sleep and maternal care (reviewed in Hu et al., 2020 and Lecourtier & Kelly, 2007) whilst inactivating the LHb also disrupts social behaviour (van Kerkhof et al.,2013). These studies set a platform for deeper investigation into neural mechanisms underlying the LHb's role in these processes. As denoted by intense expression of vesicular glutamate transporter markers (Aizawa et al., 2012; Herzog et al., 2004), LHb cellular composition is considered to be almost exclusively glutamatergic projection neurons, however a small population of putative interneurons positive for GABAergic markers have also recently been described (Flanigan et al., 2020; Webster et al., 2020; Zhang et al., 2016, 2018b). LHb neurons can be categorised based on three distinct patterns of spontaneous firing activity: Silent, tonic and burst firing cells (Weiss & Veh, 2011). The LHb can be subdivided into medial and lateral portions with distinct functional relevancies dictated by their individual connectivity profiles.

The majority of work examining the behavioural function of LHb activity have focussed on its role in encoding aversive stimuli and mediating appropriate behavioural responses. Seminal experiments conducted by Matsumoto & Hikosaka (2007; 2009) in non-human primates demonstrated a role of LHb activity in the encoding of reward and aversion. LHb activity was shown to encode unpredicted reward (sucrose) or stress (airpuff) with opposing activity – LHb neurons spiking increased following an unpredicted airpuff but were inhibited by unpredicted sucrose. Moreover, when the delivery became predictable by preceding cues, LHb activity transferred to the cues predicting imminent reward or aversion. Finally, when delivery of an expected reward was withheld, LHb neurons were excited (Matsumoto & Hikosaka, 2007; 2009). Similar activity dynamics have since been confirmed in rodents (Wang et al., 2017). This profile of activity provides an almost perfect mirror to that of RPE encoding VTA DA neurons (Shultz et al., 1997). Recent work has built upon these findings to demonstrate a necessary role of LHb activity during reward omission for reward-guided learning (Nuno-Perez et al., 2021). Furthermore, LHb neural activity and synaptic transmission has been shown to be necessary for both innate and learned escape behaviours (Lecca et al., 2017, 2020; Trusel et al, 2019). Intriguingly, these negative RPE signals may be distorted following stress such that rewards are encoded with phasic excitation rather than inhibition (Shabel et al., 2019).

1.4.2 Afferent connectivity of the LHb

The LHb receives input from a broad range of limbic structures (Figure 8). Particularly dense innervation arises from the lateral hypothalamus (LH) which targets the entirety of the LHb with mostly glutamatergic projections which convey aversive signals to the LHb and are necessary for the execution of escape behaviours (Lecca et al., 2017, Lazaridis et al., 2019, Trusel et al., 2019). Similarly strong connections from axons of the neighbouring entopeduncular nucleus (EPN) co-release glutamate and GABA selectively on to neurons in the lateral portion

and are also thought to contribute to LHb encoding of aversive stimuli (Shabel et al., 2014). Mixed glutamate and GABA projections also emanate from the medial VTA (Root et al., 2014) whilst serotonergic and glutamatergic afferents come from the DRN and median raphe nucleus (MRN) respectively (Cardozo Pinto et al., 2019; Szőnyi et al., 2019). LHb receives additional confirmed afferent innervation from basal forebrain structures including the BNST, medial septum (MS), ventral pallidum (VP) and lateral preoptic area (LPO) (Knowland et al., 2017; Lazaridis et al., 2019; Nuno-Perez et al., 2021; Zhang et al., 2018a). Whilst the precise behavioural importance of each of these individual inputs is yet to be fully elucidated, a general principle repeatedly shown by optogenetically stimulating inputs in Place preference/avoidance experiments is that excitatory innervation of LHb neurons is aversive and whilst stimulation of inhibitory afferents is rewarding, in-keeping with data demonstrating a key role of the LHb in aversion encoding.

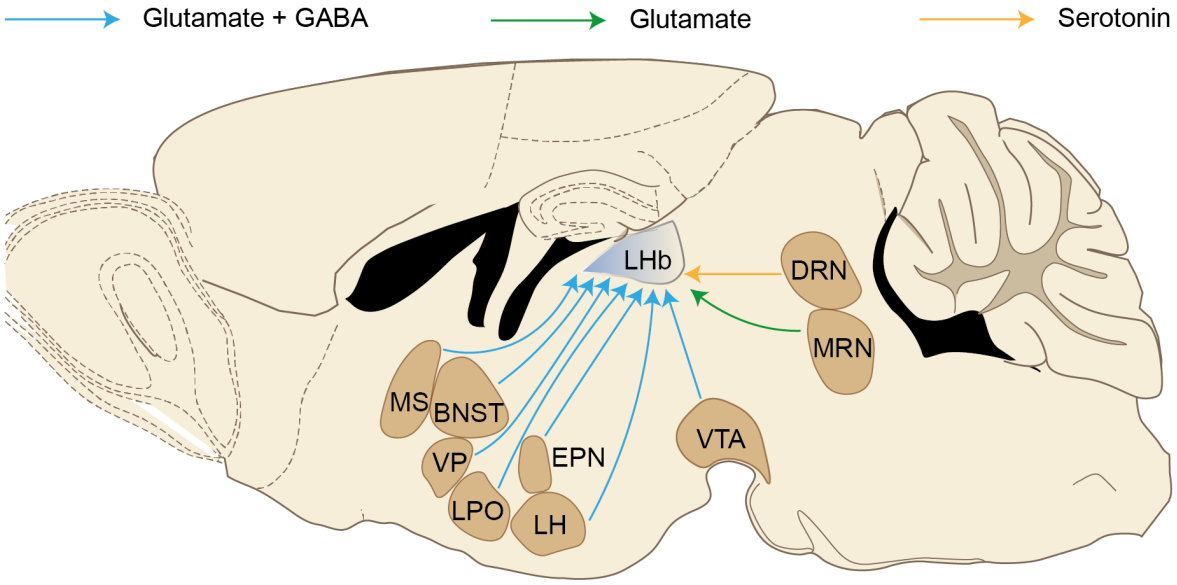

Figure 8. Afferent connectivity of the LHb. LHb inputs from both EPN and VTA co-release Gluatamate and GABA from the same axon terminals whilst distinct glutamate and GABA populations from numerous other regions target the LHb. These include the LH, which is predominantly an excitatory input, as well as a collection of basal forebrain structures such as the MS, BNST, LPO and VP. Finally, the LHb also receives input from glutamate and serotonergic neurons of both the DRN and MRN.

1.4.3 Efferent connectivity of the LHb

LHb projections (Figure 9) travel through a dense fibre bundle – the fasciculus retroflexus – towards the midbrain. Here, there is innervation of the rostromedial tegmental nucleus (RMTg) which contains a mass of inhibitory projection neurons. RMTg GABA neurons act to inhibit reward encoding VTA DA neurons, as well as serotonergic neurons of the DRN (Jhou et al, 2009; Kaufling et al., 2010; Lecca et al., 2012). It has been repeatedly shown in several animal species that direct electrical stimulation of LHb drives powerful feedforward inhibition of VTA DA neurons (Ji & Shepherd, 2007; Matsumoto & Hikosaka, 2007). This potent control is likely a strong contributor to negative RPE signals in DA neurons, particularly those arising following omission of an expected reward (Matsumoto & Hikosaka, 2009; Tian & Uchida, 2015). RMTg projecting neurons of the LHb are distributed mostly in the lateral portion where they receive prominent afferent input from glutamate/GABA co-releasing axons of the EPN (Meye et al., 2016; Li et al., 2019).

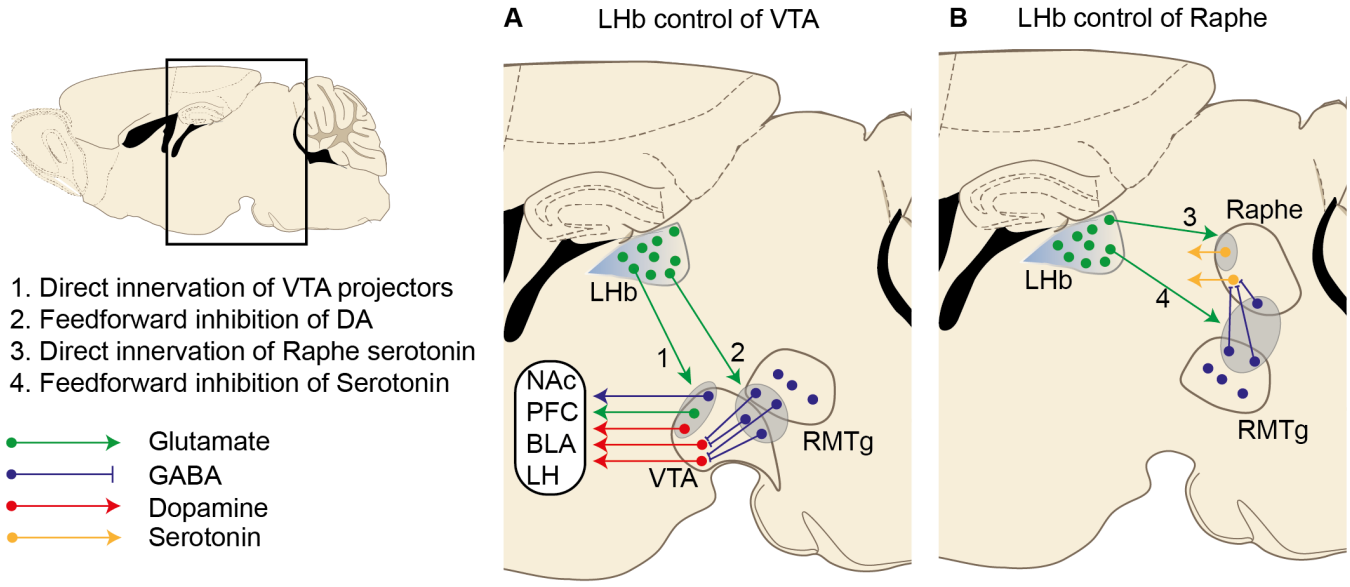

Figure 9. Efferent connectivity of the LHb. Excitatory projections of the LHb regulate the activity of neurons in both the VTA and Raphe through a series of distinct pathways. **A.** LHb provides direct innervation of projection neurons of the VTA (1), targetting all neurochemical cell types. Additionally, the LHb activity can also powerfully inhibit a subset of DA neurons by targetting local inhibitory neurons in both the VTA and RMTg (2). **B.** Similarly, in the Raphe the LHb also directly targets serotonergic projection neurons (3), whilst also exciting inhibitory relays located in both the RMTg and Raphe nuclei (4).

The LHb also provides direct excitatory input to the VTA and DRN (Figure 9). Both nuclei contain an array of neurochemical cell types. Estimates of LHb innervation of VTA neuronal subtypes vary with some studies showing a predominant innervation of VTA GABA neurons (Brinschwitz et al 2010), similarly contributing to overall feedforward inhibition of VTA DA neurons. Whilst this is undoubtedly a prime function of LHb activity, several reports show that LHb axons also provide direct innervation to VTA DA neurons and that proportionally, within the VTA, targeting of GABA and DA may be roughly equal (Omolchenko et al., 2009). Output-specific monosynaptic viral tracing with a modified rabies virus (Beier et al., 2015; 2019) reveals that LHb neurons target VTA projection neurons of all three transmitter phenotypes (DA, GABA and glutamate). Of studies examining the functional relevance of this direct innervation of VTA projection, rather than interneurons, it was shown that LHb projections directly target VTA DA projections to the mPFC and that conditioned place aversion following LHb terminal stimulation in the VTA was dependent on intact DA signalling in the mPFC (Lammel et al., 2012). Less is known concerning LHb projections to the DRN, although tracing studies demonstrate that LHb provides monosynaptic innervation of both serotonin and GABA neurons located there (Pollak-Doricic et al., 2014; Liu et al., 2021). The DRN plays a key role in regulating a broad range of behavioural functions including motivation, mood and social behaviour. Studies examining innervation of this complex and highly heterogenous system by limbic regions such as the LHb could help to elucidate the circuit logic underlying DRN control over precise behavioural roles within these broader functions.

1.4.4 LHb adaptations in the emergence of aversive states

Following the logic that LHb activity transiently encodes aversive stimuli, experiments recording LHb during aversive states both in-vivo and in acute brain slices have revealed persistent elevations in LHb activity/excitability, as well as synaptic adaptations favouring excitatory drive on to LHb neurons. These adaptations have been shown to critically underlie the emergence of these aversive states. Here I will provide an overview of LHb adaptations

implicated in mediating the aversive states arising during depression and drug withdrawal, which account for the majority of published literature to date.

1.4.4.1 Depression

Early indications of a putative role of LHb dysfunction in depression came via human neuroimaging studies in which patients experienced a transient depressed mood following depletion of tryptophan, an essential amino acid and critical to the synthesis of serotonin. It was shown that LHb metabolic activity was altered by this intervention (Morris et al., 1999). Further neuroimaging studies have since linked Habenular volume to severity of depressive symptoms in patients whilst LHb activity during aversive stimuli is altered in depressed patients (Lawson et al., 2017). Additional clinical evidence of aberrant LHb activity in depression was demonstrated by a seminal study showing that Deep Brain Stimulation (DBS) of the LHb in a patient with treatment resistant depression was able to significantly alleviate symptoms (Sartorius et al., 2010).

These clinical data are complemented by a wealth of preclinical data implicating LHb adaptations in the emergence of depression and elucidating the circuit, synaptic and cellular mechanisms underpinning these adaptations. A consistent finding in a variety of different mouse models of depression including those bred for depressive traits, and models where a depressive state is induced through exposure to severe and/or persistent stressors, is that LHb neurons are hyperactive/hyperexcitable. Interventions using chemogenetics to directly reduce LHb hyperactivity (Tchenio et al., 2017) or to reverse/prevent LHb hyperactivity by targeting molecular pathways instrumental its induction (Lecca et al., 2016) reliably abolish or prevent depressive-like behaviours. Reports of both an increase in the proportion of LHb neurons exhibiting burst like firing (Cui et al., 2018) and increased rate of tonic firing (Liu et al., 2021) may account for the overall hyperactivity. Among these studies, ground-breaking research demonstrated a novel mechanism involving astrocytes in producing an increase in the proportion of bursting neurons. Cui et al (2018) showed that an upregulation of Kir4.1, a potassium channel exclusively located on astrocytic cell bodies, in the LHb in multiple models of depression, altered the potassium buffering properties of these cells. This resulted in a knock-on effect on of hyperpolarizing the resting membrane potential of LHb neurons which is a critical determinant of LHb firing properties (Weiss & Veh, 2011), due to the presence of low-threshold voltage gated calcium channels causing rebound bursting. Reversing the Kir4.1 upregulation in the LHb rescued the depressive phenotype, along with the increase in bursting neurons (Cui et al., 2018). These results come amidst a growing appreciation of the importance of glial cells in regulating neuronal function and psychiatric disorders. Further studies are required to better understand the contributions of glia, including non-astrocyte glial cells such as microglia, to LHb adaptions in aversive states.

Accompanying, and most likely contributing to, LHb hyperactivity in depression are several reports of synaptic plasticity of both excitatory and inhibitory transmission. Li et al (2011) show that glutamate release probability of excitatory inputs in the LHb is increased in the congenital learned helplessness (cLH) model of depression. In the same model, the ratio of glutamate and GABA released from EPN terminals in the LHb was altered such that excitatory drive increased due to diminished levels of glutamic acid decarboxylase, the rate limiting enzyme in GABA synthesis (Shabel et al., 2014). Further depression related plasticity of GABA transmission in LHb is evident in studies demonstrating reduced surface expression of $GABA_B$ receptors mediating LHb hyperactivity and depressive-like symptoms induced by foot-shock stress (Lecca et al., 2016) and maternal separation (Tchenio et al., 2017).

Altogether, it is clear that LHb adaptations represent a key player in the pathology of depression. Both hyperactivity of the LHb, and synaptic plasticity favouring excitatory transmission on to LHb neurons, are necessary elements for the emergence of depressive-like

behaviours. Similar functional adaptations occur despite the recruitment of a variety of different induction mechanisms in these studies. This suggests that LHb adaptations could mediate the aversive states arising from various different initial stimuli, including during drug withdrawal.

1.4.4.2 Drug withdrawal

In lieu of its well-documented prominent connection with monoaminergic nuclei, critical for motivational processes disrupted in addiction, LHb adaptations have long been hypothesised to play a role in drug-driven behaviours. Studies providing early evidence of this showed that in rats who received slow-release formulas of several drugs of abuse to maintain consistent, yet relatively low, plasma concentrations had significant degeneration of the fr fibre tract connecting the LHb to the midbrain after 2 days of withdrawal, hypothesised to be due to excitotoxicity (Carlson et al., 2000; Ellison, 2002). In line with this hypothesis of increased excitation of LHb neurons during withdrawal, protracted (14 days) withdrawal from chronic heroin treatment in rats revealed an increase in immunoreactivity for the immediate early gene cFos – an indicator of recent neuronal activity – specifically in the medial portion of the LHb (Zhang et al., 2005).

These studies provided circumstantial evidence of aberrant LHb activity in drug withdrawal, yet without direct electrophysiological data demonstrating this to be the case. Many studies since have shown that, much like in depression, drug-withdrawal drives adaptations both in the activity of LHb neurons and of LHb synaptic plasticity (Figure 10). Compelling data now firmly implicates LHb adaptations in the pathogenesis of aversive states emerging in both cocaine and ethanol withdrawal.

1.4.2.2.1 Cocaine withdrawal

On short time scale, likely representing the initial “crash” phase of cocaine withdrawal emerging soon after the drug has been degraded, in-vivo recordings showed increased LHb activity, which opposed a decrease in activity immediately following administration (Jhou et al., 2013). Withdrawal at stages after this crash phase has passed, from either chronic cocaine i.p. injections (Meye et al., 2015) or self-administered intravenous cocaine (Neumann et al., 2014) results in hyperexcitability of LHb neurons. Meye et al (2015) demonstrated that this increase in hyperexcitability in acute slices translated to increased LHb activity in-vivo and was specific to RMTg-projecting LHb neurons. Increases in excitability were driven by a decrease in potassium conductances which provide an inhibitory driving force crucial in regulating neuronal firing (Friedman et al., 2014). The hyperexcitability occurred in concert with a potentiation of AMPA transmission in these cells previously reported (Maroteaux & Mameli, 2012). Both these adaptations were shown to be the result of increased trafficking of GluA1 containing AMPA receptors (the most abundant type in the LHb) to the cell surface following increased phosphorylation of the serine-845 (S845) residue on the GluA1 C terminus (Meye et al., 2013; 2015). Blocking this process prevented the synaptic potentiation, hyperexcitability and the emergence of depressive-like symptoms (Meye et al., 2015). As is the case in cLH mice (Shabel et al., 2014) the same cocaine regimen also shifts EPN co-release in LHb to favour excitation, albeit with a different mechanism. Cocaine withdrawal resulted in a decrease of vesicular GABA transporter (VGAT), causing deficient GABA vesicle filling in the EPN thus decreasing GABAergic transmission from these terminals, an effect visible in both $GABA_A$ (Meye et al., 2016) and $GABA_B$ mediated currents (Tan et al., 2019). Selectively overexpressing VGAT in LHb-projecting EPN neurons restored EPN GABA transmission. Furthermore, this intervention rescued depressive-like symptoms in cocaine withdrawal and abolished stress induced reinstatement of cocaine CPP (Meye et al., 2016). Overall cocaine withdrawal drives hyperexcitability in RMTg projecting LHb neurons, which also undergo strengthening of excitatory strength and diminished inhibitory input (EPN neurons preferentially target midbrain GABA neurons (Meye et al., 2016)).

1.4.2.2.2 Ethanol withdrawal

Ethanol withdrawal, whether from i.p. injections, or self-administration, reliably elicits both depressive-like and anxiety-like phenotypes in rodents that are dependent on LHb adaptations. Interestingly, many of the LHb changes present in cocaine withdrawal also emerge during ethanol withdrawal, suggesting that certain changes in LHb activity and neurotransmission may represent common features of drug withdrawal. Ethanol withdrawal also results in LHb hyperexcitability in slices and hyperactivity in-vivo which are dependent on reduced potassium currents (specifically currents passing through M-type potassium channels) (Kang et al., 2017; Li et al., 2017). Furthermore, ethanol withdrawal drives a potentiation of AMPA transmission in LHb neurons dependent on phosphorylation of another GluA1-C terminus serine residue (S831) and the resultant increase in GluA1 receptor trafficking (Li et al.,2017). As in cocaine withdrawal, interventions targeted to these induction mechanisms reversed the LHb adaptations and in doing so ameliorated the associated behavioural phenotypes (Kang et al., 2017; Li et al., 2017). Interestingly, ethanol withdrawal-driven hyperactivity was also shown to be regulated by decreased astrocytic glutamate buffering through the GLT-1 transporter, providing further support to the notion that glial cells play a key role in regulating LHb adaptations in aversive states (Cui et al., 2018; Kang et al., 2018).

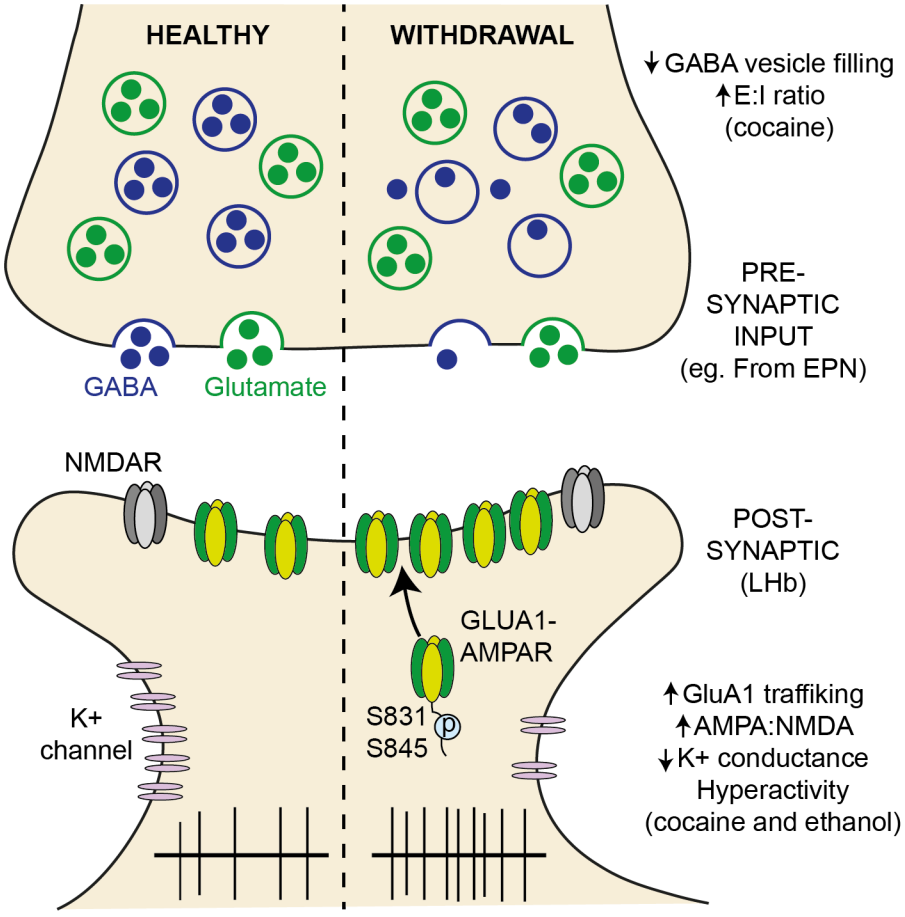

Figure 10. Cellular/Synaptic adaptations emerging in the LHb during drug withdrawal. Withdrawal from cocaine and ethanol drive common adaptations in LHb neurons. Cocaine and ethanol: Phosphorylation of GluA1-serine residues potentiates trafficking of AMPA receptors to the cell membrane, thus increasing the AMPA:NMDA ratio - strengthening excitatory synaptic transmission. Reductions in potassium conductance ultimately drive hyperactivity. Cocaine: Impaired presynaptic (from EPN) GABAergic vesicle filling drives an increase in E:I ratio at this input. Adapted from [Clerke et al., 2021b: Neuronal adaptations in the lateral habenula during drug withdrawal: Preclinical evidence for addiction therapy]

1.4.5 Objectives and rational of the thesis work

Altogether, several studies in the last decade using models of withdrawal from both cocaine and ethanol demonstrate the importance of LHb adaptations in mediating the aversive state emerging in withdrawal, providing concrete electrophysiological and mechanistic evidence to back up early anatomical studies. Yet many open questions remain.

Whilst the majority of studies describing output-specific adaptation in the LHb during aversive states have focused on VTA and RMTg projecting neurons, a population also project to the DRN, the main source of serotonin neurons in the brain. Given serotonins well characterised role in mood regulation, disrupted in depression, it is likely that specific adaptations may also occur in LHb projections to the DRN in depression. Regarding drug withdrawal, early studies using cFos indicate that withdrawal from heroin results in aberrant LHb activity (Zhang et al., 2005), specifically in the medial portion which projects to the DRN. Additionally, a study reporting that depleted NAc serotonin levels may account for increased morphine preference during withdrawal (Harris & Ashton-Jones, 2001) suggests a role of aberrant DRN serotonin in mediating the withdrawal state from opioids. Thus, it is plausible that morphine withdrawal may alter the LHb-DRN pathway. To this end we sought to determine whether morphine-withdrawal driven adaptations occurring upstream in the LHb could mediate components of the withdrawal aversive state.

How cocaine withdrawal affects LHb output to the midbrain remains unknown. Despite the absence of clear changes in VTA projecting neurons (Meye et al., 2015), the great heterogeneity and complexity of this region, with a variety of cell types and projection targets each receiving LHb input (Beier et al., 2015; 2019), means that diverse and potentially important adaptations not detectible in VTA projecting LHb neurons may become visible downstream in the VTA. In light of this we decided to investigate cocaine withdrawal driven plasticity of LHb projections to the midbrain.

These are the questions I aim to tackle in my PhD thesis to provide a broader understanding of LHb circuit adaptations during the drug-withdrawal driven aversive state.

Chapter 2. Morphine withdrawal adaptations in the LHb drive social deficits

Opiate withdrawal produces aversive symptoms, which collectively acts as a strong source of negative reinforcement to continue, or resume drug use. Among the psychological disturbances present at this time are social deficits (Goeldner et al., 2011; Powell & Taylor, 1991). Despite a large body of clinical data acknowledging a link between social isolation and opioid addiction (Christie, 2021), the neural substrates underpinning this link remain unclear. Several lines of evidence implicate a role for the LHb. Heroin withdrawal drives an increase in cells positive for the activity marker cFos in the LHb (Zhang et al., 2005), whilst the functional integrity of this nucleus is necessary for social play behaviours in rats (van Kerkhof et al., 2013). Moreover, functional adaptations in the LHb are well recognized to underlie aversive states emerging in other types of drug withdrawal. Excitatory transmission is potentiated on to LHb neurons in both cocaine and ethanol withdrawal, accounting for the emergence of depressive-like symptoms in both (Li et al., 2017; Meye et al., 2015). However, it is unknown how morphine withdrawal alters LHb glutamatergic transmission, and if such adaptations could, like in cocaine and ethanol withdrawal, be causal for specific components of the ensuing aversive state.

In the present study, we first assessed the impact of naloxone-precipitated morphine withdrawal upon excitatory synaptic strength in the LHb using whole-cell patch clamp slice electrophysiology. We found that morphine withdrawal diminished AMPA/NMDA ratios specifically in medially located LHb neurons projecting to the DRN, and not to the VTA. Following reports that local elevations in neuroinflammation drive drug withdrawal driven plasticity elsewhere in the brain (Lewitus et al., 2014) we demonstrated that morphine withdrawal driven elevations in LHb tumour necrosis factor alpha (TNFα) mediated synaptic depression during morphine withdrawal. Furthermore, we showed that the action of TNFα in the LHb during withdrawal accounted for the emergence of sociability deficits. The extent of social impairment in withdrawal inversely correlated with synaptic strength in the LHb and chemogenetic inhibition of the LHb-to-DRN pathway mimicked the social deficits present in morphine withdrawal. Altogether these results support the concept that morphine withdrawal drives a local TNFα-mediated depression of excitatory transmission in the LHb-to-DRN pathway that in turn leads to impaired sociability.

My contributions to this study involved a series of experiments employing whole-cell patch clamp recordings in acute brain slices. I helped to demonstrate the localisation of TNFα driven LTD was specific to medially located LHb neurons (Figure 2), and that this plasticity was dependent on endogenous TNFα signalling (Figure S3). I additionally helped to show that the morphine withdrawal driven plasticity was present in spontaneous withdrawal and persisted for up to 30 days (Figure S1). Finally, I contributed to experiments showing a correlation between synaptic strength and morphine withdrawal driven sociability impairment (Figure 3).

The following section includes the manuscript for this study as published in Nature Neuroscience.

Valentinova K, Tchenio A, Trusel M, **Clerke JA**, Lalive AL, Tzanoulinou S, Matera A, Moutkine I, Maroteaux L, Paolicelli RC, Volterra A, Bellone C, Mameli M. Morphine withdrawal recruits lateral habenula cytokine signaling to reduce synaptic excitation and sociability. Nat Neurosci. 2019 Jul;22(7):1053-1056. doi: 10.1038/s41593-019-0421-4. Epub 2019 Jun 17.

nature neuroscience

BRIEF COMMUNICATION

https://doi.org/10.1038/s41593-019-0421-4

Morphine withdrawal recruits lateral habenula cytokine signaling to reduce synaptic excitation and sociability

Kristina Valentinova[1,2,6], Anna Tchenio[1,6], Massimo Trusel[1], Joseph A. Clerke[1], Arnaud L. Lalive[1], Stamatina Tzanoulinou[3], Alessandro Matera[4], Imane Moutkine[5], Luc Maroteaux[5], Rosa C. Paolicelli[4], Andrea Volterra[1], Camilla Bellone[3] and Manuel Mameli[1,5*]

The lateral habenula encodes aversive stimuli contributing to negative emotional states during drug withdrawal. Here we report that morphine withdrawal in mice leads to microglia adaptations and diminishes glutamatergic transmission onto raphe-projecting lateral habenula neurons. Chemogenetic inhibition of this circuit promotes morphine withdrawal-like social deficits. Morphine withdrawal-driven synaptic plasticity and reduced sociability require tumor necrosis factor-α (TNF-α) release and neuronal TNF receptor 1 activation. Hence, habenular cytokines control synaptic and behavioral adaptations during drug withdrawal.

Opiate withdrawal produces negative states, including low mood and reduced sociability, which contribute to relapse during drug abstinence[1,2]. Dysfunction of the lateral habenula (LHb)—a nucleus that controls monoaminergic systems and processes aversive stimuli—underlies depressive symptoms typical of drug withdrawal[3]; however, how opiates affect the LHb remains poorly understood[4,5].

We subjected mice to naloxone-precipitated morphine withdrawal (MORwd) to examine its repercussions on glutamatergic synapses onto LHb neurons[1]. Indeed, aberrant LHb excitatory transmission underlies negative symptoms in rodent models of depression and addiction[3]. Spontaneous excitatory postsynaptic current (sEPSC) amplitudes, but not frequencies, were reduced only in LHb neurons located in the medial aspect (^{Med}LHb; Supplementary Fig. 1a–b). Accordingly, MORwd diminished AMPA receptor (AMPAR)/NMDA receptor (NMDAR) ratios solely in the ^{Med}LHb (Fig. 1a; Supplementary Fig. 1c) without affecting neurotransmitter release, as assessed via trains of synaptic stimulation (Supplementary Fig. 1d). Recordings obtained 1 h after the last morphine injection (without naloxone) yielded saline-comparable AMPAR/NMDAR ratios. In contrast, spontaneous MORwd decreased AMPAR/NMDAR ratios in the ^{Med}LHb up to 30 days after the last morphine injection (Supplementary Fig. 1e).

To assess whether MORwd affects AMPAR conductance or number, we analyzed peak-scaled non-stationary fluctuations of ^{Med}LHb-recorded sEPSCs[6]. While single-channel conductance remained unaffected in MORwd slices, the number of channels opened at the peak was positively correlated with amplitude values (Supplementary Fig. 1f). MORwd failed to alter AMPAR-EPSC rectification (Supplementary Fig. 1g), whereas it reduced glutamate

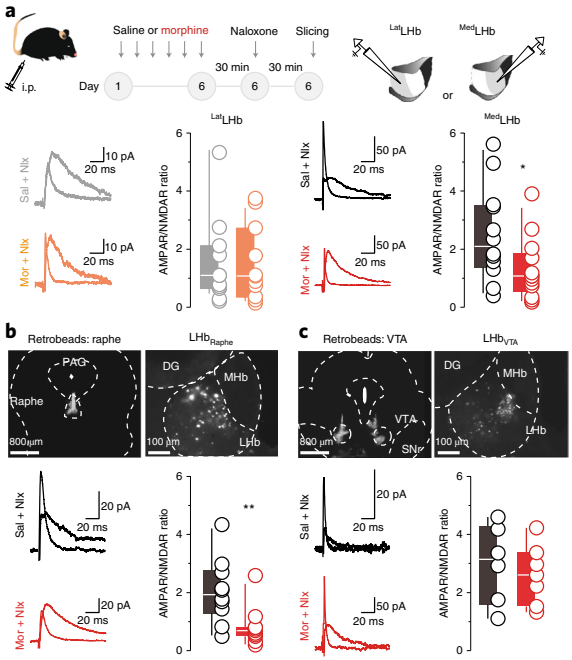

Fig. 1 | MORwd-driven projection-specific synaptic depression in the LHb. **a**, Top: naloxone-precipitated MORwd (NP-MORwd) protocol. Bottom left: traces and AMPAR/NMDAR ratios from ^{Lat}LHb slices (saline + naloxone (Sal+Nlx; $n = 7$ mice, 11 cells) versus NP-MORwd (Mor+Nlx; $n = 8$ mice, 11 cells)). Two-sided t test, $t_{20} = 0.0548$, $P = 0.957$. Bottom right: traces and AMPAR/NMDAR ratios from ^{Med}LHb slices (saline + naloxone ($n = 7$ mice, 12 cells) versus NP-MORwd ($n = 8$ mice, 13 cells)). Two-sided t test, $t_{23} = 2.210$, $^{*}P = 0.037$. i.p., intraperitoneal injection. **b**, Top: images of retrobeads in raphe and retrogradely labeled LHb_{Raphe} neurons. Bottom: Traces and AMPAR/NMDAR ratios from LHb_{Raphe} neurons (saline + naloxone ($n = 5$ mice, 10 cells) versus NP-MORwd ($n = 5$ mice, 11 cells)). Two-sided t test, $t_{19} = 3.153$, $^{**}P = 0.005$. **c**, Same as **b**, but in LHb_{VTA} neurons (saline + naloxone ($n = 2$ mice, 6 cells) versus NP-MORwd ($n = 4$ mice, 7 cells)). Two-sided t test, $t_{11} = 0.575$, $P = 0.577$. PAG, periaqueductal gray; DG, dentate gyrus; MHb, medial habenula; SNr, substantia nigra pars reticulata. Data are presented as box plots, with 10th and 90th percentiles, median and scatter.

[1]The Department of Fundamental Neuroscience, The University of Lausanne, Lausanne, Switzerland. [2]Department of Physiology, The University of Bern, Bern, Switzerland. [3]Department of Basic Neuroscience, The University of Geneva, Geneva, Switzerland. [4]Department of Physiology, The University of Lausanne, Lausanne, Switzerland. [5]Inserm, UMR-S 839, Paris, France. [6]These authors contributed equally: Kristina Valentinova and Anna Tchenio. *e-mail: manuel.mameli@unil.ch

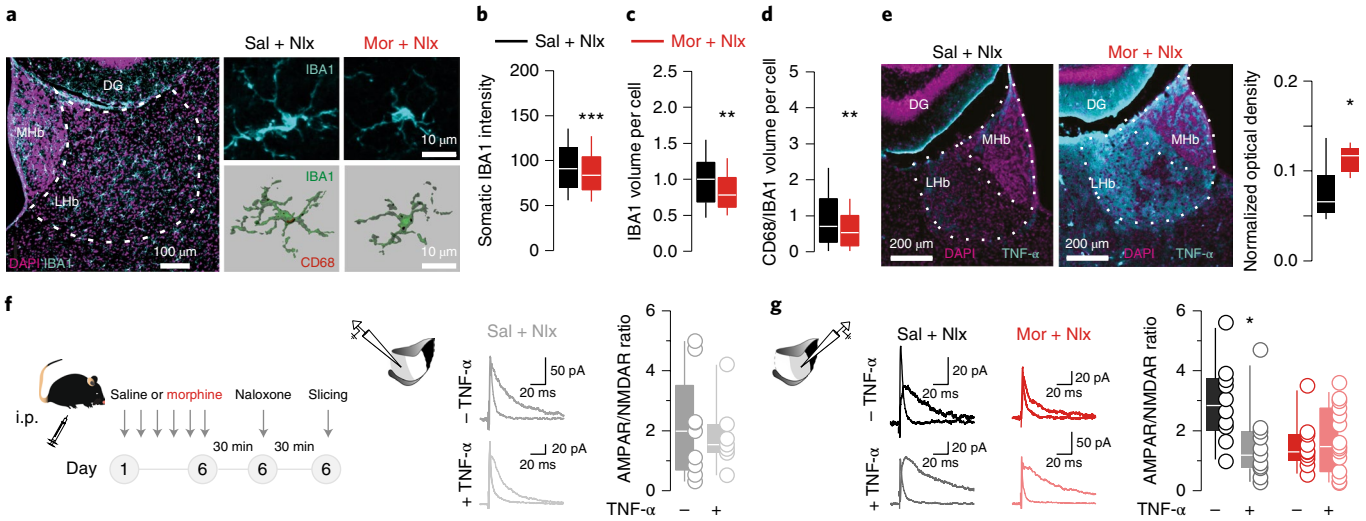

Fig. 2 | Cytokine signaling in the LHb for MORwd plasticity. a, Max-projection of confocal image of the LHb with IBA1$^+$ microglia (left). Max-projection of ^{Med}LHb microglia in saline + naloxone and NP-MORwd mice (upper right). 3D reconstruction of IBA1$^+$ microglia containing CD68 structures from slices obtained from saline + naloxone and NP-MORwd mice (lower right). **b**, Analysis of IBA1 microglia immunoreactivity in ^{Med}LHb slices (saline + naloxone ($n = 4$ mice, 366 cells), NP-MORwd ($n = 4$ mice, 328 cells)). Two-sided t test, $t_{692} = 3.305$, $^{***}P = 0.001$; 3 independent acquisition sessions. **c**,**d**, Quantitative analyses of microglial cell volume (based on IBA1 immunoreactivity) and CD68$^+$ structures. Values are normalized to saline control (saline + naloxone (black; $n_{mice/cells} = 4$ mice, 89 cells), NP-MORwd (red; $n = 4$ mice, 83 cells)). IBA1 volume (**c**): two-sided t test, $t_{170} = 3.05$, $^{**}P = 0.003$. CD68/IBA1 volume (**d**): two-sided t test, $t_{170} = 2.65$, $^{**}P = 0.008$. Measurements were obtained from independent samples. **e**, TNF-α (cyan) and DAPI (magenta) immunostaining and normalized TNF-α optical density in the LHb (saline + naloxone (black; $n = 7$ mice, 6 independent acquisitions per mouse) versus NP-MORwd (red; $n = 8$ mice, 5 independent acquisitions per mouse)). Two-sided t test, $t_{13} = 2.991$, $^{*}P = 0.0104$. **f**, Experimental protocol (left) and example traces and AMPAR/NMDAR ratios (right) in the ^{Lat}LHb with (+) or without (–) exogenous TNF-α (saline + naloxone –TNF-α ($n = 2$ mice, 9 cells) versus saline + naloxone +TNF-α ($n = 2$ mice, 9 cells)). Two-sided t test, $t_{14} = 0.37$, $P = 0.717$. **g**, AMPAR/NMDAR ratios with or without exogenous TNF-α recorded from saline + naloxone ($n = 3$ mice, 10 cells (–TNF-α) and $n = 4$ mice, 11 cells (+TNF-α)) and NP-MORwd ^{Med}LHb slices ($n = 3$ mice, 10 cells (–TNF-α) and $n = 5$ mice, 15 cells (+TNF-α)). Interaction factor $F_{(1,42)} = 4.90$, two-way ANOVA, $^{*}P = 0.039$. Data are presented as box plots, with 10th and 90th percentiles, median and scatter.

uncaging-evoked AMPAR/NMDAR ratios, yielding a decrease only in absolute AMPAR currents (Supplementary Fig. 1h). This suggests that MORwd reduces, in a territory-specific fashion, the number of AMPARs without affecting their biophysical properties, NMDAR numbers or presynaptic glutamate release.

MORwd-evoked plasticity occurs onto ^{Med}LHb neurons, which innervate downstream structures, including the raphe nucleus and the ventral tegmental area (VTA)[7]. MORwd diminished AMPAR/NMDAR ratios solely in retrobead-labeled raphe-projecting (LHb_{Raphe}) but not VTA-projecting LHb (LHb_{VTA}) neurons (Fig. 1b,c). These results point to the specificity of MORwd for discrete habenular circuits.

Which induction mechanism gates MORwd-driven plasticity onto ^{Med}LHb neurons? Inflammatory responses and glial cell activation emerge during drug withdrawal[8]. Indeed, spontaneous MORwd drives microglia adaptations and pro-inflammatory cytokine release (that is, TNF-α)[9]. Notably, cocaine also leads to reduced microglia arborization along with TNF-α-dependent AMPAR internalization, which partly underlies drug-mediated behavioral adaptations[8]. We found that within the ^{Med}LHb, MORwd reduced microglial markers, including IBA1 and CD68, and diminished microglial cell volume (Fig. 2a–d). In parallel, naloxone-induced and spontaneous MORwd increased habenular TNF-α immunolabeling (Fig. 2e; Supplementary Fig. 2a–d). Altogether, these findings support the view that there is engagement of inflammatory responses and cytokine signaling within the LHb during MORwd.

We then reasoned that if MORwd promotes TNF-α release, artificially increasing its levels should prove sufficient to recapitulate MORwd-driven synaptic plasticity. Incubating LHb-containing slices obtained from saline-injected mice with exogenous TNF-α reduced AMPAR/NMDAR ratios in the ^{Med}LHb. This effect was absent in the lateral aspect of the LHb (^{Lat}LHb), and occluded by naloxone and spontaneous MORwd (Fig. 2f,g; Supplementary Fig. 3a). TNF-α release may arise from microglial Toll-like receptor 4 (TLR4) signaling[10]. Systemically activating TLR4 with the agonist monophosphoryl lipid A (MPLA) in morphine-treated mice, instead of naloxone, mimicked MORwd plasticity (Supplementary Fig. 3b). Moreover, MPLA application in slices obtained from morphine-treated animals reduced AMPAR currents in the ^{Med}LHb, but not the ^{Lat}LHb (Supplementary Fig. 3c–d). MPLA-driven EPSC reduction did not occur in the presence of a dominant-negative peptide that blocks the soluble form of TNF-α[8] (XENP1595; Supplementary Fig. 3e). Furthermore, MORwd occluded MPLA-driven synaptic depression (Supplementary Fig. 3c), and systemic injection of XENP1595 prevented MORwd-induced plasticity (Supplementary Fig. 3f). Altogether, these results support the notion that TLR4 is expressed within the LHb (see the Allen Brain Atlas) and that its effect on AMPARs occurs via TNF-α signaling. Moreover, the results support the necessity and sufficiency of TNF-α for MORwd-driven reduction of LHb glutamatergic transmission.

TNF-α triggers its central effects partly through TNF receptor 1 (TNF-R1; encoded by *Tnfr1* (also known as *Tnfrsf1a*))[11]. We employed 129-Tnfrsf1atm3GkI (referred to as $Tnfr1^{fl/fl}$) mice in which *Tnfr1* expression in LHb neurons was knocked down via adenovirus (AAV)-Cre (Fig. 3a–c). After viral injection, AAV-Cre-$Tnfr1^{fl/fl}$ mice failed to show MORwd-driven AMPAR/NMDAR ratio reduction compared to AAV-Control-infused mice (Fig. 3d). This highlights the necessity of neuronal TNF-R1 for MORwd-driven depression of synaptic AMPARs in the LHb.

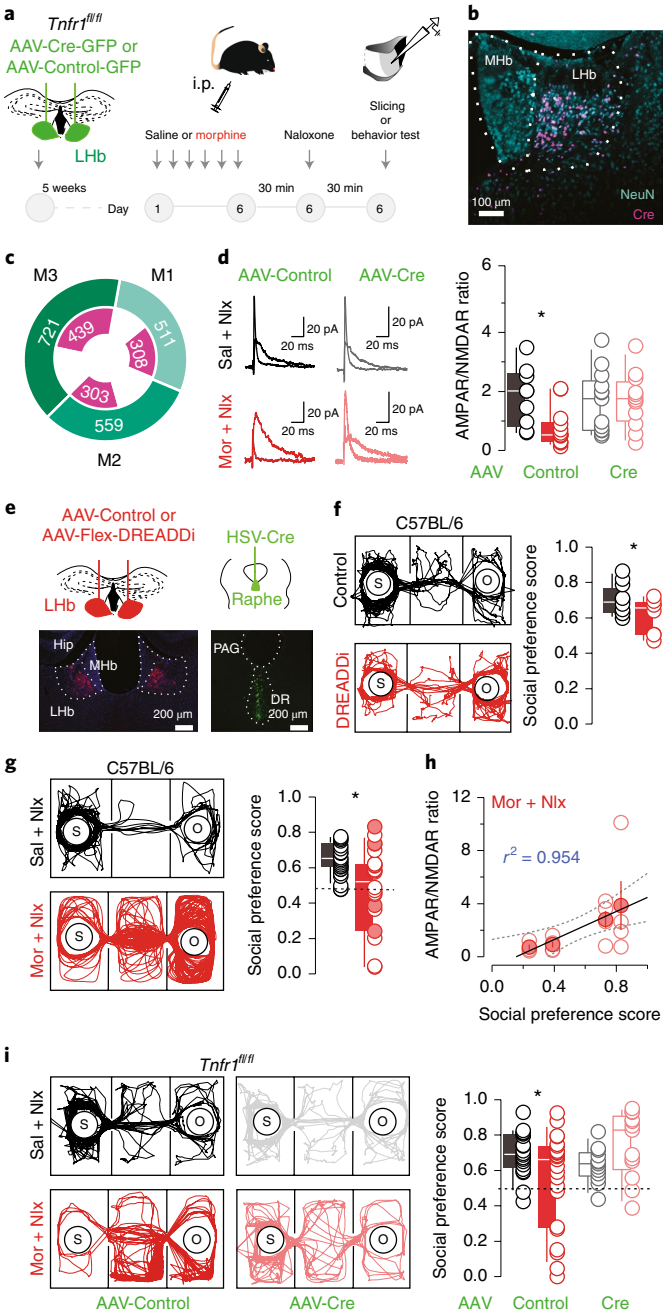

Fig. 3 | TNF-R1 requirements for MORwd-driven synaptic and behavioral adaptations. a, Experimental protocol. **b**,**c**, Image (**b**) and quantification (**c**) of AAV-Cre-infected LHb neurons (magenta) and total LHb neurons (cyan; 3 mice: M1, M2 and M3; NeuN, neuronal marker). **d**, Traces and AMPAR/NMDAR ratios from ^{Med}LHb of AAV-Control-*Tnfr1*$^{fl/fl}$ (saline + naloxone ($n = 2$ mice, 9 cells) versus NP-MORwd ($n = 3$ mice, 14 cells)) or AAV-Cre-*Tnfr1*$^{fl/fl}$ (saline + naloxone ($n = 4$ mice, 13 cells) versus NP-MORwd ($n = 3$ mice, 12 cells)). Interaction factor $F_{(1,44)} = 4.887$, two-way ANOVA, $^{*}P = 0.032$. **e**, AAV-Control or AAV-Flex-DREADDi virus injections in the LHb and HSV-Cre virus in the raphe (DR, dorsal raphe; Hip, hippocampus). **f**, Tracking plots and box and scatter plots of social preference test (SPT) in C57BL/6 mice expressing or not expressing DREADDi in LHb-to-raphe neurons (control virus versus DREADDi; $n = 8$ mice per group, $t_{18} = 2.271$, $^{*}P = 0.043$). **g**, Tracking plots of SPT in C57BL/6 mice. Box and scatter plots showing social preference score (saline + naloxone versus NP-MORwd; $n = 22$ mice per group, $t_{42} = 2.559$, $^{*}P = 0.014$). Filled circles indicate mice used for recordings in **h**. **h**, Correlation of AMPAR/NMDAR ratios and social preference score ($n = 4$ mice, 12 cells; Pearson's $r^2 = 0.954$, $^{*}P = 0.023$. Filled circles represent single cell; open circles represent average per mouse (mean and s.e.m.). **i**, Tracking plots and box and scatter plots of SPT in *Tnfr1*$^{fl/fl}$ mice (AAV-Control: saline + naloxone ($n = 20$ mice), NP-MORwd ($n = 20$ mice); AAV-Cre: saline + naloxone ($n = 13$ mice per group), NP-MORwd ($n = 13$ mice per group). Interaction factor $F_{(1,65)} = 7.20$, two-way ANOVA, $^{**}P = 0.009$. O, object, S, social stimulus. Data are presented as box plots, with 10th and 90th percentiles, median and scatter.

MORwd drives negative symptoms, including social detachment[1]. Similarly, LHb dysfunction contributes to the negative states emerging in addiction; however, the implications of LHb dysfunction with respect to sociability remains poorly addressed. We examined the contribution of the LHb-to-raphe pathway, the locus of MORwd plasticity, in social behavior. We employed an intersectional chemogenetic approach to reduce the efficiency of the LHb-to-raphe projection. This involved the combined retrograde expression of Cre-recombinase (HSV-Cre) in the dorsal raphe with the Cre-dependent expression of hM4Di (rAAV-hM4Di-mCherry, DREADDi) in the LHb (Fig. 3e). Reducing LHb-to-raphe efficiency with clozapine-*N*-oxide diminished social preference (Fig. 3f); this result supports the concept that the LHb contributes to social behaviors.

Next, we recapitulated MORwd-driven reduction in social preference in C57BL/6 mice (Fig. 3g; Supplementary Fig. 4a–d). Slices obtained from mice subjected to MORwd and exhibiting low or high sociability scores showed that ^{Med}LHb AMPAR/NMDAR ratios were positively correlated with the social score (Fig. 3h). This indicates that reduced synaptic strength in the LHb predicts opiate-withdrawal-driven sociability deficits.

Notably, microglia and TNF-α signaling also contributes to social behaviors[12]. Accordingly, MORwd-driven sociability deficits were absent after Cre-dependent LHb *Tnfr1* knockdown (Fig. 3i; Supplementary Fig. 4e–i). This genetic intervention did not affect locomotion (Supplementary Fig. 4j).

We found that MORwd-driven TNF-α release requires neuronal TNF-R1 to reduce AMPAR transmission onto raphe-projecting, medially located, LHb neurons. This ultimately gates MORwd-driven social impairment, a negative symptom typical of opiate withdrawal.

Together with sociability deficits, MORwd also leads to anxiety and hyperalgesia[1]. Since the contribution of the LHb on these two behavioral aspects remains elusive, we cannot rule out that MORwd-driven habenular plasticity is specific for withdrawal-mediated sociability defects.

The TNF-α–TNF-R1 engagement within the LHb represents a previously unidentified mechanism underlying precise cellular and behavioral aspects of MORwd. However, this is consistent with the following data: (1) drugs and drug-withdrawal-mediated modulation of AMPAR transmission partly rely on cytokine signaling[8]; (2) inhibition of TLR4 attenuates MORwd symptoms[13]; and (3) TNFRs contribute to social behaviors[14]. Notably, in pyramidal neurons of the hippocampus and cortex, TNF-α regulates AMPAR surface expression[15,16]. This phenomenon is opposite at striatal synapses where, similar to the LHb, TNF-α application results in decreased AMPAR transmission[8]. This divergence may arise from different TNF-α release dynamics, TNFR expression and signaling, or, alternatively, AMPAR anchoring properties within the LHb. MORwd modifies the morphology of microglia in the LHb. This is, at least partly, consistent with previous findings[8], yet it remains correlative with respect to TNF-α levels. This heightens the need to fill the gap in understanding regarding microglia function and its relationship with TNF-α within the habenula. Overall, while pharmacotherapies targeting pro-inflammatory pathways in substance abuse are missing, our data support cytokine signaling as a cellular pillar for aspects of drug addiction.

MORwd-driven TNF-α-dependent depression of AMPAR transmission occurs at LHb_{Raphe} neurons. From a circuit standpoint, this may provide an 'antisocial' signal that is likely produced through reduced actions onto raphe neuronal populations. This is consistent with the evidence reported here that chemogenetic manipulation of the LHb-to-raphe projection diminishes sociability. In addition, dopamine-containing and serotonin-containing raphe neurons contribute to social behaviors, and medially located LHb neurons monosynaptically connect to the latter[17–19]. Understanding the repercussions of LHb activity onto raphe neuronal subtypes during MORwd remains an important aspect for future investigation.

In conclusion, our data support the concept that cytokine-mediated plasticity participates in opiate-evoked negative symptoms, a mechanism by which the LHb ultimately contributes to the addiction spiral.

Online content

Any methods, additional references, Nature Research reporting summaries, source data, statements of code and data availability and associated accession codes are available at https://doi.org/10.1038/s41593-019-0421-4.

Received: 18 October 2018; Accepted: 7 May 2019;
Published online: 17 June 2019

References

1. Goeldner, C. et al. *Biol. Psychiatry* **69**, 236–244 (2011).
2. Lutz, P. E. et al. *Neuropsychopharmacology* **39**, 2694–2705 (2014).
3. Meye, F. J., Trusel, M., Soiza-Reilly, M. & Mameli, M. *Pharm. Biochem. Behav.* **162**, 87–93 (2017).
4. Margolis, E. B. & Fields, H. L. *PLoS One* **11**, e0159097 (2016).
5. Wang, J. et al. *Neurosci. Lett.* **653**, 64–70 (2017).
6. Valentinova, K. & Mameli, M. *Cell Rep.* **16**, 2298–2307 (2016).
7. Pollak Dorocic, I. et al. *Neuron* **83**, 663–678 (2014).
8. Lewitus, G. M. et al. *Neuron* **90**, 483–491 (2016).
9. Campbell, L. A., Avdoshina, V., Rozzi, S. & Mocchetti, I. *Brain Behav. Immun.* **34**, 130–140 (2013).
10. Michaud, M. et al. *J. Am. Med. Dir. Assoc.* **14**, 877–882 (2013).
11. Probert, L. *Neuroscience* **302**, 2–22 (2015).
12. Nie, X. et al. *Neuron* **99**, 464–479.e7 (2018).
13. Hutchinson, M. R. et al. *Brain Behav. Immun.* **22**, 1178–1189 (2008).
14. Patel, A., Siegel, A. & Zalcman, S. S. *Brain Behav. Immun.* **24**, 1276–1280 (2010).
15. He, P., Liu, Q., Wu, J. & Shen, Y. *FASEB J.* **26**, 334–345 (2012).
16. Stellwagen, D., Beattie, E. C., Seo, J. Y. & Malenka, R. C. *J. Neurosci.* **25**, 3219–3228 (2005).
17. Kane, M. J. et al. *PLoS One* **7**, e48975 (2012).
18. Lecca, S. et al. *eLife* **6**, e30697 (2017).
19. Matthews, G. A. et al. *Cell* **164**, 617–631 (2016).

Acknowledgements

The authors thank F.J. Meye and the Mameli Laboratory for comments on the manuscript. This work was supported by funds from the ERC StG SalienSy 335333 and the SNSF (31003A) to M.M. They also thank D. Szymkowski for the donation of XENP1595, and G. Kollias and H. Strubbe for the use and breeding of the *Tnfr1*$^{fl/fl}$ mouse line.

Author contributions

K.V., A.T. and M.M. performed and analyzed the ex vivo recordings and behavior experiments. A.L.L. and J.A.C. contributed to the ex vivo recordings. M.T., I.M. and L.M. performed the molecular biology experiments. C.B. and S.T. provided support for the behavioral experiments. A.M. and R.C.P. analyzed the microglia morphology. A.V. provided conceptual and experimental input related to TNF-α signaling and the *Tnfr1*$^{fl/fl}$ mice. K.V. and M.M. conceptualized, designed the study and wrote the manuscript.

Competing interests

The authors declare no competing interests.

Additional information

Supplementary information is available for this paper at https://doi.org/10.1038/s41593-019-0421-4.

Reprints and permissions information is available at www.nature.com/reprints.

Correspondence and requests for materials should be addressed to M.M.

Journal peer review information: *Nature Neuroscience* thanks David Stellwagen and the other, anonymous, reviewer(s) for their contribution to the peer review of this work.

Publisher's note: Springer Nature remains neutral with regard to jurisdictional claims in published maps and institutional affiliations.

Methods

Animals and morphine treatment. C57BL/6J wild-type mice (male) and 129-Tnfrsf1atm3GkI mice (male and female, referred to as *Tnfr1*$^{fl/fl}$) aged 4–10 weeks were group-housed (three to five per cage) on a 12–12 h light cycle (lights on at 7:00) with food and water ad libitum. All procedures aimed to fulfill the criterion of the 3Rs and were approved by the Veterinary Offices of Vaud (Switzerland; license VD3172). Part of the current study was carried out at the Institut du Fer a Moulin, Paris, France, and experiments were performed in accordance with the guidelines of the French Agriculture and Forestry Ministry. MORwd was either precipitated with naloxone or was induced naturally. For naloxone-precipitated MORwd, mice were subjected to intraperitoneal (i.p.) morphine (20 mg per kg, Cantonal Hospital of Lausanne, Switzerland) or saline injections (saline and morphine-treated animals were housed together) for 6 days. On day 6, the last morphine or saline injection was given in a separate cage. After 30 min, the animals then received an i.p. injection of naloxone hydrochloride (2 mg per kg, Abcam). MORwd-dependence symptoms were allowed to develop in the following 30 min, after which the mice were either killed for ex vivo electrophysiological recordings or were subjected to behavioral tests.

For spontaneous withdrawal, mice were treated with morphine or saline for 6 days and were killed for recording experiments 10–13, 20 or 30 days after the last injection. For recordings in morphine-treated animals not in withdrawal, mice were killed 1 h after the last morphine injection on day 6. To assess for the involvement of TNF-α in MORwd plasticity, some of the animals were subjected to an i.p. injection of MPLA (10 µg, dissolved in dimethylsulfoxide (DMSO) and saline) or saline (containing the same amount of DMSO as control)[8] instead of naloxone 30 min after the last morphine injection on day 6. Another group of the animals received an i.p. injection (30 mg per kg) of a dominant-negative peptide blocking the soluble form of TNF-α (XENP1595, Xencor)[8] 1 h before the last morphine or saline injection on day 6. Thirty minutes after the morphine or saline injection, these animals received naloxone and were killed for recording experiments as described above. No statistical methods were used to predetermine sample sizes, but our sample sizes were similar to previously reported numbers[6].

Surgery. Animals of at least 4 weeks of age were anesthetized with an i.p. injection of ketamine (150 mg per kg)/xylazine (100 mg per kg; veterinary office the University of Lausanne) and were placed on a stereotactic frame (Kopf). Bilateral injections of 200–400 nl were performed through a glass needle at a rate of approximately 100 nl min^{-1}. The injection pipette was withdrawn from the brain 10 min after the infusion. Retrobeads (Lumafluor) were infused into the dorsal raphe nucleus (anterior–posterior (AP): −3.5 mm; medial–lateral (ML): 0 mm; dorsal–ventral (DV): −3.8 mm) or the VTA (AP: −2.4 mm; ML: ±0.65 mm; DV: −4.9 mm) of C57BL/6 mice. *Tnfr1*$^{fl/fl}$ mice were injected with either rAAV2-hSyn-eGFP or rAAV2-hSyn or CMV-Cre-eGFP into the LHb (AP: −1.35 mm; ML: ±0.45 mm; DV: −3.00 mm). In another set of experiments, C57BL/6 mice were injected with a herpes simplex virus-derived hEF1α-Cre vector (MGA Gene Delivery Technology Core) in the raphe nucleus and with rAAV-DJ-EF1α-Flex-hM4D(Gi)-mCherry (Gene Vector and Virus Core, Stanford Medicine) in the LHb. Animals were allowed to recover for about 5–7 days after injection of the retrobeads or 5 weeks after viral infusion before being treated with morphine or saline. The injection sites were carefully examined during all electrophysiology experiments, and only animals with correct injections were used for recordings. Similarly, for behavioral studies, only animals with correct injection sites were included in the analyses. Brain slices obtained from mice injected with retrobeads or viruses were directly examined under an epifluorescence microscope.

Ex vivo electrophysiology. Animals aged 5 weeks were anesthetized with an injection of ketamine (150 mg kg)/ xylazine (100 mg/kg) for preparation of LHb-containing brain slices. Slicing was done in bubbled ice-cold 95% O_2/5% CO_2-equilibrated solution containing (in mM): 110 choline chloride, 25 glucose, 25 $NaHCO_3$, 7 $MgCl_2$, 116 ascorbic acid, 3.1 sodium pyruvate, 2.5 KCl, 1.25 NaH_2PO_4, and 0.5 $CaCl_2$. Coronal slices (25 µm) were prepared and transferred for 10 min to warmed solution (34 °C) of identical composition before they were stored at ~22 °C in 95% O_2/5% CO_2-equilibrated artificial cerebrospinal fluid containing (in mM): 124 NaCl, 26.2 $NaHCO_3$, 11 glucose, 2.5 KCl, 2.5 $CaCl_2$,1.3 $MgCl_2$, and 1 NaH_2PO_4. Recordings (flow rate of 2.5 ml min^{-1}) were obtained using an Olympus-BX51 microscope (Olympus) at 32 °C. Patch-clamp experiments were performed using borosilicate glass pipettes (2.7–4 MΩ; Phymep). Currents were amplified, filtered at 5 kHz and digitized at 20 kHz (Multiclamp 200B; Molecular Devices). Data were acquired using Igor Pro with NIDAQ tools (Wavemetrics). Access resistance was monitored by a step of −4 mV (0.1 Hz). Experiments were discarded if the access resistance increased by more than 20%. All recordings were made in voltage-clamp configuration. Spontaneous EPSCs were recorded either in the ^{Lat}LHb or ^{Med}LHb at −60 mV in the presence of picrotoxin (100 µM; Abcam) and APV ((2R)-amino-5-phosphonovaleric acid, 50 µM, Abcam). The internal solution contained (in mM): 130 CsCl, 4 NaCl, 2 $MgCl_2$, 1.1 ethylene glycol tetraacetic acid (EGTA), 5 HEPES buffer, 2 ATP-Na_2, 5 sodium creatine-phosphate, 0.6 GTP-Na_3, and 0.1 spermine. The liquid junction potential was −3 mV and was not compensated. For determining the AMPAR/NMDAR ratios, EPSCs were evoked through glass electrodes placed ~200 µm from the recording site using an AMPI ISO-Flex stimulator. A mixture of AMPA and NMDA currents were evoked at +40 mV (in the presence of picrotoxin). The two components were pharmacologically isolated by adding APV in the recording solution and by subsequent identification of the individual currents via digital subtraction. For glutamate uncaging experiments, MNI-glutamate (4-methoxy-7-nitroindolinyl-caged L-glutamate, 500 µM; Tocris) was added to the recording solution. Uncaging was obtained via a single-path photolysis head (Prairie Technologies) connected to a solid-state laser (Rapp Optolectronics; 405 nm, duration 1 ms, diameter 3–5 µm, 250–300 µm from the soma). AMPAR/NMDAR ratios in uncaging experiments were calculated as follows: AMPA-EPSCs at −60 mV/NMDA-EPSCs at +40 mV. The individual components were identified as previously described[6], using the late component of the EPSC at 30 ms after the onset. The rectification index was computed by recording AMPA-EPSCs at −70 mV and +40 mV and was calculated as follows: (AMPA-EPSC at −70/AMPA-EPSC at +40)/1.75. To assess presynaptic release properties, trains of AMPAR-EPSCs were evoked using an extracellular-stimulating electrode (5 pulses at 5 Hz, 10 Hz and 20 Hz). The amplitudes of EPSC trains were normalized to the amplitude of the first pulse. When indicated, recordings were performed from retrogradely labeled and fluorescently identified LHb neurons. Some experiments were performed in LHb-containing slices incubated for a minimum of 1 h with exogenous TNF-α (100 ng ml^{-1}). To test the effect of MPLA on AMPAR transmission, neurons were patched either in the ^{Lat}LHb or the ^{Med}LHb, and EPSCs were evoked with extracellular stimulation. Following a 10-min baseline, MPLA (1 µg ml^{-1}) was added to the recording solution and EPSCs were recorded for a minimum of 40 min. Some experiments were performed in the presence of the TNF-α dominant-negative peptide XENP1595 (6 mg 1 ml^{-1}; Xencor) in the recording solution.

Non-stationary fluctuation analysis. A peak-scaled non-stationary fluctuation analysis was performed on sEPSCs (number of events, 70–250) (Synaptosoft). sEPSCs were selected by applying the following criteria: fast rise time alignment, stable baseline holding current and the absence of spurious fluctuations during the sEPSC decay. The variance–amplitude relationship of sEPSC decay was plotted and fitted with the equation $\sigma^2 = iI - I^2/N + \sigma_b^2$ (where i is the mean single-channel AMPA current, I is the mean current, N is the number of channels activated at the peak, N = mean amplitude/i; and σ_b^2 is the baseline variance). i was estimated as the slope of the linear fit of the first portion of the parabola of the fitted sEPSC decay. The goodness-of-fit was assessed with a least-squares algorithm. The unitary current was converted into conductance based on the reversal potential of evoked EPSCs (~0 mV) and the holding potential (−60 mV). Conductance and average EPSC amplitude, mean rise time, mean decay time, access resistance or background noise variance had no correlation ($P > 0.4$).

Histology and immunofluorescence. Mice were injected daily with saline or morphine (20 mg per kg, i.p.) for 6 days. Some mice were left to develop spontaneous withdrawal, while others received naloxone (2 mg per kg, i.p.) injection 30 min after the last saline or morphine injection on day 6. After 10–13 days of spontaneous withdrawal or 30 min after naloxone injection, mice were anesthetized and perfused with cold 4% paraformaldehyde (PFA) in PBS. The brains were extracted, post-fixed in 4% PFA in PBS and then incubated in 30% sucrose in PBS until they sank. Slices (30 µm) were cut using a cryostat and stored in PBS containing 0.02% NaN_3 for future analyses. For immunofluorescence, the slices were incubated for 2 h in blocking buffer (5% NGS (normal goat serum), 0.3% Triton-X in PBS) and then incubated for 24 h at 4 °C with the primary antibody solution (mouse anti-TNF-α antibody, 1:100 in blocking buffer; ab1793, Abcam)[8]. After extensive rinses, the secondary antibody was applied (goat anti-mouse IgG-conjugated Alexa 488, Invitrogen, 1:400 in blocking buffer, 24 h at 4 °C). The slices were then incubated in 4,6-diamidino-2-phenylindole (DAPI) (1:400 solution in PBS), extensively rinsed, mounted on glass slides with Pro-Long Gold Antifade Reagent (Invitrogen) and coverslipped. Images were acquired with an epifluorescence microscope with a ×20 objective (AxioVision, Zeiss) using the same parameters for all the samples. The images were analyzed and processed using the software ImageJ. Optical density was measured on the whole LHb area and normalized against the neighboring thalamus using the following equation: LHb – thalamus/(LHb + thalamus). A total of three to six slices distributed in the rostrocaudal axis were analyzed per animal (eight morphine-treated, seven saline-treated).

Microglia analysis. Mice were anesthetized and perfused with cold 4% PFA in PBS. The brains were extracted, post-fixed in 4% PFA in PBS and then incubated in 30% sucrose in PBS until they sank. Slices (30 µm) were cut using a cryostat and stored in PBS containing 0.02% NaN_3 for future analyses. Brain sections were permeabilized at room temperature in 0.5% Triton X-100 (Sigma) for 1 h at room temperature, followed by blocking in 2% BSA 0.5% Triton X-100 for 1 h at room temperature and then overnight incubation with primary antibody (IBA1, 1:1,000 (cat. no. 019–19741, Wako Chemicals) and CD68, 1:400 (cat. no. MCA1957, Bio-Rad))[8] at 4 °C. After washing, sections were incubated for 2 h at room temperature with Alexa-fluorophore-conjugated secondary antibodies (Invitrogen) and counterstained with DAPI (Invitrogen).

Confocal microscopy was performed using a TCS-SP5 (Leica) Laser Scanning System with a ×20 dry objective. Images were processed and analyzed using the software Fiji or Imaris (Bitplane) as appropriate. Imaris was used for three-dimensional (3D) rendering of confocal images for quantification of volumes.

For density analyses, for each acquisition, the DAPI channel was max-projected and the ^{Med}LHb and ^{Lat}LHb were manually drawn as regions of interest. Then, stacks ranging from 15 µm to 20 µm in thickness, with a *z*-step size of 1 µm, were processed as follows: IBA1 and DAPI channels were thresholded in Fiji and multiplied to each other for each stack, with the image calculator function. The resulting thresholded stack was max-projected, and the microglia nuclei were counted using the function Analyze Particle.

For cell soma size and IBA1 intensity analyses, each acquisition was max-projected, and the contour of cell somata in the ^{Med}LHb were manually drawn based on the immunoreactivity of IBA1 and then analyzed per size in µm^2 and intensity.

3D imaging analysis was performed using Imaris and applying recorded algorithms (fixed thresholds for signal intensity) to all the images of the same experiment to produce unbiased signal quantification. In each experiment, one brain slice per animal ($n=4$) per group was acquired. The microglial cell volume and the volume of phagocytic structures were reconstructed based on the absolute intensity of IBA1 and CD68 signals, respectively. The volume of CD68 was then normalized to the IBA1 volume to take in account the cell size.

Behavior. *Social preference test.* A three-chambered social preference test was used. The arena was a rectangular Plexiglas (60 × 40 × 22 cm) (Ugo Basile) divided into three chambers. The walls of the center chamber had doors to allow free access to all compartments. The luminosity was around 10 lux. Thirty minutes after naloxone injection, each mouse was placed in the arena for a habituation period of 10 min and was allowed to freely explore the whole empty arena. The social preference test was performed immediately after the end of the habituation period: two enclosures with vertical bars were placed in the middle of the two lateral compartments, while the central chamber remained empty. One enclosure was empty (serving as an inanimate object), whereas the other contained a social stimulus (an unfamiliar juvenile mouse 25 ± 1 days old). The enclosures allowed visual, auditory, olfactory and tactile contact between the experimental mice and the social stimuli mice. The juvenile mice in the enclosures were habituated to the apparatus and the enclosures for 3 days before the experiment, and each one of them served as a social stimulus for no more than 2 experimental mice (at least 6 weeks old). The test lasted 10 min, whereby the experimental mice were allowed to freely explore the apparatus and the enclosures. The position of the empty and juvenile-containing enclosures alternated and was counterbalanced for each trial to avoid any bias effects. Every session was video-tracked and recorded using Ethovision XT (Noldus) or AnyMaze (Stoelting), which provided an automated recording of the entries and time spent in the compartments, the distance moved and the velocity. The time spent in each chamber was assessed and then used to determine the preference score for the social compartment as compared to the object compartment (social/(social + object)). The arena was cleaned with 1% acetic acid solution and dried between trials.

Analyses and statistics. Animals were randomly assigned to experimental groups. Compiled data are reported and presented as whisker box plots (the upper and lower whiskers representing the 90th and 10th percentiles, respectively, and the upper and lower boxes representing the 75th and 25th percentiles, respectively, and the horizontal line representing the median) or the mean ± s.e.m., with single data points plotted (single cell for electrophysiology and single animal for behavioral experiments). Animals or data points were not excluded unless stated, and a normality test was applied. Data collection and analyses were not performed blinded to the conditions of the experiments. When applicable, statistical tests were paired or unpaired *t*-test and one-way or two-way analysis of variance (ANOVA). Significance for correlations was obtained applying Pearson's estimates. Testing was always performed two-tailed with $\alpha=0.05$. More information on the methods and analyses can be found in the Nature Research Reporting Summary.

Reporting Summary. Further information on research design is available in the Nature Research Reporting Summary linked to this article.

Data availability

The datasets generated during and/or analyzed during the current study are available from the corresponding author upon reasonable request.

nature research

Corresponding author(s): Manuel Mameli

Last updated by author(s): April 16 2019

Reporting Summary

Nature Research wishes to improve the reproducibility of the work that we publish. This form provides structure for consistency and transparency in reporting. For further information on Nature Research policies, see Authors & Referees and the Editorial Policy Checklist.

Statistics

For all statistical analyses, confirm that the following items are present in the figure legend, table legend, main text, or Methods section.

n/a	Confirmed	
☐	☒	The exact sample size (*n*) for each experimental group/condition, given as a discrete number and unit of measurement
☐	☒	A statement on whether measurements were taken from distinct samples or whether the same sample was measured repeatedly
☐	☒	The statistical test(s) used AND whether they are one- or two-sided *Only common tests should be described solely by name; describe more complex techniques in the Methods section.*
☒	☐	A description of all covariates tested
☐	☒	A description of any assumptions or corrections, such as tests of normality and adjustment for multiple comparisons
☒	☐	A full description of the statistical parameters including central tendency (e.g. means) or other basic estimates (e.g. regression coefficient) AND variation (e.g. standard deviation) or associated estimates of uncertainty (e.g. confidence intervals)
☐	☒	For null hypothesis testing, the test statistic (e.g. *F*, *t*, *r*) with confidence intervals, effect sizes, degrees of freedom and *P* value noted *Give P values as exact values whenever suitable.*
☒	☐	For Bayesian analysis, information on the choice of priors and Markov chain Monte Carlo settings
☒	☐	For hierarchical and complex designs, identification of the appropriate level for tests and full reporting of outcomes
☐	☒	Estimates of effect sizes (e.g. Cohen's *d*, Pearson's *r*), indicating how they were calculated

Our web collection on statistics for biologists contains articles on many of the points above.

Software and code

Policy information about availability of computer code

Data collection	Data were acquired with commercially available softwares indicated in the Methods section: IGOR Wavemetrics, Anymaze Stoelting, Ethovision XT, AxioVision Zeiss.
Data analysis	Data were analyzed with commercially available softwares indicated in the Methods section: IGOR Wavemetrics, Anymaze Stoelting, Graphpad Prism, Imaris, ImageJ and Fiji Plugin.

For manuscripts utilizing custom algorithms or software that are central to the research but not yet described in published literature, software must be made available to editors/reviewers. We strongly encourage code deposition in a community repository (e.g. GitHub). See the Nature Research guidelines for submitting code & software for further information.

Data

Policy information about availability of data

All manuscripts must include a data availability statement. This statement should provide the following information, where applicable:

- Accession codes, unique identifiers, or web links for publicly available datasets
- A list of figures that have associated raw data
- A description of any restrictions on data availability

The data sets generated during and/or analysed during the current study are available from the corresponding author on reasonable request.

Field-specific reporting

Please select the one below that is the best fit for your research. If you are not sure, read the appropriate sections before making your selection.

☒ Life sciences ☐ Behavioural & social sciences ☐ Ecological, evolutionary & environmental sciences

Life sciences study design

All studies must disclose on these points even when the disclosure is negative.

Sample size	Sample size was based on the based of previous results obtained in the laboratory. This is based on the specific variance observed in the region of interest studied. This is now stated in the methods with a reference of our previously published work
Data exclusions	The methods include an exclusion criteria related to the quality of the recording (access resistance) which reflects the physiological parameters of recorded neurons and site of injection in the surgery section which was always controlled.
Replication	Each experiment was replicated at minimum three times.
Randomization	Animals were randomly assigned to experimental groups.
Blinding	The operators were not blind of the experimental groups in the case of ex-vivo recordings. Double control with the PI and peers in the lab, as well cross controlled recordings within the laboratory allow the operator to not be blind of the experimental condition with no risk in biasing the result. The experimenters were blind for the analysis of the behavioral and immunolabeling experiments.

Reporting for specific materials, systems and methods

We require information from authors about some types of materials, experimental systems and methods used in many studies. Here, indicate whether each material, system or method listed is relevant to your study. If you are not sure if a list item applies to your research, read the appropriate section before selecting a response.

Materials & experimental systems

n/a	Involved in the study
☐	☒ Antibodies
☒	☐ Eukaryotic cell lines
☒	☐ Palaeontology
☐	☒ Animals and other organisms
☒	☐ Human research participants
☒	☐ Clinical data

Methods

n/a	Involved in the study
☒	☐ ChIP-seq
☒	☐ Flow cytometry
☒	☐ MRI-based neuroimaging

Antibodies

Antibodies used	mouse anti-TNFα antibody, ab1793, clone number 52B83, Lot#GR66942 Abcam, 1:100 in blocking buffer goat anti-mouse IgG-conjugated Alexa 488, Catalog # A28175, Lot#1874804 (No clone# available), Invitrogen, 1:400 in blocking buffer, 24h at 4°C Iba1 1:1000, Wako Chemicals, Cat. 019-1974 Clone NCNP24, Lot. PTN5930 CD68 1:400, Bio-Rad Cat. MCA1957, Clone FA-11, Lot. 1807
Validation	mouse anti-TNFα antibody validation was based on published results from Lewitus et al., 2016. This is now stated in the manuscript, methods session. Iba1 and CD68 validation was based on previous publication including Lewitus et al., 2016 and Paolicelli et al., 2011. Dr. Paolicelli is an authors of this manuscript therefore the validation of these antibodies were based on her experience in the field. The entire validation reported here is valid for the species used in this study which is mice.

Animals and other organisms

Policy information about studies involving animals; ARRIVE guidelines recommended for reporting animal research

Laboratory animals	C57Bl/6J wild-type (male) and 129-Tnfrsf1atm3Gkl (male and female, referred as TNF-R1fl/f) mice of 4–10 weeks were used
Wild animals	This study did not involve the use of wild animals
Field-collected samples	This study did not involve the use of field collected samples
Ethics oversight	All procedures were approved by the Veterinary Offices of Vaud (Switzerland; License VD3172)

Note that full information on the approval of the study protocol must also be provided in the manuscript.

nature neuroscience

SUPPLEMENTARY INFORMATION

https://doi.org/10.1038/s41593-019-0421-4

In the format provided by the authors and unedited.

Morphine withdrawal recruits lateral habenula cytokine signaling to reduce synaptic excitation and sociability

Kristina Valentinova[1,2,6], Anna Tchenio[1,6], Massimo Trusel[1], Joseph A. Clerke[1], Arnaud L. Lalive[1], Stamatina Tzanoulinou[3], Alessandro Matera[4], Imane Moutkine[5], Luc Maroteaux[5], Rosa C. Paolicelli[4], Andrea Volterra[1], Camilla Bellone[3] and Manuel Mameli[1,5]*

[1]The Department of Fundamental Neuroscience, The University of Lausanne, Lausanne, Switzerland. [2]Department of Physiology, The University of Bern, Bern, Switzerland. [3]Department of Basic Neuroscience, The University of Geneva, Geneva, Switzerland. [4]Department of Physiology, The University of Lausanne, Lausanne, Switzerland. [5]Inserm, UMR-S 839, Paris, France. [6]These authors contributed equally: Kristina Valentinova and Anna Tchenio.
*e-mail: manuel.mameli@unil.ch

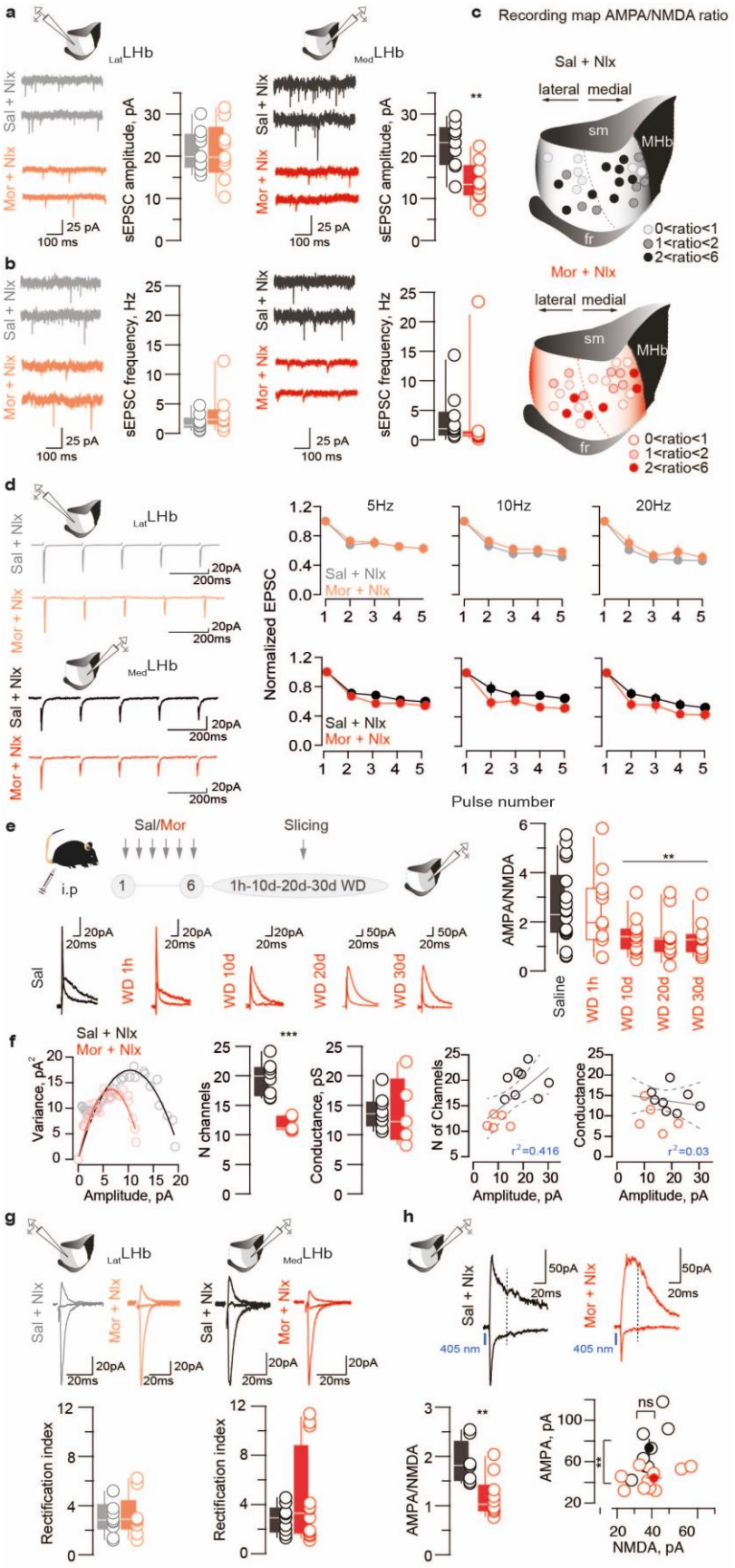

Supplementary Figure 1

MORwd induces postsynaptic depression of AMPAR-mediated neurotransmission in medial LHb.

(a) Left: sample traces, box and scatter plots of sEPSCs amplitudes recorded in ^{Lat}LHb (saline+naloxone ($n_{cells/mice}$=9/3; gray) versus NP-MORwd ($n_{cells/mice}$=9/4; orange), two-sided t-test,, t_{16}=0.098, P=0.923). Right: same but sEPSCs were recorded in ^{Med}LHb (saline+naloxone ($n_{cells/mice}$=9/4; black) versus NP-MORwd ($n_{cells/mice}$=9/5; red), two-sided t-test, t_{16}=3.493, **P=0.003). (b) Left: sample traces, box and scatter plots of sEPSCs frequencies recorded in ^{Lat}LHb (saline+naloxone ($n_{cells/mice}$=9/4, gray) versus NP-MORwd ($n_{cells/mice}$=9/4, orange), two-sided t-test,, t_{16}=1.331, P=0.202). Right: same but sEPSCs were recorded in ^{Med}LHb (saline+naloxone ($n_{cells/mice}$=9/5, black) versus NP-MORwd ($n_{cells/mice}$=9/4,red), two-sided t-test, t_{16}=0.161, P=0.874). (c) Recording map color-coded for the value of AMPAR:NMDAR ratios recorded throughout the LHb. Lighter colors indicate smaller AMPAR:NMDAR ratios, while darker colors represent high AMPAR:NMDAR ratio. (d) Top: Sample traces and normalized EPSC versus pulse number plots recorded at 5, 10 and 20 Hz in ^{Lat}LHb (saline+naloxone ($n_{cells/mice}$=10/2, gray) versus NP-MORwd ($n_{cells/mice}$=10/3, orange), 5Hz interaction factor $F_{(4,\ 36)}$=0.227, P=0.921; 10Hz interaction factor $F_{(4,36)}$=0.251, P=0.907; 20Hz interaction factor $F_{(4,36)}$=0.573, P=0.683 two-way ANOVA Repeated Measures). Bottom: same but in ^{Med}LHb ($n_{cells/mice}$=10/3, saline+naloxone (black) versus NP-MORwd (red), 5Hz interaction factor $F_{(4,36)}$=0.1.183, P=0.334; 10Hz interaction factor $F_{(4,36)}$=1.171, P=0.34; 20Hz interaction factor $F_{(4,36)}$=0.88, P=0.485 two-way ANOVA Repeated Measures). (e) Spontaneous withdrawal timeline. AMPAR:NMDAR ratios from ^{Med}LHb 1 hour, 10, 20 or 30 days post-saline or MOR (saline 1 hour and 10 days pooled ($n_{mice/cells}$=6/22; black) versus MORwd 1 hour ($n_{mice/cells}$=5/11; open red) and MOR 10 ($n_{mice/cells}$=3/12), 20 ($n_{mice/cells}$=3/11) and 30 days withdrawal ($n_{mice/cells}$=3/11; red), $F_{(4,\ 62)}$=3.90 one-way ANOVA, **P=0.007). (f) Example of peak-scaled NSFA of ^{Med}LHb neurons in the saline- and NP-MORwd group. Pooled data for conductance (γ) and number of channels (*N*) open at the peak together with amplitude versus N of channels and conductance plots (Saline+naloxone, $n_{cells/mice}$=5/4; MORwd, $n_{cells/mice}$=8/5; N of channels, two-sided t-test, t_{11}=5.67, ***P=0.0001, $r^2_{(N\text{-}Channels)}$ = 0.416; *P=0.017; Conductance, t_{11}=0.006, P=0.99, $r^2_{(Conductance)}$ = 0.03, P=0.55). (g) Left: sample traces, box and scatter plots for rectification index calculated from AMPAR EPSCs recorded at -70, 0 and 40 mV in ^{Lat}LH (saline+naloxone ($n_{cells/mice}$=9/7, gray) versus NP-MORwd ($n_{cells/mice}$=10/7, orange), two-sided t-test, t_{17}=0.210, P=0.836). Right same but recordings in ^{Med}LHb (saline+naloxone ($n_{cells/mice}$=12/8, black) versus NP- MORwd ($n_{cells/mice}$=9/5, red), two-sided t-test, t_{19}=1.292, P=0.212). (h) Sample traces, box and scatter plots of AMPAR:NMDAR ratios recorded in ^{Med}LHb via 405 nm laser-assisted uncaging of MNI-glutamate,

500μM (saline+naloxone ($n_{cells/mice}$=8/2, black) versus NP-MORwd ($n_{cells/mice}$=10/3, red), two-sided t-test, t_{16}=3.521, **P=0.003). Bottom right: Absolute AMPAR versus absolute NMDAR uncaging-evoked current plots from saline+naloxone (open black circles) or NP-MORwd mice (open red circles). The mean with S.E.M. AMPA and NMDA currents are shown with black and red filled circles for saline versus MORwd respectively (saline+naloxone versus NP-MORwd: AMPA, two-sided t-test, t_{16}=3.536, **P=0.003; NMDA, two-sided t-test, t_{16}=0.195, P=0.848). Data are presented as box plots 10-90 percentiles and scatter.

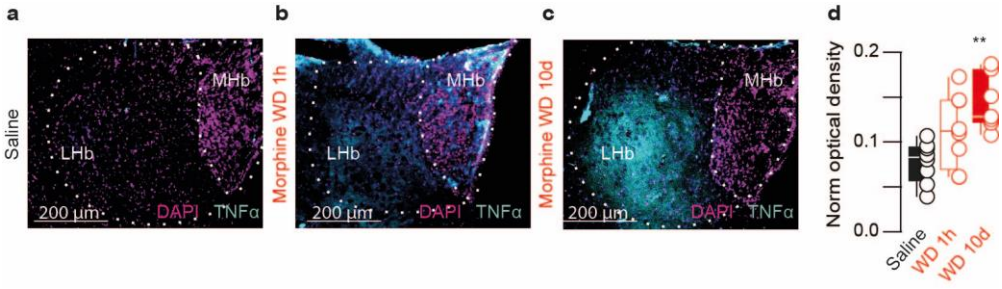

Supplementary Figure 2

TNFα levels in the LHb increase following spontaneous MORwd

(a) TNFα (cyan) and DAPI (magenta) immunostaining in slices from saline-treated, (b) MOR-treated (sacrificed 1 hour after the last MOR injection) and (c) animals in spontaneous MORwd (10-13 days post last MOR injection). (d) Normalized LHb TNFα optical density in saline (black), MOR (open red) and spontaneous MORwd (red) (n_{mice}=8, saline (black) versus MOR (open red) versus spontaneous MORwd (red), $F_{(2,20)}$=7.7 one-way ANOVA, **P=0.003). Data are presented as box plots 10-90 percentiles with median and scatter.

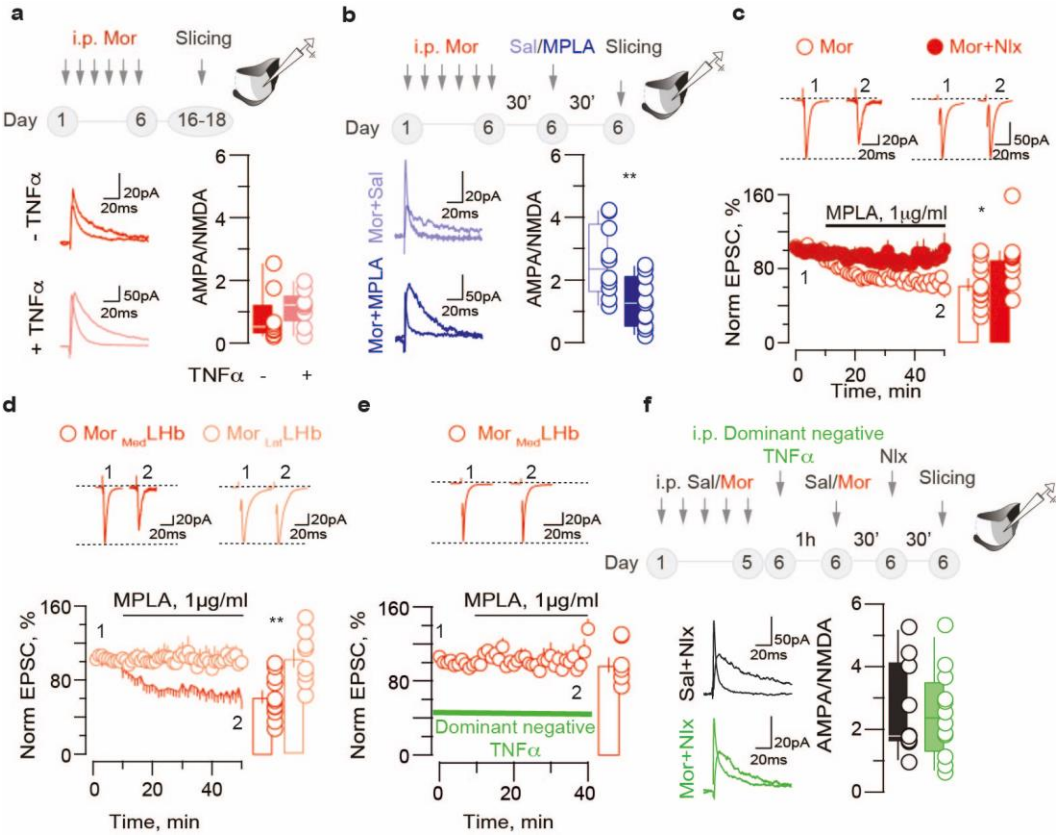

Supplementary Figure 3

TNFα signaling is necessary and sufficient for MORwd-induced plasticity

(a) Spontaneous MORwd protocol, sample traces, box and scatter plots for AMPAR:NMDAR ratios recorded in ^{Med}LHb slices incubated with (+) or without (–) exogenous TNFα from spontaneous MORwd mice (10 days). (MORwd -TNFα (red) versus +TNFα (pink), $n_{cells/mice}$=9/4, two-sided t-test, t_{16}=0.986, P=0.339). (b) ^{Med}LHb AMPAR:NMDAR ratios from saline or MPLA-injected MOR-treated mice (MOR/saline ($n_{mice/cells}$=3/10; shaded blue) versus MOR/MPLA ($n_{mice/cells}$=4/11; dark blue), two-sided t-test, t_{19}=3.070, **P=0.006). (c) Sample traces, time versus amplitude plot and bar graphs showing the effect of MPLA (1□g/ml) on AMPAR-EPSCs (MOR ($n_{mice/cells}$=4/11 ; 63.93 ± 7.06%; open red), NP-MORwd ($n_{mice/cells}$=3/10 cells; 91.63 ± 8.86%; filled red), MOR versus NP-MORwd, two-sided t-test, t_{19}=2.419, *P=0.026). Data of this panel are represented as mean and sem. (d) Sample traces, time versus amplitude plot and bar graphs showing the effect of MPLA (1µg/ml) on evoked AMPAR-EPSCs (baseline (1) vs 30 min post-MPLA (2)) recorded in ^{Lat}LHb (open orange) or ^{Med}LHb (open red) in slices obtained from morphine-treated animals ($n_{cells/mice}$=8/4, morphine ^{Lat}LHb 103.98 ± 10.13; $n_{cells/mice}$=11/5, morphine ^{Med}LHb 63.31 ± 7.06%; morphine ^{Lat}LHb versus morphine ^{Med}LHb, two-sided t-test, t_{17}=3.406, **P=0.003). Note that the data set for ^{Med}LHb is the same as in c and is used for comparison. Data are presented as mean and SEM. (e) Sample traces, time versus amplitude plot and bar graph showing the effect of MPLA (1µg/ml) on evoked AMPAR-EPSCs (baseline (1) vs 30 min post-MPLA (2)) in the presence of TNFα dominant negative peptide (XENP1595, 6mg/1ml) recorded in ^{Med}LHb in slices obtained from morphine-treated animals ($n_{cells/mice}$=7/2, 98.88 ± 8.23 %, two-sided t-test, t-test, t_6=0.073, P=0.944). Data are presented with mean and SEM. (f) NP-MORwd protocol with dominant-negative TNFα (XENP1595, 30mg/kg) pretreatment, sample traces, box and scatter plots for AMPAR:NMDAR ratios recorded in ^{Med}LHb (saline+naloxone ($n_{cells/mice}$=10/3, black) versus NP-MORwd ($n_{cells/mice}$=12/3, green), two-sided t-test, t-test, t_{20}=0.165, P=0.871). Data are presented as box plots 10-90 percentiles and scatter.

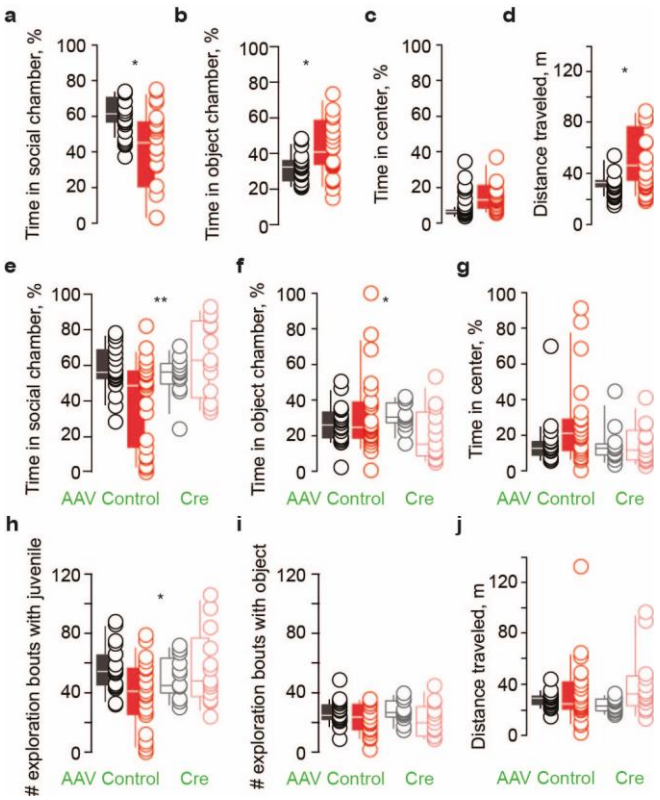

Supplementary Figure 4

Behavioral assessment of MORwd

(a) Box and scatter plot showing the percent time spent in the compartment containing the social stimulus for C57Bl6 mice (N=22 mice/group, saline+naloxone (black) versus NP-MORwd (red), two-sided t-test, t_{42}=2.401, *P=0.021). (b) Box and scatter plot showing the percent time spent in the compartment containing the object stimulus for C57Bl6 mice (N=22 mice/group, saline+naloxone (black) versus NP-MORwd (red), two-sided t-test, t_{42}=2.465, *P=0.02). (c) Box and scatter plot showing the percent time spent in the central compartment for C57Bl6 mice (N=22 mice/group, saline+naloxone (black) versus NP-MORwd (red), two-sided t-test, t_{42}=1.186, P=0.242). (d) Box and scatter plot showing locomotor activity during social preference test for C57Bl6 mice (N=22 mice/group, saline+naloxone (black) versus NP-MORwd (red), two-sided t-test, t_{42}=2.621, *P=0.012). (e) Box and scatter plot showing the percent time spent in the compartment containing the social stimulus for TNF-R1fl/fl mice (AAV-Control: 58.02 ± 2.96% saline+naloxone (N_{mice}=20, black) versus 40.45 ± 5.08% NP-MORwd (N_{mice}=23, red); AAV-Cre: 54.41 ± 3.15% saline (N_{mice}=13, open gray) versus 64.52 ± 5.94 % NP-MORwd (N_{mice}=13, open pink), interaction factor $F_{(1,65)}$=8.591 two-way ANOVA , **P=0.005). (f) Box and scatter plot showing the percent time spent in the compartment containing the object stimulus for TNF-R1fl/fl mice (N of mice same as panel e. AAV-Control: 26.42 ± 2.47 % saline+naloxone (black) versus 30.9 ± 4.79% NP-MORwd (red); AAV-Cre: 31.19 ± 2.07% saline+naloxone (open gray) versus 20.7 ± 4.13 % NP-MORwd (open pink), interaction factor $F_{(1,65)}$=4.136 two-way ANOVA, *P=0.046). (g) Box and scatter plot showing the percent time spent in the central compartment for TNF-R1fl/fl mice (N of mice same as panel e. AAV-Control: 15.38 ± 3.08% saline+naloxone (black) versus 27.82 ± 4.98% NP-MORwd (red); AAV-Cre: 14.23 ± 2.9 % saline+naloxone (open gray) versus 14.62 ± 3.08% NP-MORwd (open pink), interaction factor $F_{(1,65)}$=1.748 two-way ANOVA , P=0.191). (h) Box and scatter plot showing number of exploration bouts of TNF-R1fl/fl with the juvenile (N of mice same as panel e. AAV-Control: 56 ± 3.51 saline+naloxone (black) versus 39.30 ± 4.8 NP-MORwd (red); AAV-Cre: 50.38 ± 3.78 saline+naloxone (open gray) versus 57.15 ± 7.01 NP-MORwd (open pink), interaction factor $F_{(1.65)}$=5.519 two-way ANOVA, *P=0.022). (i) Box and scatter plot showing number of exploration bouts of TNF-R1fl/fl with the object (N of mice is the same as panel e. AAV-Control: 26.9 ± 1.88 saline+naloxone (black) versus 23.35 ± 2.13 NP-MORwd (red); AAV-Cre: 28.08 ± 2.01 saline+naloxone (open gray) versus 21.69 ± 3.16 NP-MORwd (open pink), interaction factor $F_{(1.65)}$=0.361, P=0.55). (j) Box and scatter plot showing locomotor activity during social preference test for TNF-R1fl/fl mice (N of mice is the same as panel e. AAV-Control: 28.13 ± 1.35m saline+naloxone (black) versus 33.8 ± 5.59m NP-MORwd (red); AAV-Cre: 23.78 ± 1.47m saline+naloxone (open gray) versus 40.17 ± 7.11m NP-MORwd (open pink), interaction factor $F_{(1,65)}$=1.224 two-way ANOVA , P=0.273). Data are presented as box plots 10-90 percentiles with median and scatter.

Chapter 3. Opposing forms of synaptic plasticity at precise LHb-to-VTA circuits during cocaine withdrawal

The aversive state emerging during cocaine withdrawal is dependent in part upon synaptic and cellular adaptations within the LHb (Meye et al., 2015; 2016). Additionally, core components of behavioural adaptations emerging during cocaine withdrawal are linked to precise circuits emanating from the VTA, the main source of DA in the brain. Projections from the LHb exert control over the activity of VTA neurons, via a mixture of direct excitation of VTA projection neurons (Lammel et al., 2012; Beier et al., 2015, 2019) and feedforward inhibition via inhibitory relays in the midbrain (Matsumoto & Hikosaka, 2007) with both forms of control implicated in the processing of aversive experiences. Whilst much research has explored the feedforward inhibition of VTA DA neurons via midbrain GABA neurons, the anatomical and functional characteristics of LHb innervation of distinct VTA populations is currently poorly understood. Additionally, whether, and if so how, cocaine withdrawal alters this pathway is unknown. The LHb targets VTA projections that regulate processing of reward (to the NAc) and aversion (to the mPFC). Does cocaine withdrawal impose uniform or specific alterations of synaptic strength at these connections, given their divergent behavioural functions?

The present study, which formed the largest part of my thesis work, incorporated a combination of anatomical and electrophysiological techniques to probe the LHb-to-VTA circuit in cocaine withdrawal. First, we demonstrated using brain clarification and whole brain imaging (collab. Wyss Centre, UNIGE) that the VTA constituted a major afferent projection of the LHb, in line with previous report. We then characterised the precise distribution of LHb afferent terminals within the VTA, and their projection targets in the VTA using a combination of viral-anatomical strategies. These experiments revealed a preferential innervation of the medial portion of the VTA, and a preferential targeting of non-DA VTA neurons, although a substantial portion of DA neurons were also targeted. To examine whether cocaine withdrawal produced global, or LHb-innervation specific changes in excitatory transmission we conducted whole-cell patch clamp experiments in acute slices from cocaine and saline treated mice. Surprisingly, cocaine failed to elicit significant alterations of either global excitatory input or of LHb input to all VTA neurons. Given the functional divergence of distinct output-specific VTA projection neurons, we hypothesised that functional adaptations occurring in specific input-output relationships may be being masked by grouping VTA neurons together. In line with this, we observed that cocaine withdrawal drove opposing plasticity of LHb axon glutamate release probability on to VTA neurons projecting to the mPFC and NAc. Specifically, we found that glutamate release increased on to mPFC projectors, and diminished on to NAc projectors, whilst innervation of LH projecting neurons remained unaltered. Altogether, this study provides a precise characterisation of the LHb-to-VTA pathway and demonstrates how it can be altered by cocaine withdrawal in a circuit dependent manner. Given the respective roles of the VTA projections involved, it is possible these circuit dependent adaptations could underlie distinct components of the aversive state emerging in cocaine withdrawal, a question future studies should investigate.

The following section includes the manuscript for this study as published in Frontiers in Synaptic Neuroscience.

Clerke J, Preston-Ferrer P, Zouridis IS, Tissot A, Batti L, Voigt FF, Pagès S, Burgalossi A, Mameli M. Output-Specific Adaptation of Habenula-Midbrain Excitatory Synapses During Cocaine Withdrawal. Front Synaptic Neurosci. 2021 Mar 31;13:643138. doi: 10.3389/fnsyn.2021.643138.

frontiers in Synaptic Neuroscience

BRIEF RESEARCH REPORT
published: 31 March 2021
doi: 10.3389/fnsyn.2021.643138

Output-Specific Adaptation of Habenula-Midbrain Excitatory Synapses During Cocaine Withdrawal

*Joseph Clerke[1], Patricia Preston-Ferrer[2,3], Ioannis S. Zouridis[2,3,4], Audrey Tissot[5], Laura Batti[5], Fabian F. Voigt[6,7], Stephane Pagès[5], Andrea Burgalossi[2,3] and Manuel Mameli[1,8]**

[1] The Department of Fundamental Neuroscience, The University of Lausanne, Lausanne, Switzerland, [2] Institute of Neurobiology, University of Tübingen, Tübingen, Germany, [3] Werner-Reichardt Centre for Integrative Neuroscience, Tübingen, Germany, [4] International Max Planck Research School, Graduate Training Centre of Neuroscience, University of Tübingen, Tübingen, Germany, [5] The Wyss Center for Bio and Neuroengineering, Geneva, Switzerland, [6] Brain Research Institute, University of Zurich, Zurich, Switzerland, [7] Neuroscience Center Zurich, University of Zurich & ETH Zurich, Zurich, Switzerland, [8] INSERM UMR-S 839, Paris, France

Projections from the lateral habenula (LHb) control ventral tegmental area (VTA) neuronal populations' activity and both nuclei shape the pathological behaviors emerging during cocaine withdrawal. However, it is unknown whether cocaine withdrawal modulates LHb neurotransmission onto subsets of VTA neurons that are part of distinct neuronal circuits. Here we show that, in mice, cocaine withdrawal, drives discrete and opposing synaptic adaptations at LHb inputs onto VTA neurons defined by their output synaptic connectivity. LHb axons innervate the medial aspect of VTA, release glutamate and synapse on to dopamine and non-dopamine neuronal populations. VTA neurons receiving LHb inputs project their axons to medial prefrontal cortex (mPFC), nucleus accumbens (NAc), and lateral hypothalamus (LH). While cocaine withdrawal increases glutamate release from LHb onto VTA-mPFC projectors, it reduces presynaptic release onto VTA-NAc projectors, leaving LHb synapses onto VTA-to-LH unaffected. Altogether, cocaine withdrawal promotes distinct adaptations at identified LHb-to-VTA circuits, which provide a framework for understanding the circuit basis of the negative states emerging during abstinence of drug intake.

Keywords: ventral tegmental area, lateral habenula, cocaine, synaptic plasticity, glutamatergic transmission

OPEN ACCESS

Edited by:
Emmanuel Valjent, Centre National de la Recherche Scientifique (CNRS), France

Reviewed by:
Nicholas Michael Graziane, Pennsylvania State University, United States
Margaret E. Rice, New York University, United States

****Correspondence:***
Manuel Mameli
manuel.mameli@unil.ch

Received: *17 December 2020*
Accepted: *01 March 2021*
Published: *31 March 2021*

Citation:
Clerke J, Preston-Ferrer P, Zouridis IS, Tissot A, Batti L, Voigt FF, Pagès S, Burgalossi A and Mameli M (2021) Output-Specific Adaptation of Habenula-Midbrain Excitatory Synapses During Cocaine Withdrawal. Front. Synaptic Neurosci. 13:643138. doi: 10.3389/fnsyn.2021.643138

INTRODUCTION

The functional role of distinct ventral tegmental area (VTA) neuronal populations is a matter of long-standing interest as through the innervation of their target structures, these cells underlie core components of rewarding and aversive behaviors as well as of neuropsychiatric disorders including drug addiction (Nestler and Lüscher, 2019). To mediate this, the VTA relies on neuronal populations that are heterogeneous in their anatomical location, and especially in the targets to which they project (Lammel et al., 2014). Indeed, VTA neurons projecting to the medial prefrontal

cortex (mPFC), the nucleus accumbens (NAc) and the lateral hypothalamus (LH) are crucial for motivated behaviors and the related pathological states (Lammel et al., 2014).

VTA neurons receive, among others, glutamatergic innervation from the epithalamic lateral habenula (LHb) (Omelchenko et al., 2009). LHb axons onto the midbrain exert profound control of neuronal activity, by directly exciting some VTA cells as well as reducing the activity of other VTA neurons. As a consequence this control leads to the expression of aversive behaviors (Matsumoto and Hikosaka, 2007; Lammel et al., 2012). Drug withdrawal increases excitatory synaptic efficacy and neuronal activity within the LHb leading to the emergence of drug-driven depressive states (Meye et al., 2015, 2017). Along with this, cocaine withdrawal also produces a wealth of synaptic adaptations and changes in excitability of VTA neuronal populations (Chen et al., 2008; Ishikawa et al., 2013). However, little is known about the repercussions cocaine withdrawal may have on LHb-dependent control of VTA neuronal populations, especially in light of the circuits in which they are embedded.

By employing brain clarification, and viral-based anatomical tracing in combination with *ex vivo* electrophysiology, here we define functional differences between identified LHb-to-VTA output circuits undergoing synaptic adaptations during cocaine withdrawal.

MATERIALS AND METHODS

Animals and Cocaine Treatment

4–10 week old male wild-type mice (C57/BL6J) were group-housed (five per cage) with food and water *ad libitum* on a 12–12 h light cycle (lights on at 7:00). All procedures aimed to fulfil the criterion of the 3Rs and were approved by the Veterinary Offices of Vaud (Switzerland; license VD3172.1). Mice received five consecutive daily intraperitoneal (i.p.) cocaine (20 mg/kg) or saline injections (saline and cocaine-treated animals were housed together) and were sacrificed for electrophysiology experiments 10–15 days after the last injection.

Stereotactic Injections

4–5 week old male mice were anesthetized with ketamine (150 mg/kg)/xylazine (100 mg/kg) and placed on a stereotactic frame (Kopf, Germany). Bilateral injections (200–300 nl) obtained through a glass pipette were performed at a rate of approximately 100 nl min^{-1}. The injection pipette was slowly retracted from the brain 10 min following injection. The following coordinates (in mm relative to bregma and skull surface) were used for injections: lateral habenula [LHb: Anterior-Posterior (AP) −1.4, Media-Lateral (ML) ± 0.45 mm, Dorsal-Ventral (DV) −3.1]; medial prefrontal cortex (mPFC: AP 1.9, ML ± 0.37, −2.2); nucleus accumbens (NAc: AP 1.6, ML ± 0.5 mm, DV −4.5); lateral hypothalamus (LH: AP −1.34, ML ± 0.9, DV −5.08); medial VTA (mVTA: AP −2.7, ML ± 0.3, DV −4.6). A minimum of 5 days recovery were allowed after viral infusion prior to treatment with cocaine or saline. Viral constructs used in the study: rAAV8-hSyn-Chrimson-tdTomato (rAAV8-tdTomato; University of Pennsylvania viral vector core; titer: 7 × 10^{12} gc/ml). HSV-pEF1α-mCherry (HSV-mCherry; R Neve, Viral Gene Transfer Core Facility of the Massachusetts Institute of Technology; titer: 3.5 × 10^{9} gc/ml). rAAV1-hSyn-Cre-WPRE-hGH (rAAV1:ht-Cre; University of Pennsylvania viral vector core; titer:2.5 × 10^{13} gc/ml). rAAV8-hSyn-ChR2 (H134R)-GFP (rAAV8-ChR2-GFP; Addgene 58880; titer: 3.3 × 10^{13} gc/ml). rAAV8-HSyn-dLox-EGFP-dLox-WPRE-HGHp(A) (rAAV8-Flex-EGFP; Viral Vector Facility UZH, titer: 6.4 × 10^{12} gc/ml). rAAV2.5-hSyn-mRuby-T2A-Synaptophysin-eGFP (rAAV5-mRuby-T2A-Synaptophysin-eGFP; B.K. Lim, UCSD; titer: 10^{13} gc/ml). Injection sites were carefully examined during all electrophysiology and anatomical experiments, and only animals with correct injections were included in the study. For injections of viruses leaving no visible fluorescent trace within the injections site (HSV-mCherry; rAAV1:ht-Cre) a small amount of diluted red retrobeads (Lumaflor) were concurrently injected to enable identification *post hoc* of injection site.

Ex vivo Electrophysiology

7–9 week old male mice were anesthetized with an injection of ketamine (150 mg/kg)/xylazine (100 mg/kg) for preparation of acute brain slices as previously published (Li et al., 2011; Meye et al., 2015). Following sacrifice, brains were rapidly extracted and placed in ice cold 95% O^2/5% CO^2 – equilibrated bubbled slicing solution containing (pH 7.4, 298-302 mOsm, in mM): 110 choline chloride, 25 glucose, 25 NaHCO3, 7 MgCl2, 11.6 ascorbic acid, 3.1 sodium pyruvate, 2.5 KCl, 1.25 NaH2PO4, and 0.5 CaCl2. Horizontal slices (250 μm) containing the VTA were prepared and transferred for 5 min to heated solution (34°C) of identical composition before they were stored at room temperature in 95% O^2/5% CO^2 -equilibrated artificial cerebrospinal fluid (aCSF, pH 7.4, 310 mOsm) containing (in mM): 124 NaCl, 26.2 NaHCO3, 11 glucose, 2.5 KCl, 2.5 CaCl2,1.3 MgCl2, and 1 NaH2PO4. Recordings were conducted using an Olympus-BX51 microscope (Olympus) at 31°C (flow rate of 2.5 ml min^{-1}). Borosilicate glass pipettes (2.7–4 MΩ; Phymep) were used for whole-cell patch-clamp experiments (all in voltage-clamp configuration). Currents were amplified, filtered at 5 kHz and digitized at 20 kHz (Multiclamp 200B; Molecular Devices). Data were acquired using Igor Pro with NIDAQ tools (Wavemetrics). Recordings were discarded if the access resistance (monitored using a −4 mV step per 10 s) increased by more than 20%. Spontaneous EPSCs were recorded at −60 mV whereas presynaptic stimulation trains were recorded at −50 mV. Both of these experiments were conducted in the presence of picrotoxin (100 μM, Hello Bio) and APV (100 μM, Hello Bio). The internal solution used to measure spontaneous EPSCs and presynaptic release probability contained (in mM): 140mM potassium gluconate, 4 mM NaCl, 2mM $MgCl_2$, 1.1mM EGTA, 5mM HEPES, 2mM Na2ATP, 5mM sodium creatine phosphate, and 0.6mM Na3GTP (pH 7.3 with KOH; 290–300 mOsm; Labouèbe et al., 2007). Light pulses (490 nm, 1–5 ms) for opto-stimulation of LHb nerve terminals were delivered with a LED (CoolLed, United Kingdom) illumination system. To assess LHb terminal presynaptic release properties, trains of AMPAR-EPSCs were

evoked (10 light pulses at 10 and 20 Hz). The amplitudes of EPSC trains were normalized to the amplitude of the first pulse. The internal solution used to measure AMPAR/NMDAR ratios contained (in mM): 130 CsCl, 4 NaCl, 2 MgCl2, 1.1 ethylene glycol tetraacetic acid (EGTA), 5 HEPES buffer, 2 ATP-Na2, 5 sodium creatine-phosphate, 0.6 GTP-Na3, and 0.1 spermine (pH 7.3 with KOH; 290–300 mOsm; Bellone and Lüscher, 2006). To determine AMPA/NMDA ratios at LHb-to-VTA synapses, firstly, a mixed AMPA and NMDA current was evoked using a single light pulse at + 40 mV (in the presence of picrotoxin). Next, distinct AMPA and NMDA components were pharmacologically isolated by adding APV in the aCSF and by subsequent identification of the individual currents via digital subtraction (Mameli et al., 2009; Maroteaux and Mameli, 2012). For output-specific experiments, retrogradely labeled and fluorescently identified (mCherry +) VTA neurons were recorded from.

Histology and Immunofluorescence

Male mice were anesthetized and transcardially perfused with cold PBS followed by 4% paraformaldehyde (PFA) in PBS. The brains were carefully extracted, post-fixed in 4% PFA in PBS for 24 h and then incubated in PBS until they sank prior to sectioning. For mice undergoing viral infusion with rAAV1:ht-Cre and rAAV8-Flex-EGFP mice were perfused 3 weeks following viral infusion and coronal slices (50 μm) were prepared using a vibratome and stored in PBS containing 0.1%NaAz for future analyses. For immunofluorescence, slices were incubated for 2 h in blocking buffer [10%NGS (normal goat serum) in PBS] and then incubated for 24 h at 4°C with the primary antibody solution [rabbit anti-TH: ab112, abcam (1:500) in a carrier solution containing 3% NGS in PBS]. After extensive rinses with PBS, slices were incubated in the secondary antibody solution goat anti-rabbit IgG-conjugated Alexa 647, Invitrogen (1:500 in carrier solution), for 2 h at room temperature. The slices were then extensively rinsed, mounted on glass slides with Vectashield Antifade Mounting Medium with DAPI (Vectorlabs) and coverslipped. For synaptophysin experiments, horizontal sections (50 μm) were prepared using a vibratome for preferential visualization of the VTA. Confocal microscopy was performed using a TCS-SP5 (Leica) Laser Scanning System with ×10 and ×20 dry objectives. Images were acquired using the same parameters for all the samples within each experiment, then processed and analyzed using the software ImageJ. Proportions of LHb receiving cells co-stained with TH were determined using the cell counter plugin from an average of 5 slices per mouse covering the rostrocaudal extent of the VTA. For calculation of relative arbitrary fluorescence of synaptophysin punctae, green signal intensity was normalized against a region containing no green fluorescence (background) using the formula: [(Signal-background/Signal + background)/Area)]. For synaptophysin experiments, four slices distributed in the dorsoventral axis were analyzed per animal. Example images of rAAV8-ChR2-GFP injected mice, HSV-mCherry injected (VTA output) mice, and LHb-receiving VTA projections were taken with an epifluorescence microscope with ×2.5, ×5, and ×10 objectives (AxioVision, Zeiss).

In vivo Juxtacellular Labeling

In vivo juxtacellular labeling was performed on anesthetized male C57BL/6J mice (>6 weeks old; Charles River) as described previously (Diamantaki et al., 2018). Briefly, under ketamine/xylazine anesthesia, a craniotomy was performed at the coordinates for targeting the LHb (1.3–1.6 mm posterior and 0.6 mm lateral from bregma). Glass electrodes with resistance 5–7 MΩ were filled with 1.5–2% Neurobiotin (Vector Laboratories) in Ringer's solution containing (in mM): 135 NaCl, 5.4 KCl, 5 HEPES, 1.8 $CaCl_2$, and 1 $MgCl_2$ or Intracellular solution containing (in mM): 135 K-gluconate, 10 HEPES, 10 Na_2-phosphocreatine, 4 KCl, 4 MgATP, and 0.3 Na_3GTP. Osmolarity was adjusted to 280–310 mOsm. Juxtacellular labeling was performed according to standard procedures with 200 ms-long squared current pulses. The juxtacellular voltage signal was acquired via an ELC-03XS amplifier (NPI Electronic), sampled at 20 kHz by a Power1401-3 analog-to-digital interface under the control of Spike2 software (CED, Cambridge, United Kingdom).

For histological processing, animals were euthanized with an overdose of pentobarbital and perfused transcardially with 0.1 M PBS followed by a 4% paraformaldehyde solution. Brains were sliced on a vibratome (VT1200S; Leica) to obtain 70 μm-thick coronal sections. To reveal the morphology of juxtacellularly labeled cells (i.e., filled with neurobiotin), brain slices were processed with Streptavidin-546 (Life Technologies) as described previously (Diamantaki et al., 2018). Fluorescent images were acquired by epifluorescence microscopy (Axio imager; Zeiss). After fluorescence images were acquired, the neurobiotin staining was converted into a dark DAB reaction product followed by Ni_2+-DAB enhancement protocol.

CLARITY – Sample Preparation and Lightsheet Imaging

Tissue used in CLARITY experiments underwent viral injection (unilateral injection of LHb with 250nl rAAV8-tdTomato) and perfusion/brain extraction as described above prior to being shipped to the Wyss Center, Geneva. Brains were clarified following the CLARITY protocol (Chung and Deisseroth, 2013), using a X-CLARITY^{TM} system. Brains were immersed in a refractive index matching solution (RIMS) containing Histodenz (Sigma Aldrich) for at least 24 h before being imaged. Imaging was performed using a mesoSPIM (Voigt et al., 2019) instrument at Wyss Center, Geneva. The microscope consists of a dual-sided excitation path using a fiber-coupled multiline laser combiner (405, 488, 561, and 647 nm, Toptica MLE) and a detection path comprising an Olympus MVX-10 zoom macroscope with a 1× objective (Olympus MVPLAPO 1×), a filter wheel (Ludl 96A350), and a scientific CMOS (sCMOS) camera (Hamamatsu Orca Flash 4.0 V3, 2048 × 2048 pixels). The excitation paths also contain galvo scanners for light-sheet generation and reduction of shadow artifacts due to absorption of the light-sheet. In addition, the beam waist is scanned using electrically tunable lenses (ETL, Optotune EL-16-40-5D-TC-L) synchronized with the rolling shutter of the sCMOS camera. This axially scanned light-sheet mode (ASLM) leads to a uniform axial resolution across the

field-of-view (FOV) of 6.5 μm. Image acquisition is done using custom software written in Python. Z-stacks were acquired with a zoom set at 0.8X and 2X, at 5 and 3 μm spacing, respectively, resulting in an in-plane pixel size of 8.2 μm × 8.2 μm and 3.26 μm × 3.26 μm, respectively (2048 × 2048 pixels). Excitation wavelength of the tdTomato was set at 561 nm with an emission filter LP 561 nm longpass filter (BrightLine HC, AHF).

Quantification and Statistical Analysis

Online and offline analysis for presynaptic trains data were performed using Igor Pro-6 (Wavemetrics, United States). sEPSCs recordings were manually analyzed offline using Minianalysis (Synaptosoft Inc, United States). Sample size was predetermined on the basis of published studies and in-house expertise. Animals were randomly assigned to experimental groups. Compiled data for sEPSC and AMPA/NMDA recordings are reported and represented as violin plots (median and quartiles) with single data points (cells) plotted. Compiled data for presynaptic LHb stimulation trains are represented as mean ± SEM of normalized current amplitude for each pulse. Datasets were screened for outliers using a ROUT test; outliers removed are stated in figure legends. Data collection and analyses were not performed blinded to the conditions of the experiments. Data distribution was tested for normality. When applicable, statistical tests were two-way ANOVAs or unpaired *t*-test. In case of not-normally distributed data, we used the Mann-Whitney or Kolmogorov-Smirnov tests. Testing was always performed two-tailed with $\alpha = 0.05$.

RESULTS

Midbrain Innervation by LHb Axonal Projections

To examine which VTA territory LHb projections innervate, we firstly injected the LHb of mice with a rAAV8-tdTomato and then *i.* employed CLARITY to clear the brain in a whole-mount preparation, *ii.* registered the imaged volume from a mesoscale selective plane-illumination microscope and *iii.* examined resultant axonal arborization in the midbrain (see section "Materials and Methods"; **Figures 1A,B**) (Chung and Deisseroth, 2013; Voigt et al., 2019). Qualitative image analysis revealed dense LHb projections medially within midbrain structures as well as raphe nucleus (**Figure 1B**). Despite offering a global picture for the innervation stemming from the LHb, whole brain imaging fails in providing where LHb axons are making synapses within the midbrain. To identify LHb axons as well as their presynaptic terminals, we employed rAAV5-mRuby-T2A-Synaptophysin-eGFP injected into the LHb (**Figure 1C**). Long-range projecting LHb neurons densely innervated the midbrain with the majority of green punctae located in the medial territory of the VTA, and as expected by previous data also in the rostromedial tegmental nucleus [**Figure 1D** and **Supplementary Figures 1A,B** (Jhou et al., 2009)]. Accordingly, juxtacellular labeling of single LHb neurons in anesthetized mice and subsequent histological processing revealed LHb axonal processes and presynaptic boutons within medial VTA territories (**Figures 1E–G**).

Which neuronal populations are these LHb axons innervating? The medial VTA contains heterogeneous neuronal populations including dopamine releasing cells and non-dopaminergic neurons [i.e., GABA and glutamate containing (Morales and Margolis, 2017)]. To identify which VTA neurons receive LHb synaptic input we concomitantly injected an anterograde trans-synaptic high titer rAAV1:ht-Cre in the LHb and a cre-dependent rAAV8-Flex-EGFP in the VTA. This intersectional strategy, in combination with immunohistochemical staining for tyrosine hydroxylase (TH) permits the identification of those VTA neuronal populations (dopamine and non-dopamine producing) innervated by LHb axons (**Figures 1H–J**; Zingg et al., 2017). LHb-to-VTA neurons (GFP +) were predominantly negative to TH staining. Quantification showed that only 30.9 ± 2.9% of LHb receiving neurons in the VTA also stained for TH, whilst 32.3 ± 7.6% of total VTA TH + neurons were targeted by the LHb (21 sections/4 mice; **Figure 1J**). Altogether, this indicates that a minority of the LHb-to-VTA projection target TH + cells, rather controlling a neuronal population that is mostly TH– and located in the medial aspect of the VTA.

Excitatory Synaptic Transmission Within the VTA During Cocaine Withdrawal

Glutamatergic transmission onto both LHb and VTA neuronal populations dynamically and through various mechanisms adapts during cocaine experience and withdrawal, subsequently underlying different addictive behavioral states (Meye et al., 2015; Morales and Margolis, 2017). Notably, LHb activity may, at least partly, influence the firing of VTA neurons (Matsumoto and Hikosaka, 2007). We therefore investigated whether cocaine withdrawal affects neurotransmission onto the VTA, and whether this relies on precise adaptations at LHb-to-VTA synapses. Firstly, we examined whether cocaine withdrawal alters excitatory transmission specifically onto the medial VTA by using a regime of five consecutive daily intraperitoneal injections of cocaine (20 mg/kg) followed by a 10–15 day withdrawal period. This specific protocol elicits increases in AMPA-receptors mediated neurotransmission, and leads to increased neuronal excitability within the LHb (Meye et al., 2015). As a consequence these adaptations lead to depressive-like symptoms in mice (Meye et al., 2015). First, we recorded spontaneous excitatory postsynaptic currents (sEPSCs) from neurons located within the medial territory of the VTA, and found that cocaine withdrawal did not alter overall frequency or amplitude of events (**Figure 2A**). To investigate more specifically how cocaine withdrawal may impact synaptic transmission at LHb-to-VTA synapses, we injected rAAV8-ChR2-GFP into the LHb and obtained whole-cell patch-clamp recordings from neurons in the medial VTA. Blue light stimulation of LHb terminals, in the presence of picrotoxin and APV to block GABA and NMDA receptors, respectively, evoked excitatory postsynaptic currents in virtually all medial VTA neurons (**Figures 2B,C**). Cocaine withdrawal did not significantly alter

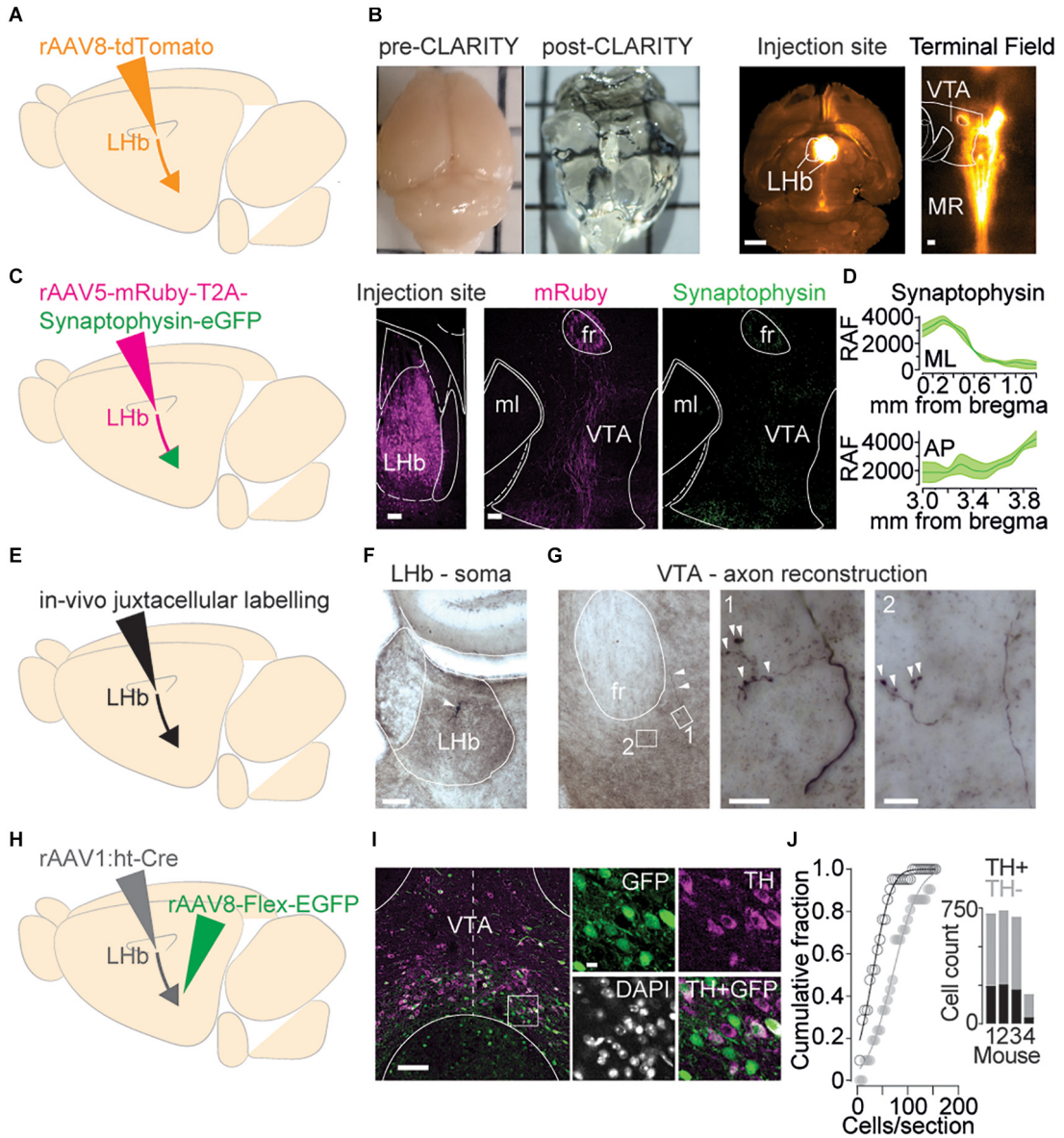

FIGURE 1 | Axons from the LHb innervate midbrain cell populations. **(A)** Viral strategy to visualize wholebrain projectome of LHb. **(B)** Left: Examples of a mouse brain before and after clarification treatment. Right: Representative images (horizontal plane) of LHb viral injection site (1 mm) and tdTomato positive terminals targeting the VTA and Median Raphe Nucleus (MRN) (100 μm). **(C)** Left: Viral strategy to identify LHb axon terminals in the midbrain. Right: images (horizontal plane, 100 μm, 10×) left to right: injection site in the LHb; mRuby positive axons in the VTA; Synaptophysin-EGFP positive terminals in the VTA. **(D)** Quantification in Relative Arbitrary Fluorescent (RAF) Units of Synaptophysin expression throughout the mediolateral (ML, top) and Anterior-Posterior (AP, bottom) extent of the VTA ($n_{hemispheres/mice}$ = 3/2) (mean ± SEM). **(E)** Strategy to identify individual LHb neuron axon terminal boutons in the VTA. **(F)** Coronal DAB-stained section showing a single LHb neuron (white arrowhead) juxtacellularly labeled *in vivo* (scale bar, 100 μm). **(G)** Left: DAB-stained section showing a single LHb axon (white arrowheads) emerging from fr into VTA (scale bar, 100 μm). Center and right, Maximum intensity z-stack projections of close-up magnifications (1 and 2) showing synaptic boutons within the VTA (white arrowheads) (scale bars, 10 μm). **(H)** Viral strategy to label LHb receiving neurons in the VTA. **(I)** Left: Representative image (coronal plane, dashed midline, 100 μm, 20×) of LHb receiving cells in the VTA (green) and TH + neurons (violet). Right: Close ups showing degree of colocalization of GFP and TH (10 μm). **(J)** Cumulative probability distribution (KS test, p = 0.0063) for the entire population of counted cells of each section; TH + (black) and TH– (gray). Inset, total cell counts for individual mice (n = 4). MR, Median Raphe; ml, medial lemniscus; fr, fasciculus retroflexus; RAF, Relative Arbitrary Fluorescence units; ML, Medial-Lateral; AP, Anterior-Posterior; GFP, Green Fluorescence Protein; TH, Tyrosine Hydroxylase.

presynaptic neurotransmitter release probability inferred from the degree of frequency depression of EPSCs during a train of blue light pulses (10 pulses, 10 Hz, and 20 Hz) (**Figure 2C** and **Supplementary Figures 2A–D**). Similarly, cocaine withdrawal left unaffected optogenetically evoked AMPAR to NMDAR ratios (AMPAR/NMDAR, + 40 mV; **Figures 2D,E**) at LHb-to-VTA synapses. Hence, despite cocaine withdrawal increasing LHb neuronal excitability, it unexpectedly does not alter LHb

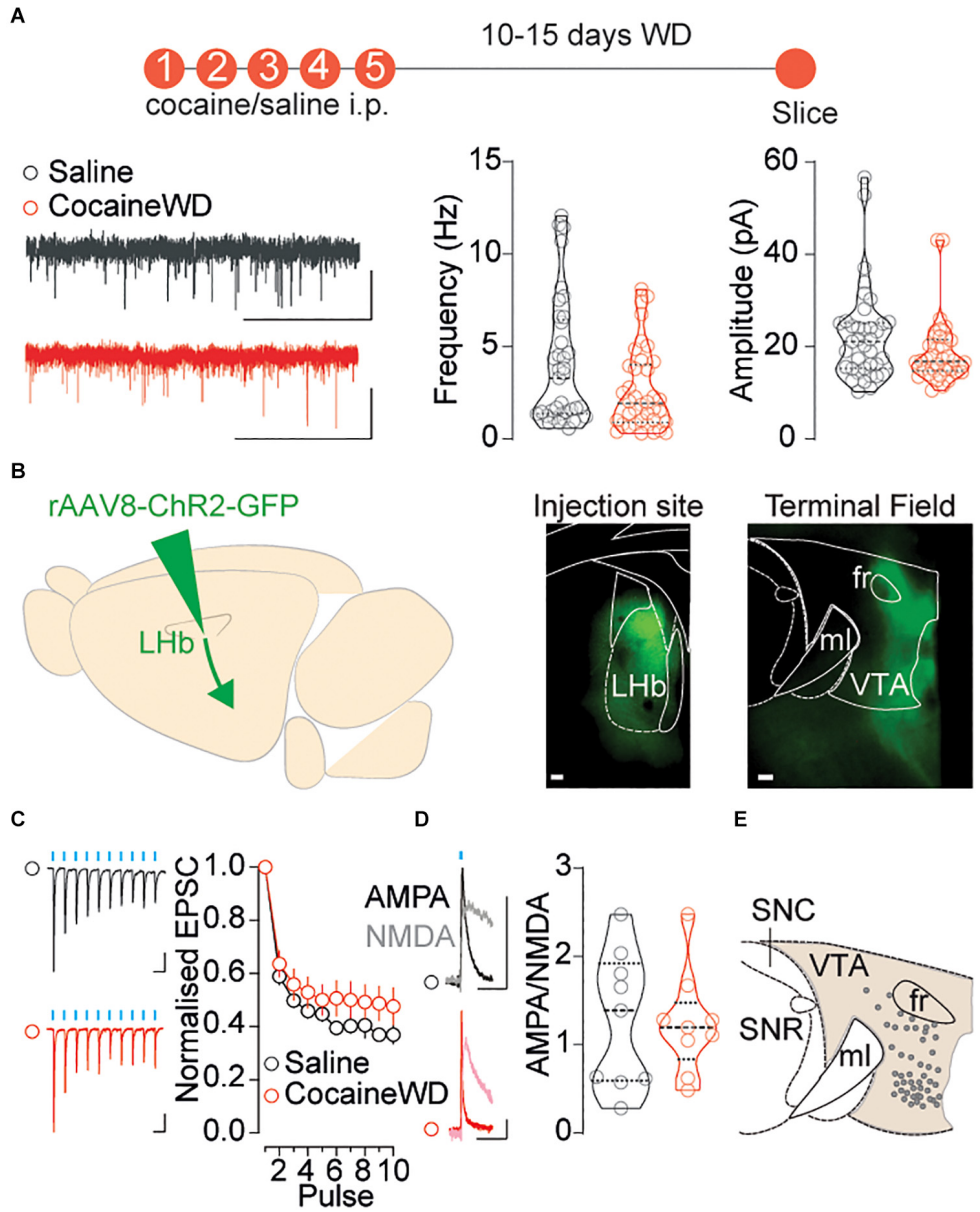

FIGURE 2 | Examining excitatory synaptic transmission on to VTA neurons during cocaine withdrawal. **(A)** Top: Cocaine/Saline treatment protocol. Left: Sample sEPSCs traces (2s, 20pA) for saline (black) and cocaine treated (red) mice. Right: Violin plots for the frequency and amplitude of events in recorded cells (saline $n_{cells/mice}$ = 37/16; cocaine $n_{cells/mice}$ = 38/12; outlier $cells_{saline/cocaine}$ = 5/6) Frequency Mann-Whitney, U = 531, p = 0.0690; Amplitude Mann-Whitney, U = 531, p = 0.0690. **(B)** Left: Viral strategy to investigate LHb innervation of VTA. Right: Injection site in the LHb and terminal field of GFP positive terminals in the VTA (both horizontal plane, 100 μm, 2.5×). **(C)** Sample traces (Saline: 50 ms, 100 pA; Cocaine: 50 ms, 20 pA) and normalized EPSC vs pulse plot (saline $n_{cells/mice}$ = 27/10; cocaine $n_{cells/mice}$ = 29/14) Interaction factor $F(9,486)$ = 1.458, P = 0.1606 two-way ANOVA Repeated Measures. **(D)** Sample traces (50 ms, 20 pA) and violin plot showing LHb-to-VTA AMPA/NMDA of recorded cells (saline $n_{cells/mice}$ = 9/4; cocaine $n_{cells/mice}$ = 9/4) Two-sided t-test, t_{16} = 0.1022, p = 0.9199. **(E)** Map of recorded VTA cells. Data are presented as mean ± SEM. SNR, Substantia Nigra pars Reticulata; SNC, Substantia Nigra pars Compacta.

excitatory transmission when macroscopically recording from medially located VTA cells.

LHb Innervation of Output-Specific VTA Populations in Cocaine Withdrawal

Neurons within the VTA project their axons to a large variety of target structures – including mPFC and NAc – and shape rewarding and aversive behaviors in an output-specific fashion (Lammel et al., 2012). Therefore, the overall absence of cocaine withdrawal-driven synaptic changes does not rule out a scenario in which the LHb-to-VTA projection adapts according to the downstream target of VTA cells. To test this, we combined the high-titer anterograde trans-synaptic rAAV1:ht-Cre in LHb and cre-dependent EGFP expression in VTA to define the output circuit of LHb receiving VTA neurons (**Figures 3A–C**). Through serial section analysis

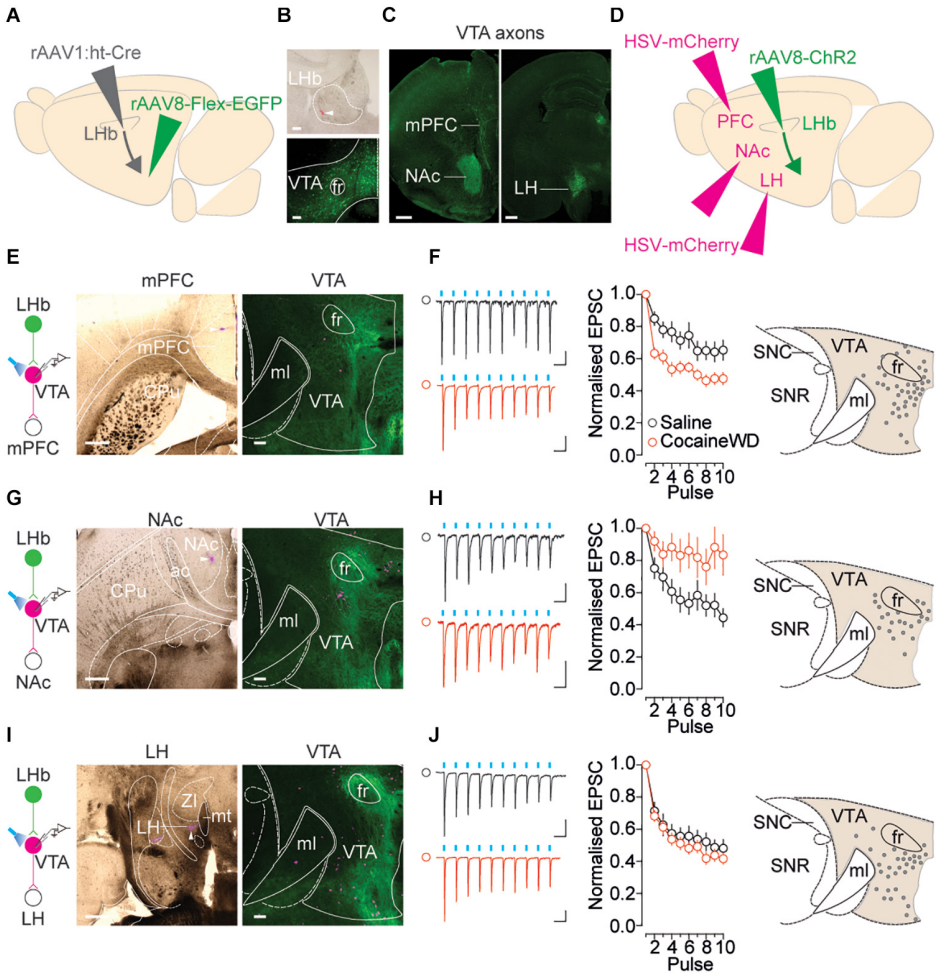

FIGURE 3 | Cocaine withdrawal re-shapes glutamatergic transmission at LHb-to-VTA output circuits. **(A)** Left: Viral strategy to visualize projection targets of LHb-receiving VTA neurons. Right: Respective terminal fields in mPFC, NAc, and LH. **(B)** Top: Site of rAAV1:ht-Cre in the LHb (tip of injection needle indicated by white arrow and small deposit of red retrobeads). Bottom: LHb-receiving, GFP positive neurons in the VTA following rAAV8-Flex-GFP injection (both coronal plane, 100 μm, 10×). **(C)** Terminal zones of axonal projections of LHb receiving VTA neurons (both coronal plane, 500 μm, 2.5×). **(D)** Viral strategy to interrogate LHb innervation of output specific VTA populations. **(E)** Left: HSV-mCherry injection site in mPFC. Right: Overlapping LHb terminals (GFP) with retrogradely labeled VTA-to-mPFC neurons. **(F)** Left: Sample traces (Saline: 50 ms, 20 pA; Cocaine: 50 ms, 100 pA) and normalized EPSC vs. pulse plots (saline $n_{cells/mice}$ = 21/16; cocaine $n_{cells/mice}$ = 21/16) Interaction factor $F(9,378) = 4.535$, $P < 0.0001$ two-way ANOVA Repeated Measures. Right: map of recorded VTA-to-mPFC cells. **(G)** Left: HSV-mCherry injection site in NAc. Right: Overlapping LHb terminals with retrogradely labeled VTA-to-NAc neurons. **(H)** Left: Sample traces (Saline: 50 ms, 20 pA; Cocaine: 50 ms, 20 pA) and normalized EPSC vs. pulse plots (saline $n_{cells/mice}$ = 11/5; cocaine $n_{cells/mice}$ = 13/3) Interaction factor $F(9,198) = 2.953$, $P = 0.0026$ two-way ANOVA Repeated Measures. Right: map of recorded VTA-to-NAc cells. **(I)** Left: HSV-mCherry injection site in LH. Right: Overlapping LHb terminals with retrogradely labeled VTA-to-LH neurons. **(J)** Left: Sample traces (Saline: 50 ms, 50 pA; Cocaine: 50 ms, 100 pA) and normalized EPSC vs. pulse plots (saline $n_{cells/mice}$ = 23/5; cocaine $n_{cells/mice}$ = 24/6) Interaction factor $F(9,405) = 0.7625$, $P = 0.6488$ two-way ANOVA Repeated Measures. Right: map of recorded VTA-to-LH cells. For images of HSV injection sites in mPFC, NAc and LH – horizontal plane, 500 μm, 2.5×. For images of VTA in same mice – horizontal plane, scale bar, 100 μm, 5×. CPu, Caudate Putamen; ac, anterior commissure; ZI, Zona Incerta; mt, mammillothalamic tract.

we examined projections of LHb-innervated cells within the VTA. Terminal fields of these VTA projections were observed in mPFC, NAc and LH, structures vulnerable to cocaine experience (Lammel et al., 2014; Aransay et al., 2015). Next, a retrograde HSV-mCherry was injected either in the mPFC, NAc or LH concomitantly with a rAAV8-ChR2-GFP within the LHb (**Figure 3D**). A vast majority of retrogradely labeled neurons emerging from the different output structures were medially located within the VTA, and mingled within the mesh of LHb terminals (**Figures 3E–I**). Based on the evidence that drug withdrawal increases neuronal activity within the LHb, we examined LHb-driven presynaptic release onto these target-identified VTA populations (Meye et al., 2015, 2017). Blue light-evoked trains of presynaptic stimulation revealed that cocaine withdrawal increased presynaptic depression at LHb inputs onto VTA-to-mPFC, reduced presynaptic depression at LHb inputs onto VTA-to-NAc and left unaffected synaptic transmission onto VTA-to-LH projections (**Figures 3F–J**). This suggests that cocaine withdrawal produces presynaptic LHb glutamate release adaptations that depend on the projection target of the connected VTA neuron.

DISCUSSION

The negative behavioral state emerging during cocaine withdrawal can persist long after cessation of drug use and can involve symptoms reminiscent of depressive states (Meye et al., 2017). Dysfunction of LHb and VTA neurons contributes to the negative behavioral phenotypes emerging during drug withdrawal. However, the detailed neuronal circuits within the VTA that are under LHb control, and are gone awry during drug withdrawal, remain to be defined. Here, we provide evidence that LHb inputs to the VTA undergo diverse synaptic adaptations onto distinct VTA neuronal populations that project to different target structures.

The behavioral relevance of distinct neural populations often segregates based on their projection targets, a concept that especially applies to VTA circuits. Indeed, VTA populations and namely dopamine releasing cells underlie aversive or appetitive behaviors depending whether they project their axons to mPFC or precise territories of the NAc (Lammel et al., 2012; de Jong et al., 2019). In light of the LHb contribution to aversive states, it is plausible that LHb innervation would control VTA cells embedded in the aversion-related neuronal circuits. The intersectional approach using anterograde trans-synaptic labeling indicates that LHb provides input not only to TH + but also and preferentially to TH– neurons (Omelchenko et al., 2009). The axons of these cells reach, in turn, structures including the mPFC, the NAc and the LH, thereby defining trisynaptic circuits that are likely (mPFC, NAc), or not (LH), underlying aspects of aversive and cocaine-experience driven states (Meye et al., 2017; de Jong et al., 2019). One caveat of the anterograde trans-synaptic tracing is that it lacks cell specificity. The experimental conditions employed do not permit distinguishing the nature of the axonal projections (TH + or TH–). Therefore, future analysis to functionally dissect whether LHb-to-TH– VTA neurons controls local or long-range synaptic transmission is required to better define this intricate connectivity.

Cocaine withdrawal differentially alters presynaptic release of glutamate from the LHb to VTA neurons depending on their output target. The increased presynaptic depression at LHb to mPFC projecting VTA neurons is in line with a reported LHb increased neuronal activity during cocaine withdrawal (Meye et al., 2015). Accordingly, this trisynaptic circuit may underlie the negative states emerging in cocaine withdrawal, given the implications of VTA-to-mPFC in aversion and depressive like behaviors (Weele et al., 2019). On the other hand, the reduction in presynaptic glutamate release at LHb-VTA-NAc projections is a surprising result and diverges from the finding describing a cocaine withdrawal-mediated increase of LHb neuronal activity (Meye et al., 2015). Several scenarios may emerge that can explain this discrepancy: (i) that cocaine withdrawal differently affects neuronal activity amongst cell populations within the LHb, a scenario yet non-described in literature, or (ii) that cocaine withdrawal alters presynaptic release independently of somatic firing. Cocaine withdrawal seems inefficient in altering LHb excitatory synapses onto LH-projecting VTA neurons. However, we cannot rule out that opposing effects at TH + and TH– VTA neurons are taking place masking net effects. Finally, the LHb-controlled TH– population may in turn provide synaptic inhibition to neighboring dopamine neurons, highlighting the need of a better understanding of synaptic inhibition after cocaine withdrawal. Altogether, the use of refined genetic tools including cre driver mouse lines together with intersectional viral strategies and electrophysiology will be necessary to parse out these distinct mechanisms.

In conclusion, this study indicates that the LHb anatomically and functionally controls distinct subpopulations of VTA neurons that are in turn embedded in distinct circuits. The diverse forms of synaptic plasticity within these LHb-to-VTA circuits may contribute to shaping reward and aversion as well as behavioral phenotypes typical of drug withdrawal.

DATA AVAILABILITY STATEMENT

The original contributions presented in the study are included in the article/**Supplementary Material**, further inquiries can be directed to the corresponding author.

ETHICS STATEMENT

The animal study was reviewed and approved by the Veterinary Offices of Vaud.

AUTHOR CONTRIBUTIONS

JC performed and analyzed immunostaining and electrophysiological experiments. IZ, PP-F, and AB performed *in vivo* juxtacellular labeling and anatomical analysis. AT, LB, and SP performed whole brain clarification, imaging, and analysis. FV conceived the MESO-Spim strategy. JC and MM conceptualized the study and wrote the manuscript with the help of all authors.

FUNDING

This work was supported by the Swiss National Funding (31003A) to MM, the Eberhard Karls University of Tübingen, the Werner Reichardt Centre for Integrative Neuroscience [Excellence Cluster funded by the Deutsche Forschungsgemeinschaft (DFG) within the framework of the Excellence Initiative EXC 307], and the DFG grants BU3126/1-1 and BU3126/2-1.

ACKNOWLEDGMENTS

We thank the whole Mameli Laboratory for the feedback on the manuscript. We thank J. C. Paterna and the Zurich Viral Vector

Facility for technical support. We also thank B. K. Lim (University of California, San Diego, United States) for kindly providing the mRuby-Synaptophysin construct. FV would like to thank F. Helmchen and members of the Helmchen laboratory for their support in developing the mesoSPIM microscope.

SUPPLEMENTARY MATERIAL

The Supplementary Material for this article can be found online at: https://www.frontiersin.org/articles/10.3389/fnsyn.2021.643138/full#supplementary-material

Supplementary Figure 1 | LHb terminal distribution in the RMTg. **(A)** Images (horizontal plane, Scale bar, 100 μm, 10×) left to right: injection site in the LHb; mRuby positive axons in the RMTg; Synaptophysin-EGFP positive terminals in the RMTg. **(B)** Quantification in Relative Arbitrary Fluorescent (RAF) Units of Synaptophysin expression throughout the mediolateral (ML, top) and Anterior-Posterior (AP, bottom) extent of the RMTg ($n_{hemispheres/mice}$ = 3/2).

Supplementary Figure 2 | 10Hz stimulation of LHb axons on to defined VTA populations. **(A)** VTA global: Sample traces (Saline: 100 ms, 20 pA; Cocaine: 100 ms, 20 pA) and normalized EPSC vs. pulse plots (saline $n_{cells/mice}$ = 27/10; cocaine $n_{cells/mice}$ = 29/14) Interaction factor $F(9,486)$ = 1.148, P = 0.3272 two-way ANOVA Repeated Measures. **(B)** VTA-to-mPFC: Sample traces (Saline: 100 ms, 20 pA; Cocaine: 100 ms, 20 pA) and normalized EPSC vs. pulse plots (saline $n_{cells/mice}$ = 21/16; cocaine $n_{cells/mice}$ = 21/16) Interaction factor $F(9,162)$ = 2.141, P = 0.0289 two-way ANOVA Repeated Measures. **(C)** VTA-to-NAc: Sample traces (Saline: 100 ms, 20 pA; Cocaine: 100 ms, 10 pA) and normalized EPSC vs. pulse plots (saline $n_{cells/mice}$ = 11/5; cocaine $n_{cells/mice}$ = 13/3) Interaction factor $F(9,198)$ = 2.012, P = 0.0397 two-way ANOVA Repeated Measures. **(D)** VTA-to-LH: Sample traces (Saline: 100 ms, 10 pA; Cocaine: 100 ms, 100 pA) and normalized EPSC vs. pulse plots (saline $n_{cells/mice}$ = 23/5; cocaine $n_{cells/mice}$ = 24/6) Interaction factor $F(9,405)$ = 1.417, P = 0.1786 two-way ANOVA Repeated Measures.

REFERENCES

Aransay, A., Rodríguez-López, C., García-Amado, M., Clascá, F., and Prensa, L. (2015). Long-range projection neurons of the mouse ventral tegmental area: a single-cell axon tracing analysis. *Front. Neuroanat.* 9:59. doi: 10.3389/fnana.2015.00059

Bellone, C., and Lüscher, C. (2006). Cocaine triggered AMPA receptor redistribution is reversed in vivo by mGluR-dependent long-term depression. *Nat. Neurosci.* 5, 636–641. doi: 10.1038/nn1682

Chen, B. T., Bowers, M. S., Martin, M., Hopf, F. W., Guillory, A. M., Carelli, R. M., et al. (2008). Cocaine but not natural reward self-administration nor passive cocaine infusion produces persistent LTP in the VTA. *Neuron* 59, 288–297. doi: 10.1016/j.neuron.2008.05.024

Chung, K., and Deisseroth, K. (2013). CLARITY for mapping the nervous system. *Nat. Methods* 10, 508–513. doi: 10.1038/nmeth.2481

de Jong, J. W., Afjei, S. A., Pollak Dorocic, I., Peck, J. R., Liu, C., Kim, C. K., et al. (2019). A Neural Circuit Mechanism for Encoding Aversive Stimuli in the Mesolimbic Dopamine System. *Neuron* 101, 133.e–151.e.

Diamantaki, M., Coletta, S., Nasr, K., Zeraati, R., Laturnus, S., Berens, P., et al. (2018). Manipulating Hippocampal Place Cell Activity by Single-Cell Stimulation in Freely Moving Mice. *Cell Rep.* 23, 32–38. doi: 10.1016/j.celrep.2018.03.031

Ishikawa, M., Otaka, M., Neumann, P. A., Wang, Z., Cook, J. M., Schlüter, O. M., et al. (2013). Exposure to cocaine regulates inhibitory synaptic transmission from the ventral tegmental area to the nucleus accumbens. *J. Physiol.* 591, 4827–4841. doi: 10.1113/jphysiol.2013.262915

Jhou, T. C., Geisler, S., Marinelli, M., Degarmo, B. A., and Zahm, D. S. (2009). The mesopontine rostromedial tegmental nucleus: A structure targeted by the lateral habenula that projects to the ventral tegmental area of Tsai and substantia nigra compacta. *J. Comp. Neurol.* 513, 566–596. doi: 10.1002/cne.21891

Laboueˋbe, G., Lomazzi, M., Cruz, H. G., Creton, C., Luján, R., Li, M., et al. (2007). RGS2 modulates coupling between GABAB receptors and GIRK channels in dopamine neurons of the ventral tegmental area. *Nat. Neurosci.* 12, 1559–1568. doi: 10.1038/nn2006

Lammel, S., Lim, B. K., and Malenka, R. C. (2014). Reward and aversion in a heterogeneous midbrain dopamine system. *Neuropharmacology* 76(Pt B), 351–359. doi: 10.1016/j.neuropharm.2013.03.019

Lammel, S., Lim, B. K., Ran, C., Huang, K. W., Betley, M. J., Tye, K. M., et al. (2012). Input-specific control of reward and aversion in the ventral tegmental area. *Nature* 491, 212–217. doi: 10.1038/nature11527

Li, B., Piriz, J., Mirrione, M., Chung, C., Proulx, C.D., Schulz, D., et al. (2011). Synaptic potentiation onto habenula neurons in the learned helplessness model of depression. *Nature* 470, 535–539. doi: 10.1038/nature09742

Mameli, M., Halbout, B., Creton, C., Engblom, D., Parkitna, J. R., Spanagel, R., et al. (2009). Cocaine-evoked synaptic plasticity: persistence in the VTA triggers adaptations in the NAc. *Nat. Neurosci.* 8, 1036–1041. doi: 10.1038/nn.2367

Maroteaux, M., and Mameli, M. (2012). Cocaine evokes projectionspecific synaptic plasticity of lateral habenula neurons. *J. Neurosci.* 32, 12641–12646. doi: 10.1523/JNEUROSCI.2405-12.2012

Matsumoto, M., and Hikosaka, O. (2007). Lateral habenula as a source of negative reward signals in dopamine neurons. *Nature* 447, 1111–1115. doi: 10.1038/nature05860

Meye, F. J., Trusel, M., Soiza-Reilly, M., and Mameli, M. (2017). Neural circuit adaptations during drug withdrawal - Spotlight on the lateral habenula. *Pharmacol. Biochem. Behav.* 162, 87–93. doi: 10.1016/j.pbb.2017.08.007

Meye, F. J., Valentinova, K., Lecca, S., Marion-Poll, L., Maroteaux, M. J., Musardo, S., et al. (2015). Cocaine-evoked negative symptoms require AMPA receptor trafficking in the lateral habenula. *Nat. Neurosci.* 18, 376–378. doi: 10.1038/nn.3923

Morales, M., and Margolis, E. B. (2017). Ventral tegmental area: cellular heterogeneity, connectivity and behaviour. *Nat. Rev. Neurosci.* 18, 73–85. doi: 10.1038/nrn.2016.165

Nestler, E. J., and Lüscher, C. (2019). The Molecular Basis of Drug Addiction: Linking Epigenetic to Synaptic and Circuit Mechanisms. *Neuron* 102, 48–59. doi: 10.1016/j.neuron.2019.01.016

Omelchenko, N., Bell, R., and Sesack, S. R. (2009). Lateral habenula projections to dopamine and GABA neurons in the rat ventral tegmental area. *Eur. J. Neurosci.* 30, 1239–1250. doi: 10.1111/j.1460-9568.2009.06924.x

Voigt, F. F., Kirschenbaum, D., Platonova, E., Pagès, S., Campbell, R. A. A., Kastli, R., et al. (2019). The mesoSPIM initiative: open-source light-sheet microscopes for imaging cleared tissue. *Nat. Methods* 16, 1105–1108. doi: 10.1038/s41592-019-0554-0

Weele, C. M. V., Siciliano, C. A., and Tye, K. M. (2019). Dopamine tunes prefrontal outputs to orchestrate aversive processing. *Brain Res.* 1713, 16–31. doi: 10.1016/j.brainres.2018.11.044

Zingg, B., Chou, X. L., Zhang, Z. G., Mesik, L., Liang, F., Tao, H. W., et al. (2017). AAV-Mediated Anterograde Transsynaptic Tagging: Mapping Corticocollicular Input-Defined Neural Pathways for Defense Behaviors. *Neuron* 93, 33–47. doi: 10.1016/j.neuron.2016.11.045

Conflict of Interest: The authors declare that the research was conducted in the absence of any commercial or financial relationships that could be construed as a potential conflict of interest.

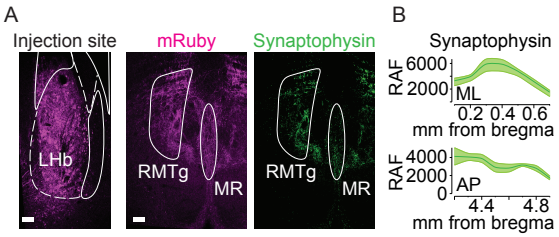

Clerke et al., Figure S1

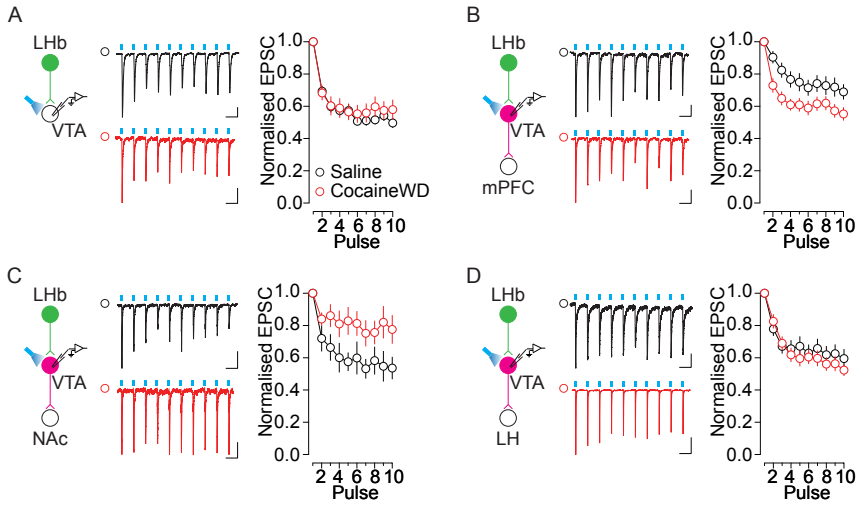

Clerke et al., Figure S2

Chapter 4. Discussion

The work presented in my PhD thesis demonstrate that withdrawal from distinct classes of drugs of abuse result in profound changes in precise LHb circuits, which regulate downstream nuclei critical to motivated behaviours. In the first part of the thesis, I show that morphine withdrawal drives a synaptic depression on to LHb neurons projecting to the DRN. This plasticity is dependent on the recruitment of locally released TNFα from activated microglia in the LHb acting on TNF-receptor 1 (TNF-R1). Further experiments demonstrated that the TNFα mediated LHb plasticity in morphine withdrawal was necessary for the emergence of sociability deficits – a component of the aversive state arising in withdrawal opioids. This behavioural function was also shown to be regulated by the same LHb neurons projecting to the Raphe where the morphine withdrawal driven plasticity occurred. Together these results present a key role for local inflammation in mediating morphine withdrawal driven plasticity in the LHb and underscore the importance of adaptations in LHb circuits for mediating central components of withdrawal-driven aversive states.

In the second part of my manuscript, I show that cocaine withdrawal dynamically alters precise sub-circuits within the LHb projection to the VTA. In line with previous results, we see that cocaine withdrawal does not alter the global LHb innervation of VTA when neglecting to specify the VTA sub-circuits which LHb axons innervate. We show that the LHb preferentially projects to the medial portion of the VTA, a highly heterogenous region composed of numerous distinct sub-populations particularly with regard to output projections. LHb-receiving VTA neurons were predominantly non-DA in nature and projected to various output structures enabling targeting of these distinct sub-circuits using intersectional viral approaches. I observe that LHb glutamatergic transmission on to distinct VTA output-specific populations is altered in opposing directions on to VTA circuits believed to encode opposite valence. Therefore, I propose that these sub-circuit specific adaptations could underlie the emergence of an aversive state arising during cocaine withdrawal.

Taken together, my thesis work serves to highlight the importance of LHb circuit adaptations during drug withdrawal as well as demonstrate the nuanced complexity of this node in the brain. Previous experiments studying LHb plasticity in drug withdrawal have universally uncovered adaptations serving increased excitation of the LHb. Here I provide evidence that cocaine withdrawal can also scale down the excitatory drive on to LHb neurons, and their output to the midbrain. The LHb targets a vast array of different cell types in its output projections, likely controlling various important functions of motivated behaviours. Ultimately, adaptations in each of these circuits could underlie specific components of the composite aversive state emerging during withdrawal from drugs of abuse. In my discussion I will discuss the results of my thesis work in the context of literature in the field and consider how future work could build upon the findings we present here.

4.1 Mechanisms for drug withdrawal driven plasticity

In the two studies presented within my thesis work, we demonstrate that withdrawal from drugs of abuse result in synaptic plasticity of glutamatergic transmission in LHb circuits. Whilst the nature of the plasticity is clear in both instances (altered presynaptic glutamate release probability in cocaine withdrawal; depression of postsynaptic AMPA transmission in morphine withdrawal), the precise mechanisms at the cellular and/or circuit level that could be driving this plasticity are unclear. In the case of morphine withdrawal, we showed that the depression of AMPA:NMDA ratio is dependent on TNFα acting on TNF-R1 yet the cellular pathway linking these two events is unknown. Concerning cocaine withdrawal, a variety of different factors are known to regulate long term plasticity of axonal neurotransmitter release probability, some of

which are known to be modified by drug exposure. Many of these cellular mechanisms are instigated by alterations of neural activity upstream of the synaptic adaptations.

4.1.1 Cellular mechanisms for morphine withdrawal plasticity

Our data show that locally released TNFα acting on TNF-R1 receptors is critical for the postsynaptic depression observed in LHb neurons projecting to the Raphe in morphine withdrawal. The means by which TNFα release is induced by morphine withdrawal remains unclear however. Endogenous release of TNFα from microglia was induced by bath application of monophosphoryl lipid A (MPLA), which acts on microglial Toll-like receptor 4 (TLR4) to drive TNFα release. This pharmacological manipulation of neuro-immune signalling reduced AMPA currents in mice which received chronic morphine treatment. However, this depression of AMPA by MPLA was occluded in mice which received a subsequent injection of the μ-opioid receptor (MOR) antagonist naloxone, which precipitates the emergence of withdrawal symptoms. Further experiments confirmed the MPLA driven AMPA depression was dependent on endogenous TNFα. This data indicates that LHb TLR4 engagement could represent a pathway activated during morphine withdrawal to drive an increase in local TNFα levels thus depressing AMPA transmission (Figure 11). In line with this both spontaneous and precipitated morphine withdrawal resulted in increased TNFα immunoreactivity in the LHb, a phenomenon also observed in the striatum following spontaneous morphine withdrawal (Campbell et al., 2013). Adaptations within this neuroimmune pathways are perhaps unsurprising given the interaction of opioid drugs on immune regulators, however the direction of these changes are in contrast to literature evaluating the nature of opioid drug action on TLR4. Acute morphine applied onto spleen cultures acts as an agonist for TLR4 pathways whilst naloxone instead acts as an antagonist (Hutchinson et al., 2010). In line with this, acute, subcutaneous morphine injections result in a transient increase in blood levels of inflammatory cytokines, followed by a sharp decrease in their levels (Pacifici et al., 2000). Together, these data would predict for a suppression of inflammatory cytokines during naloxone precipitated withdrawal, the opposite of what we observe in the LHb. A possible reason for this discrepancy lies in differential action of morphine at TLR4 in the brain vs spleen/blood, or adaptations to the system following chronic, rather than acute morphine treatment. Future experiments will be needed to confirm whether TLR4 activation is the means by which morphine withdrawal drives TNFα release in the brain, and if so, to determine the precise means by which brain TLR4 signalling is recruited.

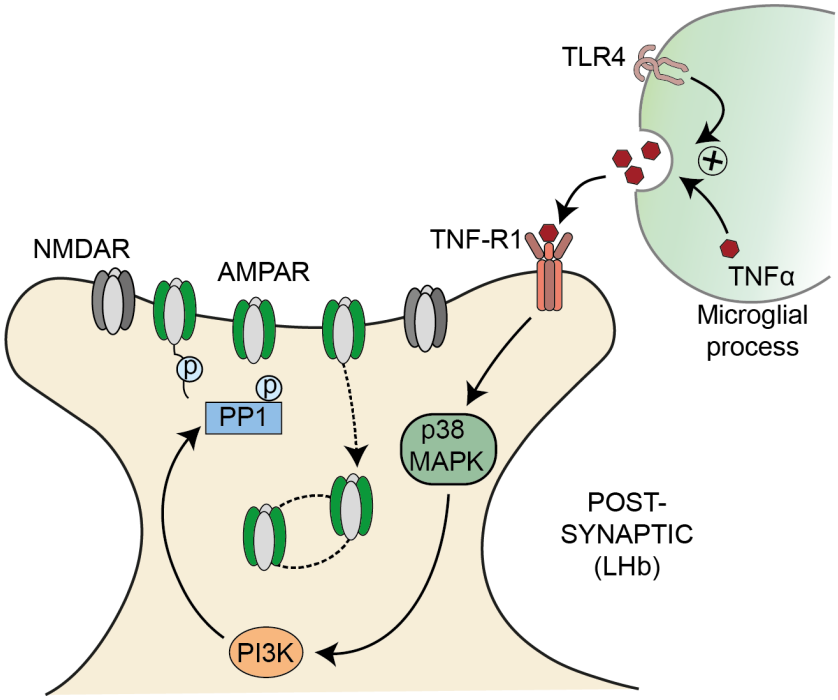

Figure 11. Putative cellular mechanism for morphine withdrawal LTD in LHb. Activation of TLR4 induces TNFα release from microglia. TNFα acting on postsynaptic TNF-R1 triggers a molecular cascade involving the kinases p38 MAPK and PI3K. This leads to the activation of PP1. PP1 has been shown to mediate forms of AMPA LTD elsewhere in the brain by dephosphorylating AMPA receptors, driving their endocytosis and thus decreasing the relative proportion of AMPA receptors to NMDA receptors.

Another outstanding question stemming from the data presented in the first portion of my thesis concerns the cellular/molecular pathway linking TNFα acting on LHb TNF-R1 and the resultant suppression of AMPA transmission (Figure 11). TNFα modulation of both glutamatergic and GABAergic transmission has previously been described in other regions of the brain. The majority of studies to date present a scenario whereby excitatory transmission is potentiated and inhibitory transmission suppressed (Heir & Stellwagen., 2020). However, in line with our results, suppression of AMPA by TNFα has also been described previously in the Striatum (Lewitus et al., 2014). In pyramidal neurons of the hippocampus, exogenous application of TNFα to cell cultures results in a rapid exocytosis of AMPA receptors, doubling the amount present on the cell membrane (Stellwagen et al., 2005). Concomitant with this increase in AMPAR surface expression is an endocytosis of $GABA_A$ receptors. Altogether this dramatically alters the ratio of Excitatory:Inhibitory (E:I ratio) synaptic transmission on to these neurons (Stellwagen et al., 2005). These adaptations to acute TNFα are thought to contribute to excitotoxicity mediated cell death following damage to the nervous system. More recent experiments have provided a thorough examination of the molecular pathway downstream of TNF-R1 activation driving the insertion of $GABA_A$ receptors by inhibiting the activity of individual elements of the cascade to block the plasticity. This process acts via p38 mitogen-activated protein kinases (p38 MAPK) which in turn activates Phosphoinositide 3-kinase (PI3K). The activity of these kinases results in the dephosphorylation of $GABA_A$ receptors by Protein phosphatase 1 (PP1) (Pribiag & Stellwagen, 2013) leading to their endocytosis. Interestingly, PP1, which is expressed throughout several regions of the brain including within the habenular nuclei (da Cruz e Silva et al., 1995) is also capable of driving endocytosis of AMPA receptors (Morishita et al., 2001). Additionally, blocking the activity of p38 MAPK specifically in the LHb reverses depressive symptoms induced by neuroinflammation (Zhao et al., 2018) and stress has been shown to increase levels of PI3K in the LHb (Levinstein et al., 2020). Thus, whilst this molecular cascade downstream of TNFα downscales $GABA_A$ in the hippocampus, it is possible it could instead act in the LHb to drive AMPAR internalization during morphine withdrawal, independently of any potential effects on GABA transmission (Figure 11).

4.1.2 Mechanisms for cocaine withdrawal plasticity

Our data shows that cocaine withdrawal drives opposing forms of presynaptic plasticity of glutamate release probability from LHb axons innervating VTA neurons projecting to the mPFC and NAc. Two important questions arising from this result are: What mechanisms are mediating the cocaine withdrawal driven presynaptic Long-term Depression (LTD) and Long-term Potentiation (LTP)? And are these mechanisms a result of altered activity in corresponding sub-circuits upstream to the LHb during cocaine withdrawal?

4.1.2.1 Factors regulating plasticity of glutamate release probability

Synaptic glutamate transmission occurs following the generation of action potentials in glutamatergic cell somas, driving depolarisation and resultant influx of calcium into axon terminals, driving the exocytosis of synaptic vesicles to the cell membrane. glutamate released into the synaptic cleft acts on a variety of postsynaptic receptors resulting in excitatory postsynaptic currents which cumulatively serve to drive the postsynaptic neuron to emit action potentials itself. Plasticity of this process, either strengthening or weakening of synaptic transmission, is well recognised to underlie fundamental learning processes as well as maladaptive behaviours and states emerging in psychiatric disorders such as addiction. Historically, a large debate in the field concerned the origin of such plasticity – whether it concerned adaptation of presynaptic neurotransmitter release, or postsynaptic alterations affecting the efficacy of these neurotransmitters at the postsynaptic membrane. Early research favoured a postsynaptic locus of expression, driven predominantly by alterations in glutamate

receptor subtypes. However, it is now clear that long-term modifications to either side of the synapse occur. As we see in our data, presynaptic plasticity involves the scaling up or down of neurotransmitter release.

Presynaptic plasticity can be observed by various electrophysiological measures, of which the most commonly applied is changes in paired pulse ratio (PPR) – the ratio of the Excitatory Postsynaptic Current (EPSC) generated by the second of two high frequency pulses relative to the first. The extent of depression of these EPSCs correlates with neurotransmitter release probability (in most, but not all cases). We employed pulse stimulation trains - which apply the same principle – to unveil cocaine withdrawal driven plasticity. Presynaptic plasticity of neurotransmitter release is achieved by numerous distinct mechanisms throughout the brain (for a review see Yang & Calakos, 2013). Rather than providing an exhaustive description of all the possible mechanisms discovered to date, I will consider the applicability of certain mechanisms to the plasticity we observe in the LHb projection to the VTA during cocaine withdrawal (Figure 12).

The first described LTP of glutamate release was observed at mossy fiber synapses – connecting granule cells of the dentate gyrus with pyramidal neurons in the CA3 region of the hippocampus (Zalutsky & Nicoll, 1990). Brief, high frequency stimulation of mossy fibre afferents resulted in a potentiation of EPSCs due to an increase in glutamate release probability. This activity-driven plasticity was shown to be dependent on calcium influx both in the granule cell soma and at the axon terminal. Interestingly, and unlike other plasticity previously unearthed it occurred independent of postsynaptic membrane potential, NMDA receptors or calcium concentration (Zalutsky & Nicoll, 1990). This represented evidence that presynaptic activity alone could drive presynaptic plasticity, irrespective of postsynaptic activity. This phenomenon, albeit with diverse mechanistic underpinnings, has since been observed in numerous other brain circuits. Alternatively, induction of certain forms of presynaptic plasticity relies on the release of retrograde messengers from postsynaptic neurons, typically upon depolarisation.

BDNF-TrkB dependent plasticity

The plasticity of mossy fiber synapses was dependent on tropomyosin receptor kinase B (TrkB) signalling (Huang et al., 2008; Schildt et al., 2013). Interestingly, levels of brain derived neurotrophic factor (BDNF), a high-affinity ligand of TrkB, are dramatically increased in many brain regions during cocaine withdrawal, including the VTA (Grimm et al., 2003; Pu et al., 2006). Furthermore, it has been shown that BDNF infused into the VTA drives increased cocaine-seeking following withdrawal in rats (Lu et al., 2004) and clinical studies have found that heightened BDNF levels are predictive of cocaine relapse (D'sa et al., 2011). BDNF-TrkB signalling is well recognised to regulate synaptic plasticity processes in many portions of the brain (Kowiański et al., 2017). This increase in VTA BDNF facilitates the induction of presynaptic LTP of glutamate release on to VTA DA neurons. A weak presynaptic afferent stimulation protocol results in LTP of glutamate release only in cocaine withdrawn rats and is also dependent on BDNF-TrkB signalling (Pu et al., 2006). Interestingly, whilst the LTP could be elicited purely by weak presynaptic stimulation, its induction was dependent specifically on postsynaptic BDNF-TrkB signalling as well as postsynaptic NMDA receptors. This involvement of the postsynaptic neuron suggests the potential role of a retrograde messenger, downstream of BDNF-TrkB signalling, emitted from the postsynaptic DA neuron to act on presynaptic release mechanisms. Whilst these BDNF-TrkB mediated adaptations occur at excitatory inputs to putative VTA DA neurons, rather than output-defined VTA neurons as is the case in our study, it is plausible that BDNF elevations during cocaine withdrawal similarly impact excitatory LHb input to VTA projections to the mPFC by lowering the threshold for LTP induction in this pathway.

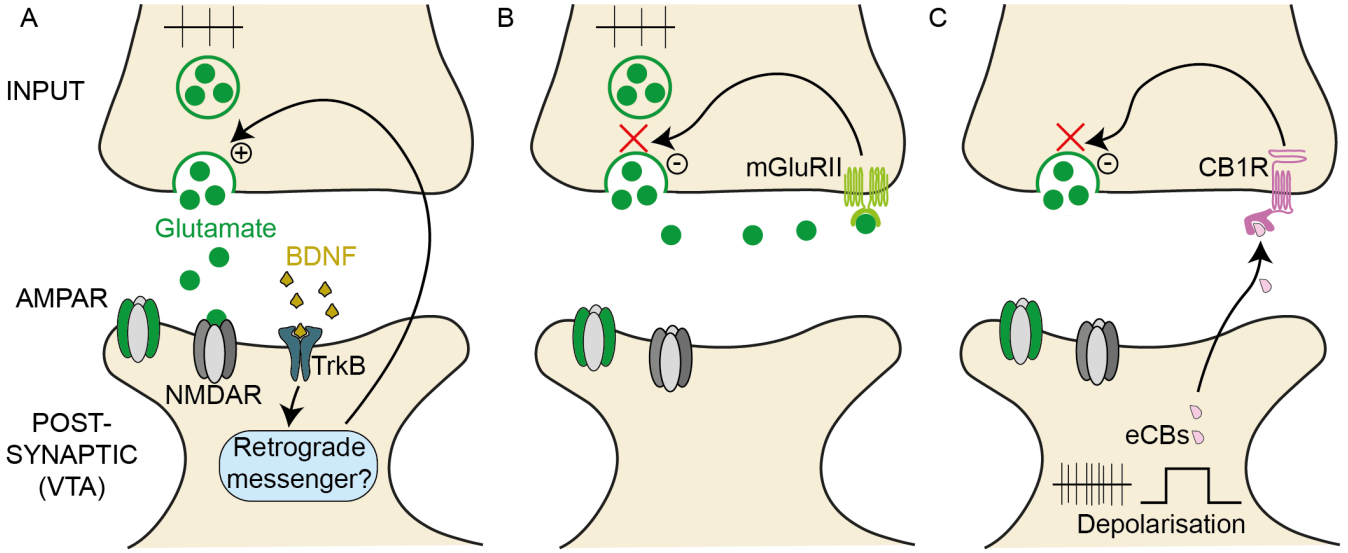

Figure 12. Regulation of presynaptic glutamate release in the VTA can be hijacked by drugs. **A**. Cocaine withdrawal facilitates the induction of presynaptic LTP in the VTA - a process mediated by postsynaptic AMPAR and BDNF-TrkB signalling, possibly resulting in release of retrograde messengers that promote glutamate release. **B.** Many instances of presynaptic LTD require the function of presynaptic mGluRII during weak stimulation. mGluRII agonism diminishes glutamate release, an effect that is attenuated in the VTA during morphine withdrawal. **C.** Alternatively LTD of presynaptic glutamate release is mediate by eCB release following postsynaptic depolarisation. eCBs are retrogradely transported and act on presynaptic CB1Rs to suppress glutamate release. CB1R agonism mediated depression of glutamate release in the VTA is attenuated following cocaine exposure.

mGluRII dependent plasticity

glutamate release is also regulated by its own action at presynaptic type II metabotropic glutamate receptors (mGluRII). Activation of mGluRII drives a reduction in glutamate release. This acute action has been shown to play a pivotal role in LTD of glutamate release. mGluRII dependent LTD, induced by low frequency stimulation was also first described at mossy fiber synapses (Kobayashi et al., 1996; Yokoi et al., 1996) but has since been found in several other regions including in the NAc (Robbe et al., 2002). The agonism of mGluRII receptors is also sufficient to drive this plasticity in the absence of electrical stimulation and occludes further LTD driven by electrical stimulation of afferents (Robbe et al., 2002; Tzounopoulos et al., 1998). Concerning the involvement of mGluRII mediated LTD in addiction, it was shown that the mGluRII mediated presynaptic depression of excitatory currents in VTA DA neurons was potentiated in morphine withdrawn rats (Manzoni & Williams, 1999). This could suggest for an increase in number/function of mGluRIIs at this synapse which may drive a decrease in glutamate release. An additional possibility is that glutamate release on to VTA DA is scaled up in morphine withdrawal, thus increasing the effective window of mGluRII action. In this scenario, mGluRII agonism could be seen to be rectifying maladaptations of glutamatergic transmission. To this end, mGluRII agonists/positive allosteric modulators have been shown to ameliorate addictive behaviours in preclinical models of both opioid and cocaine addiction (Bossert et al., 2006; Cannella et al., 2013; Jin et al., 2010). Whether mGluRII mediated adaptations could occur following cocaine withdrawal, and could impinge upon LHb transmission in the VTA to evoke output specific alterations in glutamate release remains to be tested.

Endocannabinoid dependent plasticity

Presynaptic plasticity is also tightly regulated in many regions of the brain by the release of retrograde messengers from postsynaptic neurons in response to depolarisation. These messengers act on receptors located on presynaptic axon terminals to regulate neurotransmitter release properties. Principle among these are endocannabinoids (eCBs). eCBs can diminish the

release of both glutamate and GABA by acting at CB1 receptors on presynaptic terminals. They are abundantly expressed in several specific nuclei of the brain. Electrical stimulation protocols eliciting LTD of glutamate/GABA release have been revealed in numerous brain regions including those critical for drug-driven behaviours such as the VTA, NAc and mPFC.

The eCB system is highly implicated in drug addiction for a range of drugs, not just cannabis. Acute cocaine intake drives the release of eCBs in the VTA where they act to supress GABA inputs to DA neurons (Wang et al., 2015a). In this way they disinhibit DA neurons thus regulating DA release and the behavioural rewarding effects of cocaine intake (Cheer et al., 2007; Li et al., 2009). Cocaine applied to VTA slices facilitates the establishment of LTD of inhibitory transmission in DA neurons mediated by eCB signalling, a process which is occluded following repeated exposure to cocaine (Pan et al., 2008). Whilst most work into eCB mediated presynaptic plasticity during cocaine has focused on inhibitory transmission, it also potently regulates excitatory input to VTA DA neurons. Combining electrical stimulation (2Hz) of afferents with postsynaptic depolarisation of DA neurons results in a robust LTD of glutamate release that is dependent on eCB signalling (Haj-Dahmane & Shen, 2010). The ability to induce this LTD is abolished following repeated cocaine exposure, due to impaired function of presynaptic CB1 receptors (Wang et al., 2020). This could be the result of occlusion, that this eCB mediated LTD has already occurred and underlies a reduction in excitatory transmission. Whether such an LTD would persist into cocaine withdrawal and if it occurs globally throughout the VTA or in specific population such as those deliniated in our study remains unknown. Interestingly, CB1 receptors are also present in the LHb where they regulate presynaptic plasticity and are proposed to control impulsive drug-seeking behaviours (Valentinova & Mameli, 2016; Zapata & Lupica, 2021). Thus, both the VTA and the LHb are influenced by eCB signalling to guide cocaine-related behaviours. This opens the possibility that the synaptic connections between the two, and the plasticity of these synapses during cocaine withdrawal, could be under the control of eCB signalling also.

4.1.2.2 Neural circuit activity driving LHb-to-VTA plasticity

Whilst these previously described forms of presynaptic plasticity of glutamate release may account for cocaine withdrawal driven output specific plasticity in LHb-to-VTA transmission, they do not consider the neural activity dynamics preceding and leading to such plasticity. Both the BDNF mediated potentiation of glutamate release in the VTA and classical protocols of mGluRII mediated LTD only require stimulation of afferent inputs, although the former requires intact postsynaptic BDNF-TrkB signalling. eCB mediated LTD additionally required DA neurons depolarisation to drive the release of eCBs. Thus, both the activity of LHb afferents to the VTA and of distinct VTA projections must be considered as either or both could be involved in producing the opposing forms of plasticity we observe (Figure 13).

Previous work from our laboratory and others have shown that LHb neurons undergo myriad adaptations during cocaine withdrawal that collectively serve to increase their activity (Maroteaux & Mameli, 2012; Meye et al., 2015, 2016; Neumann et al., 2014; Tan et al., 2019). However, the large focus of this work has been on these alterations occurring in RMTg projecting LHb neurons, rather than VTA projecting neurons as is the case in my thesis work. In fact, no changes in either the frequency or amplitude of spontaneous EPSCs were observed in VTA projecting LHb neurons during cocaine withdrawal (Meye et al., 2015). However, the data presented in our study demonstrate that LHb targets different VTA projections and that cocaine withdrawal modifies glutamate release in opposite directions in these two populations. It is thus plausible that these output specific populations are innervated by distinct sets of LHb neurons which may undergo corresponding opposing shifts in activity, resulting in activity dependant plasticity of glutamate release at these output specific VTA synapses. Independent studies employing the same foot-shock stress protocol have previously shown that this experience

drives hyperactivity of LHb neurons (Lecca et al., 2016) and well as a corresponding increase in neurotransmitter release probability at downstream synapses (Stamatakis & Stuber, 2012). This suggests that altered LHb activity could lead to downstream adaptations in glutamate release probability. Unfortunately, viral methods to date are unable to disentangle whether output-specific neuronal populations of one brain region could be targeted by distinct or overlapping populations of another. However, the field of viral tracing is rapidly developing. Should such technology become available it would be possible to discern if these output-specific VTA populations are targeted by independent LHb populations – supporting a circuit activity led plasticity originating in diverging activity of these LHb populations during withdrawal. An alternative solution, although technically challenging and laborious, would be to perform juxtacellular labelling of individual VTA-projecting LHb neurons identified by antidromic VTA stimulation. Combining axonal reconstruction with retrograde tracer injections of different indicators into the NAc and mPFC, one would be able to visualise whether individual LHb neurons make synaptic contacts on to both of these populations or are specialised.

Given the importance of activity-dependent release of retrograde messengers such as eCBs on afferent glutamate release, it is possible that differential activity of output specific VTA populations during either acute cocaine intake or during cocaine withdrawal could precede, and be causal for, the emergence of plasticity in the LHb-to-VTA circuit. In such a case it would be possible that this divergent plasticity on to these output-specific populations would also be present in other inputs providing excitatory input to both. Viral tracing studies indicate such an input may arise from the LH (Beier et al 2015; 2019). Whilst this specific issue remains untested, cocaine use does not evoke uniform VTA responses, both in terms of acute activity and persistent adaptations. A single injection of cocaine potentiates excitatory postsynaptic strength in NAc projecting but not mPFC projecting VTA neurons, which persists for up to days (Lammel et al., 2011). Additionally, Mejias-Aponte and colleagues (2015) demonstrated that acute cocaine administration drove a mixture of excitatory and inhibitory responses in both DA and non-DA neurons. What factors underlie this functional diversity remain unknown. Future experiments should continue to probe VTA adaptations in addiction using modern viral tools allowing for selection of precise subpopulations as understanding their different roles will provide a more refined understanding of the aetiology of addictive behaviour.

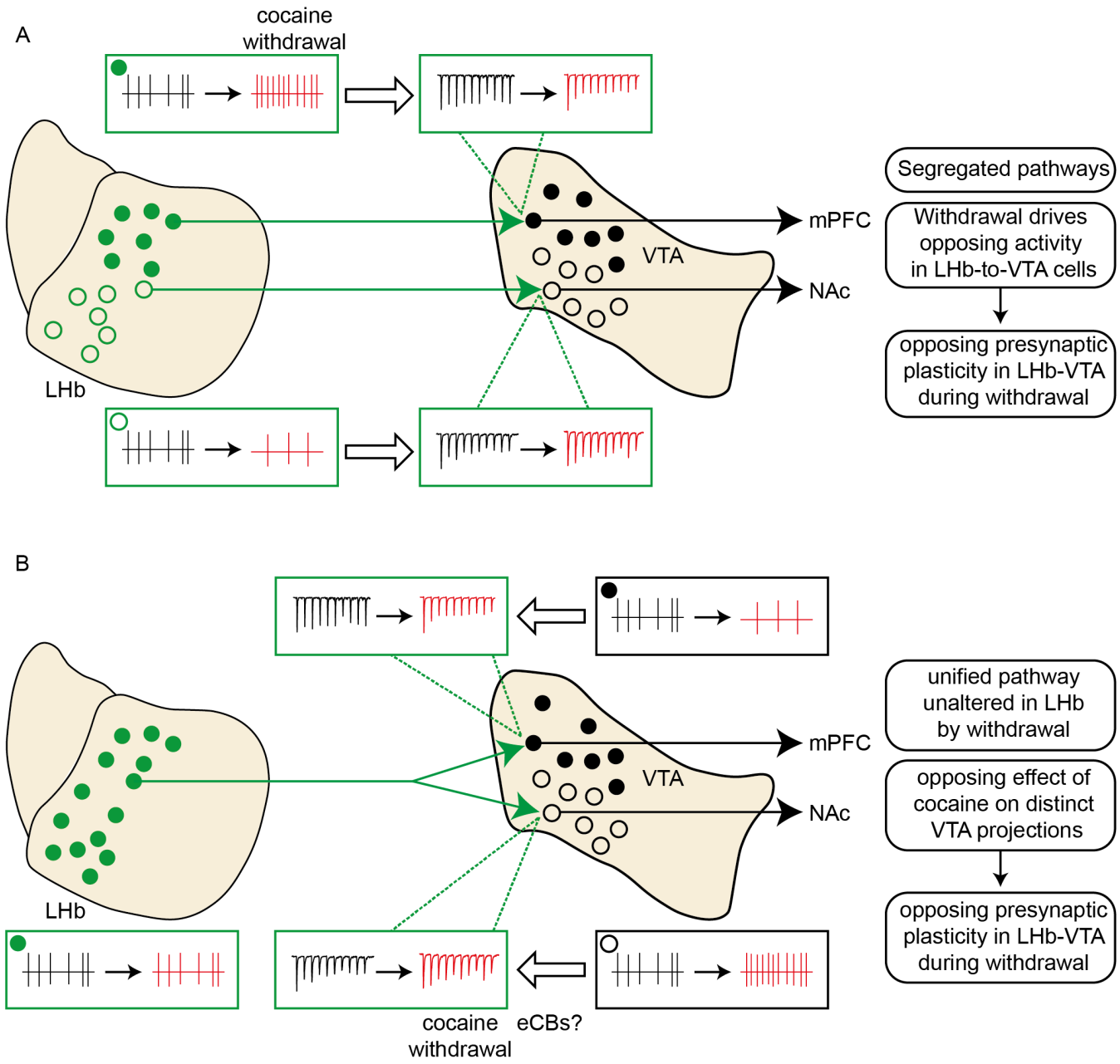

Figure 13. Potential circuit activity promoting cocaine withdrawal plasticity of LHb-to-VTA circuit. A. VTA neurons projecting to mPFC and NAc may be innervated by distinct sets of LHb projections. In this scenario, it is possible that the opposing synaptic plasticity at LHb-to-VTA synapses occurs downstream of opposing adaptations of activity in the LHb. Such adaptations in would have been missed by previous recordings in the LHb during cocaine withdrawal due to a net zero effect of these adapatations. **B.** Alternatively, mPFC and NAc projecting VTA neurons may be innervated by the same group of LHb neurons which do not undergo changes in activity during cocaine withdrawal. In this scenario, the opposing synaptic plasticity in LHb-to-VTA synapses may instead by the result of alterations in activity in the distinct VTA projections, and the release of retrograde messengers such as eCBs which can drive presynaptic plasticity of glutamate release.

Altogether, plasticity of LHb glutamate release in the VTA by cocaine withdrawal could be mediated by a wide range of both cellular processes (Figure 12), localised at the synapses within the VTA, as well as the activity of the neuronal populations at both sides of these synapses (Figure 13). It is possible that a combination of both of these factors intersect or are causally linked. Each of the cellular mechanisms for plasticity ultimately depend on presynaptic stimulation with some also requiring certain postsynaptic signalling mechanisms. The involvement of these cellular systems in driving LTP/LTD of LHb glutamate release in cocaine withdrawal could be evaluated by experiments testing if the generation of these forms of plasticity are occluded in cocaine withdrawal whilst remaining inducible in saline treated mice. Such

experiments have previously been applied to reveal mechanisms underlying presynaptic plasticity of GABA release in the VTA following cocaine exposure (Bocklisch et al., 2013)

4.2 Functional circuit and behavioural ramifications of drug withdrawal driven plasticity

These two articles serve to further our understanding of LHb circuit adaptations in drug withdrawal by uncovering circuit-specific plasticity in LHb projections of brain centres regulating motivated behaviours – the VTA and DRN, for cocaine and morphine withdrawal respectively. Yet the functional consequences of these adaptations are still not fully understood. Whilst we observe that plasticity of LHb projections to the Raphe during morphine withdrawal critically underlies sociability deficits, how this plasticity may influence the activity of distinct raphe populations to achieve this goal remains unknown. We also see that cocaine withdrawal drives opposing plasticity of LHb innervation of distinct output projections of the VTA, however, the behavioural consequences of these adaptations, and their contribution to the cocaine withdrawal state, remain unknown. In this section I will examine both these outstanding issues.

4.2.1 Repercussions of morphine withdrawal in LHb on Raphe circuits regulating social behaviour

We find that the LHb projection to the Raphe regulates social behaviour. Chemogenetic inhibition of this pathway decreases sociability, mimicking the morphine withdrawal driven sociability deficit. By disrupting LHb TNFα signalling we can rectify the plasticity observed exclusively in Raphe projecting LHb neurons, and thus normalize social behaviour. Yet it is unclear which populations in the Raphe the LHb could be targeting to control this behaviour. Whole brain mapping using monosynaptic rabies tracing, as well as optogenetic-assisted circuit mapping have shown that the LHb directly innervates serotonin neurons of the DRN (Pollak-Doricic et al., 2014), whilst they may also target DRN DA (Cardozo-Pinto et al., 2019) and GABA (Liu et al., 2021) neurons. Each of these three DRN populations have been shown to regulate social behaviour in distinct ways.

4.2.1.1 DRN serotonin neurons

Early indications of a role for serotonin in regulating social behaviours came from studies looking at aggression. A collection of data supports a hypothesis that serotonin inhibits aggressive behaviour (Duke et al., 2013; Quadros et al., 2010). Principle among these studies are initial works demonstrating an inverse correlation of serotonin levels and aggression in both mice (Giacalone et al., 1968) and humans (Brown et al., 1979) which were followed by causal evidence in the form of studies employing tryptophan depletion and serotonin receptor agonists to modulate aggression up and down respectively (Kantak et al., 1980; Olivier et al., 1995). More recently, activity of serotonin neurons of the DRN have been shown to encode social reward. Photometric recordings of DRN serotonin population activity show that they are excited upon presentation of numerous rewarding stimuli including during social interaction (Li et al., 2013). It is likely that this is mediated by DRN serotonin projections to the NAc. Using a modified version of CPP, Dölen and colleagues (2013) demonstrated that preference for a context associated with social interaction (vs isolation) depended on the integrity of DRN projections to the NAc and serotonin 1B receptor signalling in the NAc. The action of DRN serotonin in the NAc, and of serotonin on 1B receptors in the NAc, has also been shown to specifically mediate the prosocial effects of the commonly abused recreational drug (±)3,4-methylenedioxymethamphetamine (MDMA) (Heifets et al., 2019).

Morphine withdrawal decreases basal serotonin levels in the NAc (Antkiewicz-Michaluk et al., 1995; Harris & Ashton-Jones, 2001). This decrease is thought to underlie aspects of

negative reinforcement of drug use as locally blocking the uptake of serotonin in the NAc with fluoxetine, and thus increasing NAc serotonin levels, abolished the increased morphine preference observed during withdrawal (Harris & Ashton-Jones, 2001). Interestingly, systemic fluoxetine treatment also reversed anxiety-like symptoms during morphine withdrawal. Given that the synaptic depression on to DRN projecting LHb neurons could in turn lead to a diminished excitatory drive on to NAc projecting serotonin neurons, it is plausible that these two independent observations are at least partially related to each other (Figure 14).

Additionally, there exists combined serotonin/glutamate and serotonin/GABA neurons (Fu et al., 2010). serotonin/glutamate neurons are known to project to the VTA and where they innervate NAc-projecting DA neurons and thus drive rewarding behaviours (Wang et al., 2019). The precise role of either of these subtypes in the control of social behaviour is currently unknown.

4.2.1.2 DRN DA neurons

Whilst DA neurons principally reside in the VTA, a substantial population which has been comparatively less studied are also found in the DRN. Synaptic input to these neurons are strengthened following a period of social isolation (Matthews et al., 2016). Additionally, whilst normally not responsive to social interaction, DRN DA neurons are excited by it when it follows a period of isolation and their activation triggers increased social preference in the same 3-chamber social preference test used in our study examining morphine withdrawal. Interestingly, this modulation was bidirectional, and the rebound increase in sociability normally observed following a period of isolation was abolished by DRN DA inhibition. It could thus be hypothesised that decreased excitatory drive on to DRN DA neurons may contribute to diminished natural aversion to loneliness.

4.2.1.3 DRN GABA neurons

Local GABA interneurons of the DRN provide inhibitory tone to DRN serotonin neurons. Social defeat stress increases excitability of DRN GABA neurons, driving a consequent presynaptic strengthening of local inhibitory input on to DRN serotonin neurons which instead show a decrease in excitability (Challis et al., 2013). Further experiments demonstrated that DRN GABA neuron activity was necessary for the acquisition of social avoidance of an aggressor mouse (Challis et al., 2013). Interestingly, in morphine trained rats who underwent swim stress - which reliably drives reinstatement of extinguished drug seeking – GABAergic transmission in DRN serotonin neurons is also potentiated, however this appears to be due to postsynaptic, rather than presynaptic modifications (Staub et al., 2012). Thus, it appears that DRN GABA neurons oppose the prosocial role of DRN serotonin neurons by providing local inhibition. In light of this, it would appear contradictory if the excitatory LHb projection to the raphe were to be preferentially innervating DRN GABA, given that we show that it's inhibition/synaptic suppression is antisocial.

Altogether, all three neurochemical subtypes of serotonin neuron likely act in concert to regulate social behaviour with serotonin and GABA neurons functionally opposing each other in this regard whilst DRN DA neurons appear to specifically regulate the neural response to social isolation. Given the evidence supporting a role of DRN serotonergic projections to the NAc positively regulating social behaviour (Dölen et al., 2013), combined with studies demonstrating a role of depleted NAc serotonin in morphine withdrawal (Antkiewicz-Michaluk et al., 1995; Harris & Ashton-Jones, 2001), an enticing possibility is that LHb afferents control this projection to mediate social behaviour and this pathway is depressed in morphine withdrawal (Figure 14). Future experiments should seek to interrogate the downstream repercussions of this plasticity

by probing LHb innervation of distinct DRN populations based on cell-type and output projection and how it is altered in morphine withdrawal.

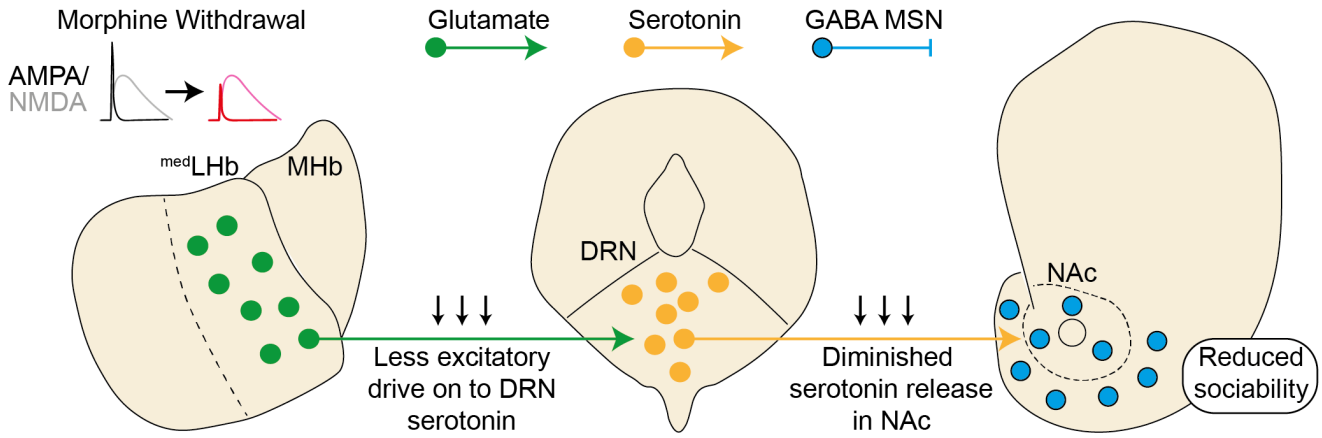

Figure 14. Candidate circuit mechanism underlying morphine withdrawal social deficits. Morphine withdrawal drives an LTD of AMPA transmission in medially located DRN-projecting LHb neurons which are known to target serotonin neurons of the DRN. This could lead do diminshed excitatory drive on to serotonin neurons, and consequently account for the decrease in serotonin release observed in the NAc during morphine withdrawal. Given the role DRN serotonin projections to the NAc play in regulating social reward, it is possible that the LHb-DRN-NAc circuit mediates social deficits during morphine withdrawal.

4.2.2 Repercussions of LHb-to-VTA plasticity in cocaine withdrawal on VTA circuits and associated behaviour

We find that cocaine withdrawal strengthens LHb input to mPFC-projecting VTA neurons, and weakens LHb input to NAc projectors. Additionally, we observe that LHb afferents to the VTA preferentially target non-DA neurons over DA neurons located in the medial portion of the VTA. This data is complemented by surprising findings that a large fraction of neurons retrogradely labelled by Herpes Simplex Virus (HSV) injected into either the NAc or mPFC, were also non-DA (Appendix – Figure 17). These findings do not corroborate with previous work using alternative retrograde tracers (Lammel et al., 2011, yet see also Yamaguchi et al., 2011), and raise the possibility that the viral tool we employed to label VTA projection neurons might have unexpected preferences for specific neuronal populations. Previous research shows that HSV infection in neurons can diminish TH activity (Price et al., 1981) however, it is inconclusive whether this was a result of viral toxicity leading to eventual cell death. More recent viral preparations, such as the one we employ in our study (Neve, 2012) have eliminated this cytotoxic action of HSV of neurons. Thus, the output-specific plasticity from the LHb may occur at either or both DA and non-DA VTA projection neurons. I will consider how both these types of projections to the NAc and mPFC can regulate motivated behaviours, as well as how cocaine withdrawal plasticity of LHb-to-VTA transmission on to these subtypes could influence the pathology of cocaine withdrawal (Figure 15). Finally, we also observed that cocaine withdrawal did not alter LHb innervation of a VTA population projecting to the LH that has been shown to be a mixture of glutamate and GABA neurons that bidirectionally regulate arousal (Yu et al., 2019). Whilst this represents a previously undiscovered synaptic connection that in itself merits further study, given its apparent lack of participation in drug-withdrawal driven adaptations of LHb circuits – the focus of this thesis - I will not discuss further this connection.

4.2.2.1 VTA DA projections to the NAc

Whilst debate concerning the precise nature of the role of DA release in the NAc, a wealth of data supports the idea that VTA DA projections to the NAc represent one of the key reward-

seeking pathways of the brain (Wise, 2008). In line with this viewpoint, deficits in DA transmission in the NAc are proposed to contribute to dysfunctional reward processing present in numerous psychiatric disorders (Whitton et al., 2015). Examples of this include depressive symptoms such as anhedonia (inability to experience pleasure from normally pleasurable activities) and amotivation (lack of motivation to obtain rewards) (Wise, 2008). Neuroimaging studies of schizophrenia patients have shown deficient activity of the ventral striatum in response to reward - in which the NAc is located and is regulated by DA transmission among other inputs – correlating with measures of anhedonia and amotivation (Lee et al., 2015). In line with these clinical data, animal studies have demonstrated that DA release in the NAc in response to food is blunted in mice who have underwent chronic mild stress to elicit a depressive-like state (Di Chiara et al., 1999), whilst depletion of DA in the NAc significantly impairs the effort animals will expend to obtain food rewards (Salamone et al., 2003). Thus, the majority of data supports the idea that overall, VTA DA projections to the NAc are a critical component of reward behaviours.

Withdrawal from cocaine leads to a decrease in basal DA release in the NAc (Weiss et al., 1992), which may account for emergence of similar depressive symptoms including anhedonia during cocaine withdrawal. Interestingly, anhedonia arising during withdrawal from nicotine – which also contains psychostimulant properties – were ameliorated by local NAc administration of bupropion, which increases DA concentrations (Paterson et al., 2007). Downstream of DA release, D2 receptor containing MSNs in the NAc project to the VP. Cocaine withdrawal driven plasticity of this circuit mediates anhedonia during this phase (Creed et al., 2016). DA neuron activity, and the subsequent release of DA in the NAc, is tightly regulated by excitatory inputs to VTA DA neurons. Whilst previous studies have shown a preferential targeting of mPFC projecting DA neurons by LHb afferent (Lammel et al., 2012) we also see EPSCs in NAc projecting VTA neurons. The strength of this connection is weakened during cocaine withdrawal, which may partially contribute to diminished NAc DA and the associated emergence of anhedonia and amotivation (Figure 15).

4.2.2.2 VTA non-DA projections to the NAc

In addition to VTA DA neurons, VTA glutamate and GABA neurons have been shown to encode both rewarding and aversive stimuli as well as their predictors with transient excitation (Root et al., 2020). Optogenetic stimulation of VTA glutamatergic afferents in the NAc has been shown to be reinforcing (Yoo et al., 2016; Zell et al., 2019), or aversive (Qi et al., 2016) depending on the temporal duration of stimulation with brief stimulation shown to be appetitive and prolonged stimulation aversive. As well as glutamate- and DA- only VTA neurons, a population of combinatorial DA and glutamate neurons have been the subject of recent research. In line with a role of VTA-to-NAc glutamate in reward, deletion of glutamate specifically from VTA DA neurons impairs extinction of cocaine seeking (Alsiö et al., 2011). Furthermore, this intervention also increases AMPA:NMDA ratios in D1-MSNs, in a manner that occludes further potentiation in cocaine withdrawal (Papathanou et al., 2018). This suggests that VTA glutamate may play a regulatory role in excitatory synaptic strength on to NAc MSNs, a critical factor concerning drug-driven behavioural adaptations. In addition, whilst stimulation of VTA GABA projections to the NAc does not influence reward consumption (Van Zessen et al., 2012), it does regulate precise features of associative reward learning (Brown et al., 2012). Interestingly, cocaine withdrawal has been shown to drive presynaptic LTP of VTA glutamate, and presynaptic LTD of VTA GABA, on to MSNs in the core subregion of the NAc (Ishikawa et al., 2013), however the functional implications of these adaptations remain to be examined.

Altogether, both VTA glutamate and GABA projections to NAc may contribute to reward-seeking and reward learning behaviour, yet more work is required to parse out the specific roles of these projections and how they are altered by drug experience to contribute to addiction pathology. Understanding of the importance of VTA non-DA projections to the NAc in reward

processing would be improved by also temporally inhibiting these projections during precise events during reward learning to determine its contribution to behaviours normally considered the domain of VTA DA. As the LHb is known to target these populations (Beier et al., 2019) it is possible that cocaine withdrawal driven plasticity of LHb transmission on to VTA glutamate and GABA neurons could also contribute to distorted reward guided behaviours in cocaine addiction.

4.2.2.3 VTA DA projections to the mPFC

Whilst DA in the NAc is well recognised to regulate rewarding behaviours, the role of DA in the mPFC is less clear. Among other potential behavioural functions, a clear line of evidence implicates VTA DA projections to the mPFC in processing of aversive stimuli. Tail-pinch in rats transiently increases the activity of mPFC projecting DA neurons (Mantz et al., 1989) and DA release in the mPFC (Di Chiara et al., 1999). This release is potentiated in stress-driven depressive like states (Di Chiara et al., 1999) suggesting the transient encoding of aversion by this pathway can be hijacked to elicit aversive states, much like the hyperactivity of LHb neurons – which transiently encode aversive stimuli (Matsumoto & Hikosaka, 2005; 2007) – in aversive states (Cui et al., 2018; Lecca et al., 2016; Meye et al., 2015; Tchenio et al., 2017). Intriguingly, LHb neurons directly innervate mPFC-projecting DA neurons, and DA transmission in the mPFC regulates the conditioned place aversion driven by stimulating LHb afferents in the midbrain (Lammel et al., 2012). Additionally, excitatory transmission on to VTA DA neurons projecting to the mPFC is strengthened following aversive stimuli (Lammel et al., 2011). Recent studies have probed more precisely why aversive stimuli may engage this circuit. Optogenetic stimulation of VTA DA afferents enhanced the ability of mPFC neurons to encode aversive stimuli (Van der Wheele et al., 2018). Thus, excessive DA transmission in the mPFC may bias processing of stimuli to favour attention on negative stimuli, contributing to aversive states.

DA transmission in the mPFC is strongly implicated in drug addiction and particularly in relapse. Numerous studies (reviewed in Kalivas & Volkow, 2005) have shown the necessity of DA receptor activation in the mPFC, but not in the NAc, for reinstatement of drug seeking following extinction of self-administration. Furthermore, cocaine withdrawal elevates cocaine driven increases in DA transmission in the mPFC. (Williams & Steketee, 2005). This suggests that cocaine withdrawal may sensitize VTA-to-PFC DA transmission.

Collectively, an interpretation of these studies concerning VTA DA projections to the mPFC is that cocaine withdrawal could strengthen this circuit, to amplify the processing of aversive stimuli thus driving an aversive state that increases susceptibility to cocaine relapse, particularly following a stressful event (Figure 15). In such circumstances, enhanced excitatory innervation from LHb afferents, which also convey aversive signals, on to mPFC projecting VTA neurons could contribute to this sensitised DA transmission in the mPFC. This would manifest in the VTA as a heightened recruitment of mPFC projecting neurons by aversive stimuli – which could be tested using in-vivo electrophysiological techniques or, alternatively, c-fos colocalization following an aversive event. Causality with LHb axon plasticity could be achieved if a means to selectively depotentiate the LHb innervation of mPFC-projecting cells is unearthed (perhaps using specific optogenetic stimulation parameters (Creed et al., 2016)). This would also allow testing of this broader behavioural theory using stress-induced reinstatement of cocaine-induced conditioned place preference. We have previously shown that impaired GABA transmission from the EPN to RMTg-projecting neurons of the LHb regulates this behaviour alongside an effect on behavioural despair (Meye et al., 2016). Therefore, these independent circuits could act synergistically in this regard to mediate both long-term depressive symptoms and heightened temporally precise processing of stressful stimuli to collectively underlie this feature of cocaine withdrawal.

4.2.2.4 VTA non-DA projections to the mPFC

glutamate and GABA neurons of the VTA also project to the mPFC, as do combined glutamate/DA neurons (Carr & Sesack, 2000; Gorelova et al., 2012; Perez-Lopez et al., 2018; Yamaguchi et al., 2011). Interestingly, several studies suggest that the VTA projection to the mPFC may infact be principally a glutamate/GABA projection rather than mostly DAergic (Yamaguchi et al., 2011; Gorelova et al., 2012 but see also Lammel et al., 2011). Despite evidence of a prominent projection, no studies to date have attempted to examine the behavioural relevance of VTA glutamate and GABA in the mPFC in either physiological or disease contexts. Previous studies have demonstrated that LHb afferents target both these populations (Beier et al., 2019).

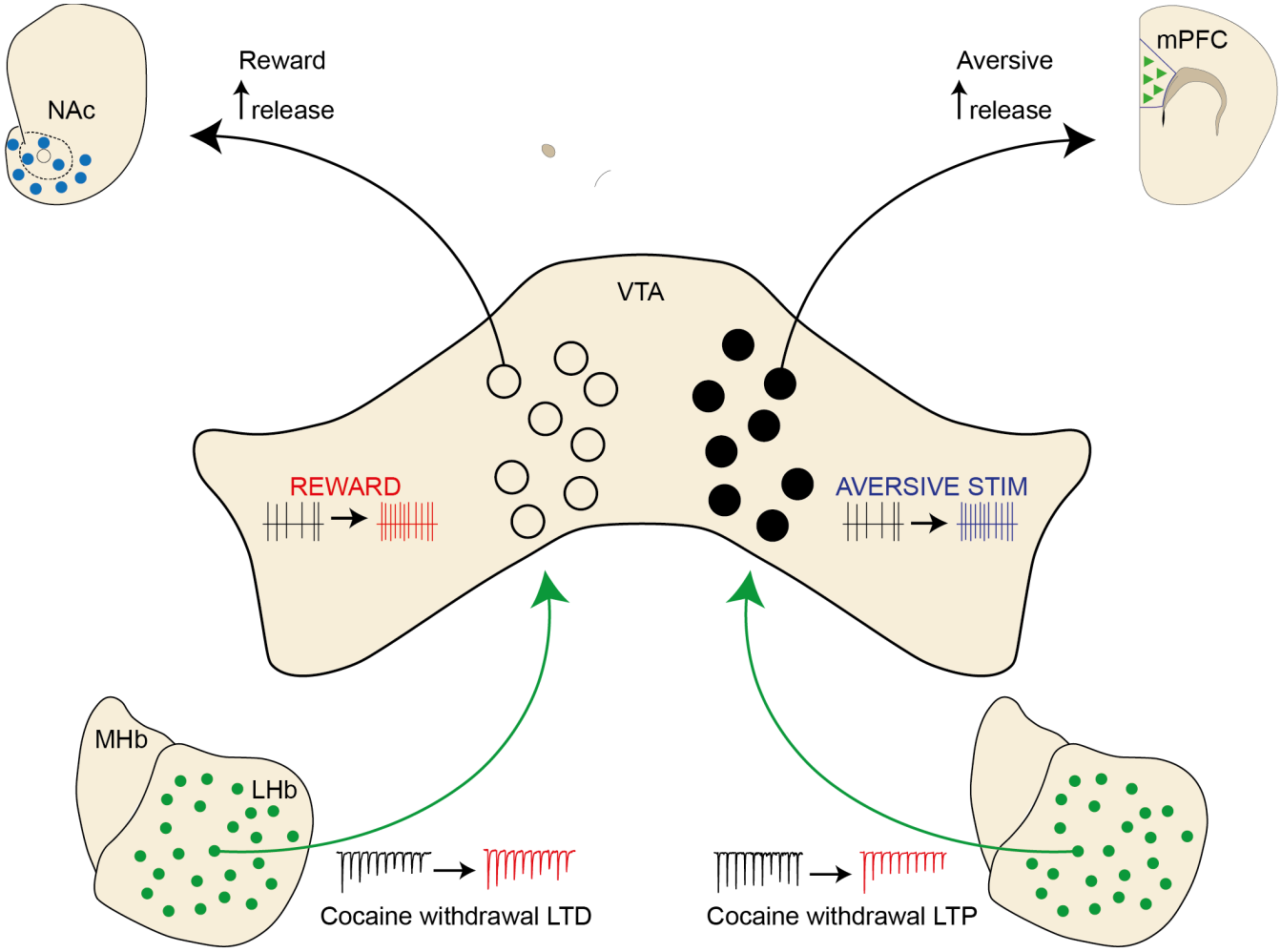

Figure 15. Medial VTA circuits involvement in motivated behaviours: theoretical framework for LHb-VTA adaptations underlying aversive state in cocaine withdrawal. VTA projections are engaged by and regulate opposing behviours. Both DA and glutamate NAc projecting neurons increase their activity in response to rewards, which also drive DA release in the NAc. Stimulation of VTA afferents in the NAc is reinforcing. On the other hand, mPFC projecting VTA DA neurons increase their firing in response to aversive stimuli which also drives DA release in the mPFC. VTA-to-mPFC DA also enhances mPFC encoding of aversive stimuli. Altogether, cocaine withdrawal driven depression of LHb projections to the rewarding NAc-projecting VTA neurons could can be considered a weakening of a rewarding pathway and drive deficient reward processing, whilst the potentiation of LHb innervation of mPFC projecting VTA neurons can be considered a strengthening of an aversive pathway and thus could contribute to enhanced aversion processing. Ultimately opposing LHb-to-VTA plasticity could contribute to the aversive state by diminishing reward and boosting aversion.

Altogether, it can be seen that VTA projections to the NAc are principally engaged in mediating features of reward related behaviours. Mice will readily self-stimulate both DA and

Glutatamte projections to the NAc, demonstrating the reinforcing, rewarding nature of these projections. Cocaine withdrawal weakens the strength of excitatory transmission from the LHb on to NAc projecting neurons. This could impair VTA-to-NAc signalling resulting in deficient reward processing. In view of this, it is possible that plasticity at LHb to NAc projecting VTA neurons may contribute to the emergence of anhedonia and amotivation in cocaine withdrawal. VTA DA projections to the mPFC are known to encode aversion and have been shown to be sensitised by cocaine withdrawal. DA release in the mPFC is strongly implicated in cocaine relapse initiate by both stress and cues. More work is required to determine if, like in the NAc, glutamate projections to the mPFC act synergistically alongside DA projections to mediate specific behavioural functions. Given available literature on stress-driven reinstatement and aversion encoding by both the LHb and VTA projections to the mPFC, it is possible that the strengthening of LHb transmission on to mPFC projectors may bias processing of negative stimuli, thus underlying increased irritability in cocaine withdrawal as well as susceptibility to stress-driven relapse (Figure 15).

4.3 Investigations into origins of LHb engagement by drugs of abuse: from acute administration to withdrawal

Whilst the data presented in my doctoral thesis describe plastic adaptations of LHb circuits associated with the negative state emerging during drug withdrawal, an open issue concerns how the LHb is engaged by drugs of abuse in the first place, and how short-term actions of drugs of abuse could lead to long term adaptations. A collection of studies at the turn of the millennia demonstrated that chronic exposure to a wide range of drugs of abuse all led to degeneration of LHb neurons and the fasciculus retroflexus, presumably through excitotoxicity (Carlson et al., 2000; Ellison, 2002). Despite considerable research since demonstrating LHb recruitment in drug driven behaviours and examining potential cellular mechanism, the link between the acute neuropharmacological actions of these drugs and LHb activity, at both acute and prolonged timescales, remains unclear.

4.3.1 Acute effects of Cocaine on LHb neurons

Acute cocaine drives pronounced effect on LHb electrophysiology in both in-vivo and slice preparations. In-vivo rat recordings revealed that a subset of LHb neurons responded with biphasic responses to cocaine administration. Cocaine at first inhibited LHb cell firing in a majority of LHb cells (13/20) before a rebound increase in firing relative to baseline in almost half of these cells (Jhou et al., 2013). This finding has since been complemented by similar proportional responses upstream in the EPN (Li et al., 2020). Interestingly, similar proportions of LHb neurons exhibited hyperpolarization only/biphasic currents in response to cocaine application in acute brain slices. Alternatively, cocaine applied to slices has been shown to result in a rapid depolarization in holding current, accompanied by an increase in presynaptic excitatory transmission and increased firing (Good et al., 2013; Zuo et al., 2013).

4.3.1.1 Does DA act in the LHb to mediate acute cocaine effects?

Despite these discrepant results, a uniform finding throughout these studies was the necessity of action at DA receptors in mediating these transient changes in response to acute cocaine administration (Good et al., 2013; Jhou et al., 2013; Zuo et al., 2013). As described earlier, cocaine acts to increase local DA concentrations in the synaptic cleft by binding DAT to prevent uptake of DA. Given the LHb receives dense innervation from the VTA, this supported a hypothesis that VTA DA is released in the LHb and its uptake would be hijacked by cocaine. However, stimulating VTA afferents in the LHb fails to elicit detectible levels of DA, instead resulting in glutamate and GABA release (Root et al., 2014; Stamatakis et al., 2013). Retrogradely labelled VTA neurons positive for the DA rate limiting enzyme Tyrosine Hydroxlase

(TH) have been consistently detected in rats (Gruber et al., 2007; Root et al., 2014), as have TH positive fibers which may or may not be from the same neurons (Aizawa et al., 2012; Gruber et al., 2007). Whether TH positive neurons in the mouse VTA send axons to the LHb is a matter of considerable debate (Lammel et al., 2015; Stamatakis et al., 2013; Stuber et al., 2015). If they do it appears they are deficient in both DAT and vesicular monoamine transporter, i.e. the machinery necessary for DA release (Stamatakis et al., 2013). Even when TH positive LHb neurons have been detected, TH-positive fibers are not present in the LHb of mice (Stamatakis et al., 2013). In light of these data, there are two possible explanations that could support an action of DA in the LHb in mediating the actions of cocaine on LHb neurons: 1) If the LHb is indeed targeted by VTA DA neurons that in standard physiological conditions do not release DA, it is possible that the profound effects of cocaine, or other compounds acting grossly and directly on DA transmission, may drive a rapid transcriptional regulation that effectively "awakens" dormant DA release from VTA-to-LHb. Cocaine is able to drive rapid (after 1 hour) changes in gene expression in the NAc (Savell et al., 2020; Zipperly et al., 2020) thus this is not inconceivable. 2) DA may be being released into the LHb from another source than the VTA. Although the majority of DA neurons reside in the VTA, they are also present in several other nuclei including regions of the hypothalamus, DRN and periaqueductal gray. The LHb is known to receive afferents from both the hypothalamus and DRN yet so far, functional demonstration of DA release from any of the many inputs to the LHb is lacking.

This ultimately leaves another possibility - that despite the involvement of DA receptors in mediating the acute effects of cocaine on LHb neurons, DA itself does not mediate these actions. As well as its primary affinity for DAT, cocaine also binds with high affinity the norepinephrine (NE) transporter (Ritz et al., 1990) and thus similarly increase NE transmission. Additionally, DAT is able to uptake NE (Torres et al., 2003). Thus, it is possible that cocaine is in fact driving considerable increases in LHb NE concentrations. Studies suggest that NE fibres are present in the LHb (Gottesfeld et al., 1983; Gruber et al., 2007) and may regulate anxious behaviour (Purvis et al., 2018). Not only does cocaine drive increases in NE concentrations, but NE has the ability to target D2-like (D2R, D3R, D4R) DA receptors and its action in the LHb, via these receptors (D4), is to depolarize LHb neurons (Root et al., 2015; Sanchez-Soto et al., 2016), similarly to the effect of cocaine observed in some studies (Good et al., 2013; Zuo et al., 2013). Further electrophysiological experiments demonstrated that selective DAT inhibition mediated a similar inward current that persisted despite prevention of impulse driven DA release, and that DAT inhibition impaired NE clearance in the LHb (Root et al., 2015).

Altogether, these results suggest that cocaine could drive acute excitation of LHb neurons mediated by increasing NE transmission. However, this does not necessarily exclude a role of DA transmission also. Cocaine in-vivo drives inhibition of a majority of LHb neurons with some showing rebound excitation – neither of which have been recapitulated by exogenous NE, but have by exogenous DA in slices and are mediated by D2 receptors (Jhou et al., 2013). Additionally, cocaine has been shown to potentiate excitatory synaptic transmission on to LHb slices, an effect mediated by D1-like receptors which, unlike D2-like receptors, is not a recognised target of NE (Zuo et al., 2013). Further experiments are required to definitively determine whether in-vivo LHb activity alterations following cocaine administration is mediated by the direct local action of DA and/or NE, as well as to probe the contribution of engaged circuits upstream – as will be discussed later.

4.3.2 Acute effects of Morphine on LHb neurons

Despite the presence of opioid receptors in the LHb (Gardon et al., 2014), there exists few data currently available examining the effect of acute Morphine on LHb activity. It has been shown that selective activation of MORs – the principle mechanism of action of Morphine - in the LHb drives a hyperpolarisation in around half of LHb neurons. Additionally, MOR agonists

decreases glutamate release on to LHb neurons, an effect shown to be dependent on MOR signalling, and principally mediated by action at MORs present on glutamatergic projections arising from the LPO (Margolis & Fields., 2016; Waung et al., 2020). In-vivo recordings of LHb neurons showed that transient increases in firing driven by noxious stimuli normally present in all recorded neurons were suppressed by morphine pre-treatment in half of these cells. Normal responses to noxious stimuli were recovered following naloxone antagonism of MORs (Benabid & Jeaugey, 1989). This aligns with studies demonstrating an analgesic effect of intra-LHb morphine (Cohen & Melzak, 1985; Khalilzadeh & Saiah, 2017; Waung et al., 2020). Interestingly, recent data has demonstrated that this analgesic effect is dependent on serotonin 5HT-3 receptor signalling in the DRN (Khalilzadeh & Saiah, 2017).

Whilst the above studies have mostly probed how drugs could directly act in the LHb, another driving force regulating LHb activity is the activity of neural circuits upstream. Drugs of abuse cause profound changes in numerous regions of the brain. How these changes could have repercussions in the LHb will be discussed below.

4.3.3 Circuit driven engagement of LHb by drugs of abuse

In addition to cocaine and opioid driven adaptations of LHb activity, ethanol also drives excitation/hyperactivity of LHb neurons at acute and withdrawal timepoint (Fu et al., 2017; Li et al., 2017). Furthermore, degeneration of fasciculus retroflexus occurs after chronic exposure to a wide range of psychostimulants including nicotine (Carlson et al., 2000; Elison, 2002). In light of these common adaptations, it is likely that circuit mechanisms universal to drug intake also regulate LHb activity following drug intake.

An obvious candidate to mediate such a mechanism, given its common role in mediating the rewarding component of all drugs of abuse, is mesolimbic DA transmission. An exhaustive discussion of all the numerous possible multi-synaptic circuits downstream or outside of this network would be overly speculative, and to propose any one as *the* circuit mechanism would be premature given available data. However, to accurately depict this theoretical concept we can use the example of the VP as an interface between mesolimbic DA transmission and the LHb in cocaine intake (Figure 16). Cocaine driven DA released in the NAc acts on GABAergic D1-MSNs to mediate positive reinforcement of cocaine administration (Baker et al., 1998). As a result, D1-MSNs become more active following cocaine intake (Calipari et al., 2016). Recent studies have demonstrated that cocaine exposure selectively potentiates excitatory transmission on to VP-projecting MSNs (Baimel et al., 2019). In line with this plasticity, presynaptic inhibitory strength of D1-MSN projections to the VP mediates cocaine locomotor sensitisation (Creed et al., 2016). Additionally, VP neurons are mostly inhibited following cocaine self-administration (Root et al., 2012), likely in part due to GABA released from excited D1-MSNs. VP neurons send predominantly GABAergic projections to the LHb (Pribiag et al., 2021), thus the effect of VP inhibition by cocaine could cause downstream disinhibition of the LHb. Interestingly, this projection, which preferentially targets RMTg-projecting LHb neurons, drives cocaine-seeking during a model of relapse following abstinence (Pribiag et al., 2021). Altogether this three-neuron link (Mesolimbic DA, D1-MSN to VP, VP GABA to LHb) between the VTA and LHb represents a possible circuit that could mediate the engagement of the LHb by acute intake of drugs of abuse. Additionally, given that adaptations in the pathway account for certain persistent behavioural features of cocaine addiction (Baimel et al., 2019; Creed et al., 2016; Pribiag et al., 2021), it is also possible that this circuit may play an upstream role in mediating LHb adaptations occurring during withdrawal (Levi et al., 2020).

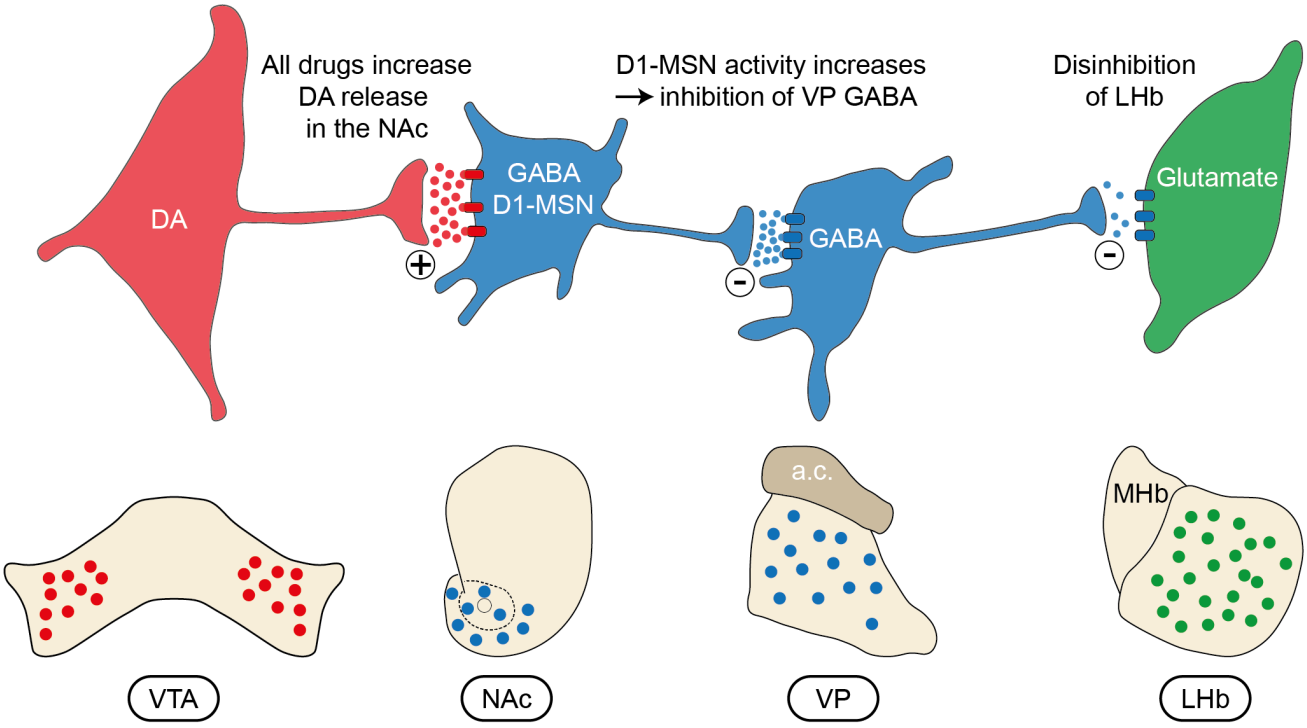

Figure 16. Putative circuit-driven engagement of LHb during acute drug intake. DA release from VTA terminals in the NAc following acute drug intake acts on D1Rs to excite GABAergic D1-MSNs. This should increase inhibition of downstream GABA neurons of the VP, which in-vivo recording show are mostly inhibited during acute cocaine intake. VP GABA neurons represent a major source of inhibition for LHb neurons, thus, acute drug intake could cause a disinhibition of LHb neurons through the engagement of this circuit.

Whether or not the activity of such a multi-synaptic circuit is causal for events downstream in the LHb during acute drug intake could be examined using hemispheric pharmacological double dissociation experiments targeting specific links within this putative pathway. Such experiments have traditionally utilised local injections of muscimol and baclofen, agonists of GABA-A and GABA-B receptors respectively, to shut down neural activity in specific brain regions. If the proposed circuit above were to drive LHb activity during cocaine intake, injections of this drug combination in the NAc of one hemisphere, and in the VP of the other, should theoretically prevent, or blunt (in the case of a partial contribution) cocaine driven changes in LHb activity. A more precise means of achieving the same target, but without potentially confounding effects stemming from contamination of inhibition of other pathways, would be to conduct injections of HSV-cre and AAV-iDREADD to allow chemogenetic inhibition of two of the three neuronal circuits implicated in opposite hemispheres during cocaine intake.

Overall, a number of potential factors could regulate the modification of LHb activity and synaptic transmission during acute drug intake. Cocaine was previously presumed to modify LHb activity by inhibiting the uptake of DA released from VTA projections. This appears unlikely given these projections do not, at least in baseline physiological conditions, release DA (Stamatakis et al., 2013). Alternatively, cocaine could act to increase local NE transmission to target DA receptors (Root et al., 2015), whilst DA may be being released into the LHb from another population of neurons. Morphine can directly act on MORs present in the LHb to modify activity and synaptic transmission in a subset of neurons (Margolis et al,. 2016). Additionally, given that a wide range of drugs engage the LHb (Carlson et al., 2000; Elison, 2002) it is possible that LHb activity is regulated by wider circuit mechanisms downstream from universal alterations of brain activity by different drugs, such as mesolimbic DA release.

4.3.4 Translating acute activity to persistent LHb adaptations in withdrawal

Acute drug intake drives a diverse mixture of responses in LHb neurons. This could be the result of the drug directly acting on LHb neurons, via circuit driven mechanisms or (most likely) a combination of both. Work from our laboratory, including the studies presented in my thesis, have demonstrated that drug withdrawal can drive output specific adaptations of the LHb. It is thus plausible that the mixture of responses – excitation, inhibition and biphasic responses – to acute drugs also occur along this criteria and shape the specific plasticity emerging in these populations.

Unfortunately, studies examining the acute effects of drugs on LHb activity have largely neglected to specify which output-specific populations are being modified. Thus, it is hard to speculate how activity during intake relates to plasticity in withdrawal. Exogenous DA, which mimics some of cocaine's actions in LHb neurons, selectively depolarizes RMTg projecting neurons (Good et al., 2013) – the same population shown to undergo synaptic strengthening and hyperactivity during cocaine withdrawal (Meye et al., 2015). This could suggest Hebbian logic guides these adaptations of glutamatergic transmission following cocaine intake. Alternatively, cocaine exposure alters rules governing synaptic plasticity induced during withdrawal in the LHb, such that protocols normally eliciting LTD of postsynaptic strength instead induce LTP specifically in RMTg projecting neurons (Maroteaux & Mameli, 2012). Additionally, persistently chemogenetically activating LHb neurons drives a postsynaptic LTD of AMPA transmission (Nuno-Perez et al., 2021). Thus, both Hebbian and non-Hebbian plasticity can occur in the LHb. By establishing a clearer picture of whether output-specific neurons of the LHb undergo distinct acute modifications during drug intake, and whether the induction of plastic adaptations in these pathways follows Hebbian or non-Hebbian logic, we can delineate how acute activity during drug intake can drive output-specific adaptations in withdrawal. Such precise investigations may also uncover important differences between subgroups of VTA-projecting neurons that may account for the opposing forms of plasticity we observed at downstream synapses during cocaine withdrawal.

A simple means to test whether the direct action of these drugs in the LHb is causal for the plasticity developing later in withdrawal, would be to locally infuse MOR/DA receptor antagonists in the LHb concomitant with morphine/cocaine administration and see whether this prevents the induction of plasticity in the LHb as well as associated behavioural phenotypes. Alternatively, if this intervention fails to prevent plasticity, but systemic injections of the same antagonists does, this would argue for a predominance of wider circuit-mediated effects.

4.4 Limitations of the thesis: Considerations of alternative approaches to support translational validity

For both studies in my PhD thesis, we have employed i.p. injections of a drug of abuse, followed by a period of forced abstinence or precipitated withdrawal to elicit an aversive state during withdrawal. This strategy has certain distinct advantages, perhaps principle among which is the ability to dissociate withdrawal adaptations from drug seeking, and thus isolate features of withdrawal specific to the sudden absence of drugs from the system. Additionally, this practice is less time and labour intensive, facilitating the generation of data. However, an overarching goal of much of addiction neuroscience research is to link brain adaptations to maintenance and progression of addiction – that is to show how these brain adaptations influence further drug seeking and taking. In this regard of translational applicability, our approach can be considered a limitation.

In this final section of the discussion I will consider an alternative approach using cocaine self-administration, that could be applied to relate the presynaptic adaptations we observe in

LHb synapses on to mPFC-projecting VTA neurons to the progression of drug use. It is poignant to state here that LHb excitability is also increased in mice withdrawn from self-administration of cocaine (Neumann et al., 2014). This suggests that the induction of this adaptation at least, and potentially also the plasticity in LHb circuits presented in this thesis, is directly related to exposure to the drug rather than drug seeking/taking per se. However, using self-administration paradigms would better enable the establishment of links between the plasticity we see and further drug use.

4.4.1 Cocaine-withdrawal driven LTP of LHb glutamate transmission at mPFC-projecting VTA neurons

As previously discussed it is possible that the LTP seen in the LHb-VTA-mPFC circuit could contribute to a heightened processing of aversive stimuli, and as a result mediate stress-driven reinstatement of previously extinguished cocaine-seeking behaviours. VTA DA projections to the mPFC are activated by aversive stimuli and they affect mPFC activity to enhance processing of aversive stimuli (Mantz et al., 1989; Vander Weele et al., 2018). Furthermore, this pathway is sensitized in drug withdrawal and DA release in the mPFC is essential for stress-induced reinstatement (McFarland et al., 2004; Williams & Steketee, 2005). This behavioural paradigm of drug self-administration models relapse during cocaine withdrawal, which is strongly linked with exposure to stress during a period in which addicts are more irritable and sensitive to minor stressors (Fox et al., 2007; Sinha, 2001).

An increase in aversion processing should theoretically amplify the emotional intensity of minor stressors. This could drive relief-craving responses (i.e. cocaine relapse) in the most affected (and likely most addicted) individuals, while resilient individuals may have less distortion of aversion processing and consequently be less prone to relapse. In this regard it has been shown that certain protocols of stress-driven reinstatement are more reliably elicited in mice undergoing extended, rather than short, access cocaine-self administration paradigms (Mantsch et al., 2008). A possible way to causally link the LTP we observe with both heightened aversive processing and stress-driven reinstatement would be to titre the intensity of the stressor such that only half of mice receiving long-access cocaine meet the criteria for stress-driven reinstatement of cocaine-seeking. It could then be assessed whether the extent of drug seeking during reinstatement could be correlated with presynaptic strength at the LHb synapse on to mPFC-projecting VTA neurons. Presuming selective depotentiation of this synapse is possible, we could probe causality of this synaptic potentiation during cocaine withdrawal for setting a lowered threshold for stress-driven relapse by examining whether this intervention increased the rate of resilience to stress-reinstatement of drug-seeking. Ultimately, if true, this would provide a multi-synaptic model of stress-driven relapse to cocaine use that could be leveraged by emerging technologies to improve addiction therapies (Clerke et al., 2021b).

This proposed research line would enable a greater examination of the role of LHb adaptations in a central tenant of addiction. As addiction progresses negative reinforcement of drug use – taking drugs to terminate aversive symptoms – becomes a progressively stronger driving force for continued drug use (Koob, 2011; Piazza & Deroche-Gamonet, 2013). A role for LHb circuit adaptations in the emergence of aversive states during drug withdrawal is becoming more established with each of the many studies published in this regard from our lab and others (Clerke et al., 2021b). Future studies aiming to further establish the translational validity regarding its role in continued drug seeking may pave the way for targeted therapeutics in drug addiction.

4.5 Concluding Remarks

My doctoral thesis provides new insight into how drug withdrawal can hijack diverse LHb neural circuits associated with the regulation of motivated behaviours. We observe that LTD of AMPA transmission in LHb projections to the Raphe underlies impaired sociability in morphine withdrawal, while cocaine withdrawal drives opposing forms of plasticity in LHb projections to output-specific populations of the VTA considered key components of both reward and aversion processing. These studies demonstrate the importance of connectivity in determining the functional role of precise circuits, and how they are altered by drugs of abuse.

The findings in my doctoral thesis align with many central observations present in addiction neuroscience studies focussing on downstream monoaminergic centres and their projections. As a prime regulator of aversion and aversive states, it is apt that the projections of the LHb to various downstream nuclei may collectively all contribute to the generation of aversive states during withdrawal. Complementing previous work demonstrating a cocaine withdrawal driven LTP and hyperactivity in RMTg-projecting neurons (Meye et al., 2015) – which should drive an enhanced inhibitory influence on NAc-projecting reward encoding DA neurons, we also see that cocaine withdrawal drives an LTD at LHb synapses on to NAc-projecting VTA neurons, well recognised to drive rewarding behaviours. Cumulatively these two adaptations may account for diminished DA levels in the NAc during cocaine withdrawal (Weiss et al., 1992) – which could drive a reward deficit in drug withdrawal, leading to depressive symptoms such as anhedonia. Alongside these inhibitory actions on rewarding pathways of the VTA, cocaine withdrawal also potentiates LHb innervation of VTA projections to the mPFC, which are critically involved in processing of aversive stimuli and stress-driven relapse (Mantz et al.,1988; McFarland et al., 2004; Vander Weele et al., 2018). Finally, the morphine withdrawal driven LTD of DRN-projecting LHb neurons may serve to unify independently observed findings that serotonin levels in the NAc are depleted in morphine withdrawal and that DRN-to-NAc signalling underlies many core aspects of social behaviour (Antkiewicz-Michaluk et al., 1995; Dölen et al., 2013; Harris & Ashton-Jones, 2001). Further studies are needed to test whether these logical postulates of LHb connectivity with monoaminergic centres and their downstream targets stand up to rigorous examination. Altogether we see that drug withdrawal adaptation of LHb circuits is non-uniform and circuit specific, suggesting a nuanced regulation of behavioural maladaptations in drug withdrawal by the LHb.

The majority of neuroscience research into drug addiction to date has focussed on the hijacked drive to seek the euphoric high present in drug addicts. However, in order for us to obtain the rounded understanding we need to develop better treatments, it is imperative we learn of the neural adaptations occurring during withdrawal. Drug withdrawal undermines attempts at abstinence by both driving relapse and disincentivising the decision to try and quit drug use in the first place (Paliwal et al.,2008; Pergolizzi et al., 2020). It represents a major pillar in the cycle of addictive behaviour that can render even those who desperately wish to be free from drugs helpless in their battle with addiction. The LHb is a key node for the withdrawal state, as repeatedly shown by work from our laboratory and others. Future work should build upon the findings of synaptic adaptations in LHb circuits presented herein using self-administration paradigms to examine the role of such plasticity in drug-withdrawal driving relapse, thus adding a stronger translational value to these findings. Emerging and future therapeutic technologies enabling specific targeting of precise brain nuclei should consider targeting the LHb to alleviate drug withdrawal symptoms, particularly following on from a case in which LHb DBS successfully ameliorated Treatment Resistant Depression (Sartorius et al., 2010).

I write this at a poignant time concerning drug use – and particularly the use of drugs to terminate aversive experiences and states. The combination of loneliness, boredom, fear, and in many cases, grief accompanying the repeated bouts of lockdown during the Covid-19

pandemic has led to a drastic increase in problem drug use, such that recent statistics estimate a record 93’000 overdose deaths in the USA over the last 12 months (Stobbe, 2021). As the world gradually emerges from such an era defining ordeal, many understandably shaken, a greater understanding of how neural pathways that process our darker moments can be hijacked to become a driving force for the destructive behaviours that define drug addiction is of great importance.

Data Appendix

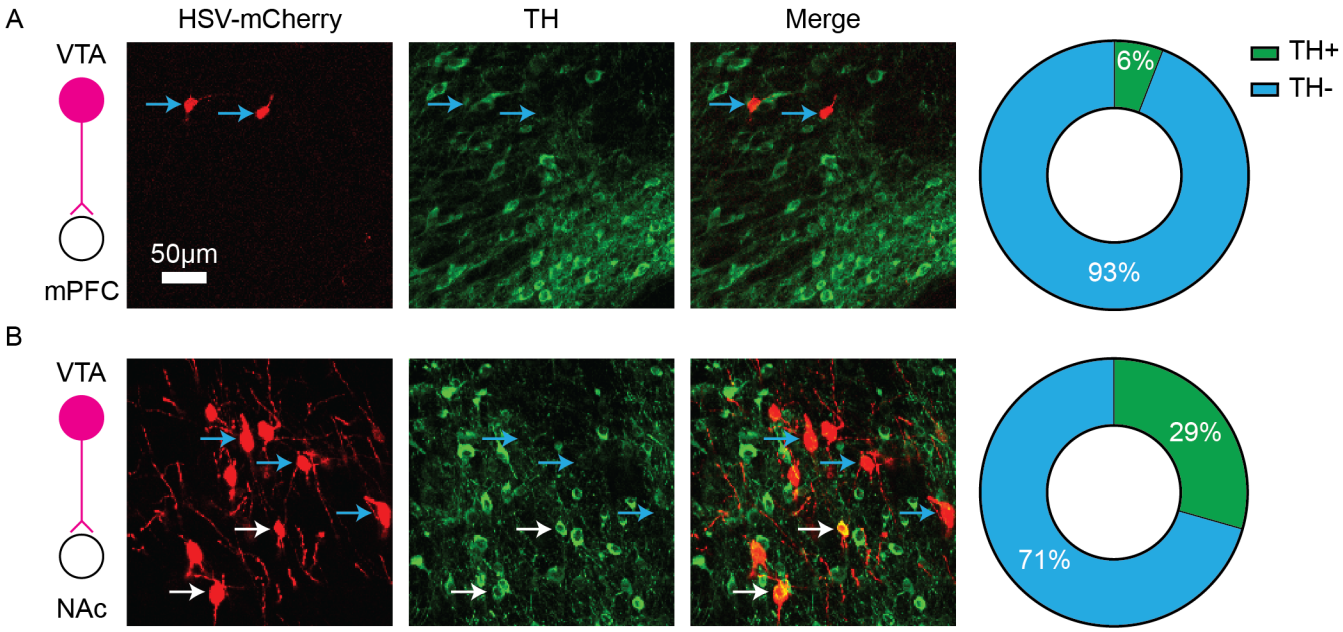

Figure 17. HSV retrogradely labelled output-specific VTA populations are mostly TH negative. A. images (left to right) of mPFC-projecting VTA neurons, TH stain, merged image. Pie chart (right) displaying percent of labelled mPFC projecting neurons that are TH+ vs TH-. **B.** Same as for A regarding NAc-projecting VTA neurons

List of publications

Research articles

Lalive, A. L., Congiu, M., **Clerke, J. A.,** Tchenio, A., Ge, Y., & Mameli, M. (2021). Synaptic inhibition in the lateral habenula shapes reward anticipation. bioRxiv.

Clerke, J., Preston-Ferrer, P., Zouridis, I. S., Tissot, A., Batti, L., Voigt, F. F., Pagès, S., Burgalossi, A., and Mameli, M. (2021a). Output-Specific Adaptation of Habenula-Midbrain Excitatory Synapses During Cocaine Withdrawal. Front Synaptic Neurosci *13*, 643138.

Valentinova, K., Tchenio, A., Trusel, M., **Clerke, J. A.,** Lalive, A. L., Tzanoulinou, S., Matera, A., Moutkine, I., Maroteaux, L., Paolicelli, R. C., Volterra, A., Bellone, C., and Mameli, M. (2019). Morphine withdrawal recruits lateral habenula cytokine signaling to reduce synaptic excitation and sociability. Nat Neurosci *22*, 1053-1056.

Review articles

Clerke, J. A., Congiu, M., and Mameli, M. (2021b). Neuronal adaptations in the lateral habenula during drug withdrawal: Preclinical evidence for addiction therapy. Neuropharmacology *192*, 108617.

References

Aizawa, H., Kobayashi, M., Tanaka, S., Fukai, T., and Okamoto, H. (2012). Molecular characterization of the subnuclei in rat habenula. J Comp Neurol *520*, 4051-4066.

Alsiö, J., Nordenankar, K., Arvidsson, E., Birgner, C., Mahmoudi, S., Halbout, B., Smith, C., Fortin, G. M., Olson, L., Descarries, L., Trudeau, L. É., Kullander, K., Lévesque, D., and Wallén-Mackenzie, A. (2011). Enhanced sucrose and cocaine self-administration and cue-induced drug seeking after loss of VGLUT2 in midbrain dopamine neurons in mice. J Neurosci *31*, 12593-12603.

Anthony, J. C., Warner, L. A., and Kessler, R. C. (1994). Comparative epidemiology of dependence on tobacco, alcohol, controlled substances, and inhalants: basic findings from the National Comorbidity Survey. Experimental and Clinical Psychopharmacology *2*, 244-268.

Antkiewicz-Michaluk, L., Romańska, I., and Vetulani, J. (1995). Immediate and "day-after" effects of morphine on dopamine and serotonin metabolism in various structures of the rat brain. Pol J Pharmacol *47*, 355-358.

Baimel, C., McGarry, L. M., and Carter, A. G. (2019). The Projection Targets of Medium Spiny Neurons Govern Cocaine-Evoked Synaptic Plasticity in the Nucleus Accumbens. Cell Rep *28*, 2256-2263.e3.

Baker, D. A., Fuchs, R. A., Specio, S. E., Khroyan, T. V., and Neisewander, J. L. (1998). Effects of intraaccumbens administration of SCH-23390 on cocaine-induced locomotion and conditioned place preference. Synapse *30*, 181-193.

Bakken, K., Landheim, A. S., and Vaglum, P. (2007). Axis I and II disorders as long-term predictors of mental distress: a six-year prospective follow-up of substance-dependent patients. BMC Psychiatry *7*, 29.

Becker, H. C. (2008). Alcohol dependence, withdrawal, and relapse. Alcohol Res Health *31*, 348-361.

Beier, K. T., Gao, X. J., Xie, S., DeLoach, K. E., Malenka, R. C., and Luo, L. (2019). Topological Organization of Ventral Tegmental Area Connectivity Revealed by Viral-Genetic Dissection of Input-Output Relations. Cell Rep *26*, 159-167.e6.

Beier, K. T., Steinberg, E. E., DeLoach, K. E., Xie, S., Miyamichi, K., Schwarz, L., Gao, X. J., Kremer, E. J., Malenka, R. C., and Luo, L. (2015). Circuit Architecture of VTA Dopamine Neurons Revealed by Systematic Input-Output Mapping. Cell *162*, 622-634.

Bellone, C., and Lüscher, C. (2006). Cocaine triggered AMPA receptor redistribution is reversed in vivo by mGluR-dependent long-term depression. Nat Neurosci *9*, 636-641.

Benabid, A. L., and Jeaugey, L. (1989). Cells of the rat lateral habenula respond to high-threshold somatosensory inputs. Neurosci Lett *96*, 289-294.

Bernard, R., and Veh, R. W. (2012). Individual neurons in the rat lateral habenular complex project mostly to the dopaminergic ventral tegmental area or to the serotonergic raphe nuclei. J Comp Neurol *520*, 2545-2558.

Bianco, I. H., and Wilson, S. W. (2009). The habenular nuclei: a conserved asymmetric relay station in the vertebrate brain. Philos Trans R Soc Lond B Biol Sci *364*, 1005-1020.

Bimpisidis, Z., and Wallén-Mackenzie, Å. (2019). Neurocircuitry of Reward and Addiction: Potential Impact of Dopamine-Glutamate Co-release as Future Target in Substance Use Disorder. J Clin Med *8*, E1887.

Bloomfield, M. A., Ashok, A. H., Volkow, N. D., and Howes, O. D. (2016). The effects of Δ^9-tetrahydrocannabinol on the dopamine system. Nature *539*, 369-377.

Bocklisch, C., Pascoli, V., Wong, J. C., House, D. R., Yvon, C., de Roo, M., Tan, K. R., and Lüscher, C. (2013). Cocaine disinhibits dopamine neurons by potentiation of GABA transmission in the ventral tegmental area. Science *341*, 1521-1525.

Bossert, J. M., Poles, G. C., Sheffler-Collins, S. I., and Ghitza, U. E. (2006). The mGluR2/3 agonist LY379268 attenuates context- and discrete cue-induced reinstatement of sucrose seeking but not sucrose self-administration in rats. Behav Brain Res *173*, 148-152.

Brecht, M. L., von Mayrhauser, C., and Anglin, M. D. (2000). Predictors of relapse after treatment for methamphetamine use. J Psychoactive Drugs *32*, 211-220.

Breton, J. M., Charbit, A. R., Snyder, B. J., Fong, P. T. K., Dias, E. V., Himmels, P., Lock, H., and Margolis, E. B. (2019). Relative contributions and mapping of ventral tegmental area dopamine and GABA neurons by projection target in the rat. J Comp Neurol *527*, 916-941.

Brischoux, F., Chakraborty, S., Brierley, D. I., and Ungless, M. A. (2009). Phasic excitation of dopamine neurons in ventral VTA by noxious stimuli. Proc Natl Acad Sci U S A *106*, 4894-4899.

Brower, K. J., and Perron, B. E. (2010). Prevalence and correlates of withdrawal-related insomnia among adults with alcohol dependence: results from a national survey. Am J Addict *19*, 238-244.

Brown, G. L., Goodwin, F. K., Ballenger, J. C., Goyer, P. F., and Major, L. F. (1979). Aggression in humans correlates with cerebrospinal fluid amine metabolites. Psychiatry Res *1*, 131-139.

Brown, M. T., Tan, K. R., O'Connor, E. C., Nikonenko, I., Muller, D., and Lüscher, C. (2012). Ventral tegmental area GABA projections pause accumbal cholinergic interneurons to enhance associative learning. Nature *492*, 452-456.

Budney, A. J., Vandrey, R. G., Hughes, J. R., Thostenson, J. D., and Bursac, Z. (2008). Comparison of cannabis and tobacco withdrawal: severity and contribution to relapse. J Subst Abuse Treat *35*, 362-368.

Calipari, E. S., Bagot, R. C., Purushothaman, I., Davidson, T. J., Yorgason, J. T., Peña, C. J., Walker, D. M., Pirpinias, S. T., Guise, K. G., Ramakrishnan, C., Deisseroth, K., and Nestler, E. J. (2016). In vivo imaging identifies temporal signature of D1 and D2 medium spiny neurons in cocaine reward. Proc Natl Acad Sci U S A *113*, 2726-2731.

Campbell, L. A., Avdoshina, V., Rozzi, S., and Mocchetti, I. (2013). CCL5 and cytokine expression in the rat brain: differential modulation by chronic morphine and morphine withdrawal. Brain Behav Immun *34*, 130-140.

Cannella, N., Halbout, B., Uhrig, S., Evrard, L., Corsi, M., Corti, C., Deroche-Gamonet, V., Hansson, A. C., and Spanagel, R. (2013). The mGluR2/3 agonist LY379268 induced anti-reinstatement effects in rats exhibiting addiction-like behavior. Neuropsychopharmacology *38*, 2048-2056.

Cardozo Pinto, D. F., Yang, H., Pollak Dorocic, I., de Jong, J. W., Han, V. J., Peck, J. R., Zhu, Y., Liu, C., Beier, K. T., Smidt, M. P., and Lammel, S. (2019). Characterization of transgenic mouse models targeting neuromodulatory systems reveals organizational principles of the dorsal raphe. Nat Commun *10*, 4633.

Carlson, J., Armstrong, B., Switzer, R. C., and Ellison, G. (2000). Selective neurotoxic effects of nicotine on axons in fasciculus retroflexus further support evidence that this a weak link in brain across multiple drugs of abuse. Neuropharmacology *39*, 2792-2798.

Carr, D. B., and Sesack, S. R. (2000). GABA-containing neurons in the rat ventral tegmental area project to the prefrontal cortex. Synapse *38*, 114-123.

Challis, C., Boulden, J., Veerakumar, A., Espallergues, J., Vassoler, F. M., Pierce, R. C., Beck, S. G., and Berton, O. (2013). Raphe GABAergic neurons mediate the acquisition of avoidance after social defeat. J Neurosci *33*, 13978-88, 13988a.

Cheer, J. F., Wassum, K. M., Sombers, L. A., Heien, M. L., Ariansen, J. L., Aragona, B. J., Phillips, P. E., and Wightman, R. M. (2007). Phasic dopamine release evoked by abused substances requires cannabinoid receptor activation. J Neurosci *27*, 791-795.

Chen, B. T., Yau, H. J., Hatch, C., Kusumoto-Yoshida, I., Cho, S. L., Hopf, F. W., and Bonci, A. (2013). Rescuing cocaine-induced prefrontal cortex hypoactivity prevents compulsive cocaine seeking. Nature *496*, 359-362.

Christie, N. C. (2021). The role of social isolation in opioid addiction. Soc Cogn Affect Neurosci *16*, 645-656.

Clem, R. L., and Huganir, R. L. (2010). Calcium-permeable AMPA receptor dynamics mediate fear memory erasure. Science *330*, 1108-1112.

Clerke, J., Preston-Ferrer, P., Zouridis, I. S., Tissot, A., Batti, L., Voigt, F. F., Pagès, S., Burgalossi, A., and Mameli, M. (2021a). Output-Specific Adaptation of Habenula-Midbrain Excitatory Synapses During Cocaine Withdrawal. Front Synaptic Neurosci *13*, 643138.

Clerke, J. A., Congiu, M., and Mameli, M. (2021b). Neuronal adaptations in the lateral habenula during drug withdrawal: Preclinical evidence for addiction therapy. Neuropharmacology *192*, 108617.

Cohen, S. R., and Melzack, R. (1985). Morphine injected into the habenula and dorsal posteromedial thalamus produces analgesia in the formalin test. Brain Res *359*, 131-139.

Conrad, K. L., Tseng, K. Y., Uejima, J. L., Reimers, J. M., Heng, L. J., Shaham, Y., Marinelli, M., and Wolf, M. E. (2008). Formation of accumbens GluR2-lacking AMPA receptors mediates incubation of cocaine craving. Nature *454*, 118-121.

Corbit, L. H., Nie, H., and Janak, P. H. (2012). Habitual alcohol seeking: time course and the contribution of subregions of the dorsal striatum. Biol Psychiatry *72*, 389-395.

Corre, J., van Zessen, R., Loureiro, M., Patriarchi, T., Tian, L., Pascoli, V., and Lüscher, C. (2018). Dopamine neurons projecting to medial shell of the nucleus accumbens drive heroin reinforcement. Elife *7*, e39945.

Creed, M., Ntamati, N. R., Chandra, R., Lobo, M. K., and Lüscher, C. (2016). Convergence of Reinforcing and Anhedonic Cocaine Effects in the Ventral Pallidum. Neuron *92*, 214-226.

Cui, Y., Yang, Y., Ni, Z., Dong, Y., Cai, G., Foncelle, A., Ma, S., Sang, K., Tang, S., Li, Y., Shen, Y., Berry, H., Wu, S., and Hu, H. (2018). Astroglial Kir4.1 in the lateral habenula drives neuronal bursts in depression. Nature *554*, 323-327.

D'Sa, C., Fox, H. C., Hong, A. K., Dileone, R. J., and Sinha, R. (2011). Increased serum brain-derived neurotrophic factor is predictive of cocaine relapse outcomes: a prospective study. Biol Psychiatry *70*, 706-711.

da Cruz e Silva, E. F., Fox, C. A., Ouimet, C. C., Gustafson, E., Watson, S. J., and Greengard, P. (1995). Differential expression of protein phosphatase 1 isoforms in mammalian brain. J Neurosci *15*, 3375-3389.

de Jong, J. W., Afjei, S. A., Pollak Dorocic, I., Peck, J. R., Liu, C., Kim, C. K., Tian, L., Deisseroth, K., and Lammel, S. (2019). A Neural Circuit Mechanism for Encoding Aversive Stimuli in the Mesolimbic Dopamine System. Neuron *101*, 133-151.e7.

Deroche-Gamonet, V., Belin, D., and Piazza, P. V. (2004). Evidence for addiction-like behavior in the rat. Science *305*, 1014-1017.

DeWeerdt, S. (2019). Tracing the US opioid crisis to its roots. Nature *573*, S10-S12.

Di Chiara, G. (1999). Drug addiction as dopamine-dependent associative learning disorder. Eur J Pharmacol *375*, 13-30.

Di Chiara, G., Loddo, P., and Tanda, G. (1999). Reciprocal changes in prefrontal and limbic dopamine responsiveness to aversive and rewarding stimuli after chronic mild stress: implications for the psychobiology of depression. Biol Psychiatry *46*, 1624-1633.

Dölen, G., Darvishzadeh, A., Huang, K. W., and Malenka, R. C. (2013). Social reward requires coordinated activity of nucleus accumbens oxytocin and serotonin. Nature *501*, 179-184.

Dong, Y., Saal, D., Thomas, M., Faust, R., Bonci, A., Robinson, T., and Malenka, R. C. (2004). Cocaine-induced potentiation of synaptic strength in dopamine neurons: behavioral correlates in GluRA(-/-) mice. Proc Natl Acad Sci U S A *101*, 14282-14287.

Duke, A. A., Bègue, L., Bell, R., and Eisenlohr-Moul, T. (2013). Revisiting the serotonin-aggression relation in humans: a meta-analysis. Psychol Bull *139*, 1148-1172.

Ellison, G. (2002). Neural degeneration following chronic stimulant abuse reveals a weak link in brain, fasciculus retroflexus, implying the loss of forebrain control circuitry. Eur Neuropsychopharmacol *12*, 287-297.

Engblom, D., Bilbao, A., Sanchis-Segura, C., Dahan, L., Perreau-Lenz, S., Balland, B., Parkitna, J. R., Luján, R., Halbout, B., Mameli, M., Parlato, R., Sprengel, R., Lüscher, C., Schütz, G., and Spanagel, R. (2008). Glutamate receptors on dopamine neurons control the persistence of cocaine seeking. Neuron *59*, 497-508.

Everitt, B. J., and Robbins, T. W. (2016). Drug Addiction: Updating Actions to Habits to Compulsions Ten Years On. Annu Rev Psychol *67*, 23-50.

Farassat, N., Costa, K. M., Stojanovic, S., Albert, S., Kovacheva, L., Shin, J., Egger, R., Somayaji, M., Duvarci, S., Schneider, G., and Roeper, J. (2019). In vivo functional diversity of midbrain dopamine neurons within identified axonal projections. Elife *8*, e48408.

Flanigan, M. E., Aleyasin, H., Li, L., Burnett, C. J., Chan, K. L., LeClair, K. B., Lucas, E. K., Matikainen-Ankney, B., Durand-de Cuttoli, R., Takahashi, A., Menard, C., Pfau, M. L., Golden, S. A., Bouchard, S., Calipari, E. S., Nestler, E. J., DiLeone, R. J., Yamanaka, A., Huntley, G. W., Clem, R. L., and Russo, S. J. (2020). Orexin signaling in GABAergic lateral habenula neurons modulates aggressive behavior in male mice. Nat Neurosci *23*, 638-650.

Fox, H. C., Hong, K. I., Siedlarz, K., and Sinha, R. (2008). Enhanced sensitivity to stress and drug/alcohol craving in abstinent cocaine-dependent individuals compared to social drinkers. Neuropsychopharmacology *33*, 796-805.

Foy, A., Kay, J., and Taylor, A. (1997). The course of alcohol withdrawal in a general hospital. QJM *90*, 253-261.

Friedman, A. K., Walsh, J. J., Juarez, B., Ku, S. M., Chaudhury, D., Wang, J., Li, X., Dietz, D. M., Pan, N., Vialou, V. F., Neve, R. L., Yue, Z., and Han, M. H. (2014). Enhancing depression mechanisms in midbrain dopamine neurons achieves homeostatic resilience. Science *344*, 313-319.

Fu, R., Mei, Q., Zuo, W., Li, J., Gregor, D., Bekker, A., and Ye, J. (2017). Low-dose ethanol excites lateral habenula neurons projecting to VTA, RMTg, and raphe. Int J Physiol Pathophysiol Pharmacol *9*, 217-230.

Garavan, H., Pankiewicz, J., Bloom, A., Cho, J. K., Sperry, L., Ross, T. J., Salmeron, B. J., Risinger, R., Kelley, D., and Stein, E. A. (2000). Cue-induced cocaine craving: neuroanatomical specificity for drug users and drug stimuli. Am J Psychiatry *157*, 1789-1798.

Garcés, L. (2005). Colombia: the link between drugs and terror. Journal of Drug Issues *35*, 83-106.

Gardon, O., Faget, L., Chu Sin Chung, P., Matifas, A., Massotte, D., and Kieffer, B. L. (2014). Expression of mu opioid receptor in dorsal diencephalic conduction system: new insights for the medial habenula. Neuroscience *277*, 595-609.

Gawin, F. H. (1991). Cocaine addiction: psychology and neurophysiology. Science *251*, 1580-1586.

Gawin, F. H., and Kleber, H. D. (1988). Evolving conceptualizations of cocaine dependence. Yale J Biol Med *61*, 123-136.

Giacalone, E., Tansella, M., and Valzelli…, L. (1968). Brain serotonin metabolism in isolated aggressive mice. Biochemical pharmacology *17*, 1315-1327.

Global Burden of Disease, A. A. D. U. C. (2018). The global burden of disease attributable to alcohol and drug use in 195 countries and territories, 1990-2016: a systematic analysis for the Global Burden of Disease Study 2016. Lancet Psychiatry *5*, 987-1012.

Goldstein, R. Z., and Volkow, N. D. (2002). Drug addiction and its underlying neurobiological basis: neuroimaging evidence for the involvement of the frontal cortex. Am J Psychiatry *159*, 1642-1652.

Good, C. H., Wang, H., Chen, Y. H., Mejias-Aponte, C. A., Hoffman, A. F., and Lupica, C. R. (2013). Dopamine D4 receptor excitation of lateral habenula neurons via multiple cellular mechanisms. J Neurosci *33*, 16853-16864.

Gorelova, N., Mulholland, P. J., Chandler, L. J., and Seamans, J. K. (2012). The glutamatergic component of the mesocortical pathway emanating from different subregions of the ventral midbrain. Cereb Cortex *22*, 327-336.

Gottesfeld, Z. (1983). Origin and distribution of noradrenergic innervation in the habenula: a neurochemical study. Brain Res *275*, 299-304.

Gruber, C., Kahl, A., Lebenheim, L., Kowski, A., Dittgen, A., and Veh, R. W. (2007). Dopaminergic projections from the VTA substantially contribute to the mesohabenular pathway in the rat. Neurosci Lett *427*, 165-170.

Guillemin, R., Dear, W. E., Nichols, B., and Lipscomb, H. S. (1959). ACTH releasing activity in vivo of a CRF preparation and lysine vasopressin. Proc Soc Exp Biol Med *101*, 107-111.

Haber, S. N., Fudge, J. L., and McFarland, N. R. (2000). Striatonigrostriatal pathways in primates form an ascending spiral from the shell to the dorsolateral striatum. J Neurosci *20*, 2369-2382.

Haj-Dahmane, S., and Shen, R. Y. (2010). Regulation of plasticity of glutamate synapses by endocannabinoids and the cyclic-AMP/protein kinase A pathway in midbrain dopamine neurons. J Physiol *588*, 2589-2604.

Hanes, W. T., and Sanello, F. (2002). The Opium Wars: The Addiction of One Empire and the Corruption of Another

Harris, G. C., and Aston-Jones, G. (2001). Augmented accumbal serotonin levels decrease the preference for a morphine associated environment during withdrawal. Neuropsychopharmacology *24*, 75-85.

Hearing, M. C., Jedynak, J., Ebner, S. R., Ingebretson, A., Asp, A. J., Fischer, R. A., Schmidt, C., Larson, E. B., and Thomas, M. J. (2016). Reversal of morphine-induced cell-type-specific synaptic plasticity in the nucleus accumbens shell blocks reinstatement. Proc Natl Acad Sci U S A *113*, 757-762.

Heifets, B. D., Salgado, J. S., Taylor, M. D., Hoerbelt, P., Cardozo Pinto, D. F., Steinberg, E. E., Walsh, J. J., Sze, J. Y., and Malenka, R. C. (2019). Distinct neural mechanisms for the prosocial and rewarding properties of MDMA. Sci Transl Med *11*, eaaw6435.

Heilig, M., Koob, G. F., Ekman, R., and Britton, K. T. (1994). Corticotropin-releasing factor and neuropeptide Y: role in emotional integration. Trends Neurosci *17*, 80-85.

Heir, R., and Stellwagen, D. (2020). TNF-Mediated Homeostatic Synaptic Plasticity: From in vitro to in vivo Models. Front Cell Neurosci *14*, 565841.

Herkenham, M., and Nauta, W. J. (1979). Efferent connections of the habenular nuclei in the rat. J Comp Neurol *187*, 19-47.

Herzog, E., Gilchrist, J., Gras, C., Muzerelle, A., Ravassard, P., Giros, B., Gaspar, P., and El Mestikawy, S. (2004). Localization of VGLUT3, the vesicular glutamate transporter type 3, in the rat brain. Neuroscience *123*, 983-1002.

Hodos, W. (1961). Progressive ratio as a measure of reward strength. Science *134*, 943-944.

Hu, H., Cui, Y., and Yang, Y. (2020). Circuits and functions of the lateral habenula in health and in disease. Nat Rev Neurosci *21*, 277-295.

Huang, Y. Z., Pan, E., Xiong, Z. Q., and McNamara, J. O. (2008). Zinc-mediated transactivation of TrkB potentiates the hippocampal mossy fiber-CA3 pyramid synapse. Neuron *57*, 546-558.

Hutchinson, M. R., Zhang, Y., Shridhar, M., Evans, J. H., Buchanan, M. M., Zhao, T. X., Slivka, P. F., Coats, B. D., Rezvani, N., Wieseler, J., Hughes, T. S., Landgraf, K. E., Chan, S., Fong, S., Phipps, S., Falke, J. J., Leinwand, L. A., Maier, S. F., Yin, H., Rice, K. C., and Watkins, L. R. (2010). Evidence that opioids may have toll-like receptor 4 and MD-2 effects. Brain Behav Immun *24*, 83-95.

Ikemoto, S. (2007). Dopamine reward circuitry: two projection systems from the ventral midbrain to the nucleus accumbens-olfactory tubercle complex. Brain Res Rev *56*, 27-78.

Ishikawa, M., Otaka, M., Neumann, P. A., Wang, Z., Cook, J. M., Schlüter, O. M., Dong, Y., and Huang, Y. H. (2013). Exposure to cocaine regulates inhibitory synaptic transmission from the ventral tegmental area to the nucleus accumbens. J Physiol *591*, 4827-4841.

Jin, X., Semenova, S., Yang, L., Ardecky, R., Sheffler, D. J., Dahl, R., Conn, P. J., Cosford, N. D., and Markou, A. (2010). The mGluR2 positive allosteric modulator BINA decreases cocaine self-administration and cue-induced cocaine-seeking and counteracts cocaine-induced enhancement of brain reward function in rats. Neuropsychopharmacology *35*, 2021-2036.

Jhou, T. C., Fields, H. L., Baxter, M. G., Saper, C. B., and Holland, P. C. (2009). The rostromedial tegmental nucleus (RMTg), a GABAergic afferent to midbrain dopamine neurons, encodes aversive stimuli and inhibits motor responses. Neuron *61*, 786-800.

Jhou, T. C., Good, C. H., Rowley, C. S., Xu, S. P., Wang, H., Burnham, N. W., Hoffman, A. F., Lupica, C. R., and Ikemoto, S. (2013). Cocaine drives aversive conditioning via delayed activation of dopamine-responsive habenular and midbrain pathways. J Neurosci *33*, 7501-7512.

Kalivas, P. W., and Volkow, N. D. (2005). The neural basis of addiction: a pathology of motivation and choice. Am J Psychiatry *162*, 1403-1413.

Kang, S., Li, J., Bekker, A., and Ye, J. H. (2018). Rescue of glutamate transport in the lateral habenula alleviates depression- and anxiety-like behaviors in ethanol-withdrawn rats. Neuropharmacology *129*, 47-56.

Kang, S., Li, J., Zuo, W., Fu, R., Gregor, D., Krnjevic, K., Bekker, A., and Ye, J. H. (2017). Ethanol Withdrawal Drives Anxiety-Related Behaviors by Reducing M-type Potassium Channel Activity in the Lateral Habenula. Neuropsychopharmacology *42*, 1813-1824.

Kantak, K. M., Hegstrand, L. R., and Whitman…, J. (1980). Effects of dietary supplements and a tryptophan-free diet on aggressive behavior in rats. Pharmacology Biochemistry and Behavior *12*, 173-179.

Kaufling, J., Veinante, P., Pawlowski, S. A., Freund-Mercier, M. J., and Barrot, M. (2010). gamma-Aminobutyric acid cells with cocaine-induced DeltaFosB in the ventral tegmental area innervate mesolimbic neurons. Biol Psychiatry *67*, 88-92.

Kaufman, J. N., Ross, T. J., Stein, E. A., and Garavan, H. (2003). Cingulate hypoactivity in cocaine users during a GO-NOGO task as revealed by event-related functional magnetic resonance imaging. J Neurosci *23*, 7839-7843.

Khalilzadeh, E., and Saiah, G. V. (2017). The possible mechanisms of analgesia produced by microinjection of morphine into the lateral habenula in the acute model of trigeminal pain in rats. Res Pharm Sci *12*, 241-248.

Knowland, D., Lilascharoen, V., Pacia, C. P., Shin, S., Wang, E. H., and Lim, B. K. (2017). Distinct Ventral Pallidal Neural Populations Mediate Separate Symptoms of Depression. Cell *170*, 284-297.e18.

Kobayashi, K., Manabe, T., and Takahashi, T. (1996). Presynaptic Long-Term Depression at the Hippocampal Mossy Fiber--CA3 Synapse. Science *273*, 648-650.

Koob, G. F. (2008). A role for brain stress systems in addiction. Neuron *59*, 11-34.

Koob, G. F. (2011). Neurobiology of addiction. Focus *9*, 55-65.

Koob, G. F., and Le Moal, M. (1997). Drug abuse: hedonic homeostatic dysregulation. Science *278*, 52-58.

Koob, G. F., and Le Moal, M. (2001). Drug addiction, dysregulation of reward, and allostasis. Neuropsychopharmacology *24*, 97-129.

Kowiański, P., Lietzau, G., Czuba, E., Waśkow, M., Steliga, A., and Moryś, J. (2018). BDNF: A Key Factor with Multipotent Impact on Brain Signaling and Synaptic Plasticity. Cell Mol Neurobiol *38*, 579-593.

Lammel, S., Hetzel, A., Häckel, O., Jones, I., Liss, B., and Roeper, J. (2008). Unique properties of mesoprefrontal neurons within a dual mesocorticolimbic dopamine system. Neuron *57*, 760-773.

Lammel, S., Ion, D. I., Roeper, J., and Malenka, R. C. (2011). Projection-specific modulation of dopamine neuron synapses by aversive and rewarding stimuli. Neuron *70*, 855-862.

Lammel, S., Lim, B. K., and Malenka, R. C. (2014). Reward and aversion in a heterogeneous midbrain dopamine system. Neuropharmacology *76*, 351-359.

Lammel, S., Lim, B. K., Ran, C., Huang, K. W., Betley, M. J., Tye, K. M., Deisseroth, K., and Malenka, R. C. (2012). Input-specific control of reward and aversion in the ventral tegmental area. Nature *491*, 212-217.

Lammel, S., Steinberg, E. E., Földy, C., Wall, N. R., Beier, K., Luo, L., and Malenka, R. C. (2015). Diversity of transgenic mouse models for selective targeting of midbrain dopamine neurons. Neuron *85*, 429-438.

Lawson, R. P., Nord, C. L., Seymour, B., Thomas, D. L., Dayan, P., Pilling, S., and Roiser, J. P. (2017). Disrupted habenula function in major depression. Mol Psychiatry *22*, 202-208.

Lazaridis, I., Tzortzi, O., Weglage, M., Märtin, A., Xuan, Y., Parent, M., Johansson, Y., Fuzik, J., Fürth, D., Fenno, L. E., Ramakrishnan, C., Silberberg, G., Deisseroth, K., Carlén, M., and Meletis, K. (2019). A hypothalamus-habenula circuit controls aversion. Mol Psychiatry *24*, 1351-1368.

Lecca, S., Melis, M., Luchicchi, A., Ennas, M. G., Castelli, M. P., Muntoni, A. L., and Pistis, M. (2011). Effects of drugs of abuse on putative rostromedial tegmental neurons, inhibitory afferents to midbrain dopamine cells. Neuropsychopharmacology *36*, 589-602.

Lecca, S., Melis, M., Luchicchi, A., Muntoni, A. L., and Pistis, M. (2012). Inhibitory inputs from rostromedial tegmental neurons regulate spontaneous activity of midbrain dopamine cells and their responses to drugs of abuse. Neuropsychopharmacology *37*, 1164-1176.

Lecca, S., Meye, F. J., Trusel, M., Tchenio, A., Harris, J., Schwarz, M. K., Burdakov, D., Georges, F., and Mameli, M. (2017). Aversive stimuli drive hypothalamus-to-habenula excitation to promote escape behavior. Elife *6*, e30697.

Lecca, S., Namboodiri, V. M. K., Restivo, L., Gervasi, N., Pillolla, G., Stuber, G. D., and Mameli, M. (2020). Heterogeneous Habenular Neuronal Ensembles during Selection of Defensive Behaviors. Cell Rep *31*, 107752.

Lecca, S., Pelosi, A., Tchenio, A., Moutkine, I., Lujan, R., Hervé, D., and Mameli, M. (2016). Rescue of GABAB and GIRK function in the lateral habenula by protein phosphatase 2A inhibition ameliorates depression-like phenotypes in mice. Nat Med *22*, 254-261.

Lecourtier, L., and Kelly, P. H. (2007). A conductor hidden in the orchestra? Role of the habenular complex in monoamine transmission and cognition. Neurosci Biobehav Rev *31*, 658-672.

Lee, J. S., Jung, S., Park, I. H., and Kim, J. J. (2015). Neural Basis of Anhedonia and Amotivation in Patients with Schizophrenia: The Role of Reward System. Curr Neuropharmacol *13*, 750-759.

Levi, L. A., Inbar, K., Nachshon, N., Bernat, N., Gatterer, A., Inbar, D., and Kupchik, Y. M. (2020). Projection-Specific Potentiation of Ventral Pallidal Glutamatergic Outputs after Abstinence from Cocaine. J Neurosci *40*, 1276-1285.

Levinstein, M. R., Coffey, K. R., Marx, R. G., Lesiak, A. J., and Neumaier, J. F. (2020). Stress induces divergent gene expression among lateral habenula efferent pathways. Neurobiol Stress *13*, 100268.

Li, B., Piriz, J., Mirrione, M., Chung, C., Proulx, C. D., Schulz, D., Henn, F., and Malinow, R. (2011). Synaptic potentiation onto habenula neurons in the learned helplessness model of depression. Nature *470*, 535-539.

Li, H., Pullmann, D., and Jhou, T. C. (2019). Valence-encoding in the lateral habenula arises from the entopeduncular region. Elife *8*, e41223.

Li, H., Eid, M., Pullmann, D., Chao, Y. S., Thomas, A. A., and Jhou, T. C. (2021). Entopeduncular Nucleus Projections to the Lateral Habenula Contribute to Cocaine Avoidance. J Neurosci *41*, 298-306.

Li, J., Kang, S., Fu, R., Wu, L., Wu, W., Liu, H., Gregor, D., Zuo, W., Bekker, A., and Ye, J. H. (2017). Inhibition of AMPA receptor and CaMKII activity in the lateral habenula reduces depressive-like behavior and alcohol intake in rats. Neuropharmacology *126*, 108-120.

Li, X., Hoffman, A. F., Peng, X. Q., Lupica, C. R., Gardner, E. L., and Xi, Z. X. (2009). Attenuation of basal and cocaine-enhanced locomotion and nucleus accumbens dopamine in cannabinoid CB1-receptor-knockout mice. Psychopharmacology (Berl) *204*, 1-11.

Li, Y., Zhong, W., Wang, D., Feng, Q., Liu, Z., Zhou, J., Jia, C., Hu, F., Zeng, J., Guo, Q., Fu, L., and Luo, M. (2016). Serotonin neurons in the dorsal raphe nucleus encode reward signals. Nat Commun *7*, 10503.

Liu, H., Rastogi, A., Narain, P., Xu, Q., Sabanovic, M., Alhammadi, A. D., Guo, L., Cao, J. L., Zhang, H., Aqel, H., Mlambo, V., Rezgui, R., Radwan, B., and Chaudhury, D. (2021). Blunted diurnal firing in lateral habenula projections to dorsal raphe nucleus and delayed photoentrainment in stress-susceptible mice. PLoS Biol *19*, e3000709.

Lloyd, C. (1998). Risk factors for problem drug use: identifying vulnerable groups. Drugs: education, prevention and policy *5*, 217-232.

Logrip, M. L., Koob, G. F., and Zorrilla, E. P. (2011). Role of corticotropin-releasing factor in drug addiction: potential for pharmacological intervention. CNS Drugs *25*, 271-287.

Lu, L., Dempsey, J., Liu, S. Y., Bossert, J. M., and Shaham, Y. (2004). A single infusion of brain-derived neurotrophic factor into the ventral tegmental area induces long-lasting potentiation of cocaine seeking after withdrawal. J Neurosci *24*, 1604-1611.

Lüscher, C. (2016). The Emergence of a Circuit Model for Addiction. Annu Rev Neurosci *39*, 257-276.

Lüscher, C., and Janak, P. H. (2021). Consolidating the Circuit Model for Addiction. Annu Rev Neurosci *44*, 173-195.

Lüscher, C., Robbins, T. W., and Everitt, B. J. (2020). The transition to compulsion in addiction. Nat Rev Neurosci *21*, 247-263.

Mameli, M., Halbout, B., Creton, C., Engblom, D., Parkitna, J. R., Spanagel, R., and Lüscher, C. (2009). Cocaine-evoked synaptic plasticity: persistence in the VTA triggers adaptations in the NAc. Nat Neurosci *12*, 1036-1041.

Mantsch, J. R., Baker, D. A., Francis, D. M., Katz, E. S., Hoks, M. A., and Serge, J. P. (2008). Stressor- and corticotropin releasing factor-induced reinstatement and active stress-related behavioral responses are augmented following long-access cocaine self-administration by rats. Psychopharmacology (Berl) *195*, 591-603.

Mantsch, J. R., Baker, D. A., Funk, D., Lê, A. D., and Shaham, Y. (2016). Stress-Induced Reinstatement of Drug Seeking: 20 Years of Progress. Neuropsychopharmacology *41*, 335-356.

Mantz, J., Thierry, A. M., and Glowinski, J. (1989). Effect of noxious tail pinch on the discharge rate of mesocortical and mesolimbic dopamine neurons: selective activation of the mesocortical system. Brain Res *476*, 377-381.

Manzoni, O. J., and Williams, J. T. (1999). Presynaptic regulation of glutamate release in the ventral tegmental area during morphine withdrawal. J Neurosci *19*, 6629-6636.

Margolis, E. B., and Fields, H. L. (2016). Mu Opioid Receptor Actions in the Lateral Habenula. PLoS One *11*, e0159097.

Maroteaux, M., and Mameli, M. (2012). Cocaine evokes projection-specific synaptic plasticity of lateral habenula neurons. J Neurosci *32*, 12641-12646.

Matsumoto, M., and Hikosaka, O. (2007). Lateral habenula as a source of negative reward signals in dopamine neurons. Nature *447*, 1111-1115.

Matsumoto, M., and Hikosaka, O. (2009). Representation of negative motivational value in the primate lateral habenula. Nat Neurosci *12*, 77-84.

Matthews, G. A., Nieh, E. H., Vander Weele, C. M., Halbert, S. A., Pradhan, R. V., Yosafat, A. S., Glober, G. F., Izadmehr, E. M., Thomas, R. E., Lacy, G. D., Wildes, C. P., Ungless, M. A., and Tye, K. M. (2016). Dorsal Raphe Dopamine Neurons Represent the Experience of Social Isolation. Cell *164*, 617-631.

McFarland, K., Davidge, S. B., Lapish, C. C., and Kalivas, P. W. (2004). Limbic and motor circuitry underlying footshock-induced reinstatement of cocaine-seeking behavior. J Neurosci *24*, 1551-1560.

McFarland, K., and Kalivas, P. W. (2001). The circuitry mediating cocaine-induced reinstatement of drug-seeking behavior. J Neurosci *21*, 8655-8663.

McGregor, C., Srisurapanont, M., Jittiwutikarn, J., Laobhripatr, S., Wongtan, T., and White, J. M. (2005). The nature, time course and severity of methamphetamine withdrawal. Addiction *100*, 1320-1329.

McKendrick, G., and Graziane, N. M. (2020). Drug-Induced Conditioned Place Preference and Its Practical Use in Substance Use Disorder Research. Front Behav Neurosci *14*, 582147.

McLellan, A. T., Lewis, D. C., O'Brien, C. P., and Kleber, H. D. (2000). Drug dependence, a chronic medical illness: implications for treatment, insurance, and outcomes evaluation. JAMA *284*, 1689-1695.

Mejias-Aponte, C. A., Ye, C., Bonci, A., Kiyatkin, E. A., and Morales, M. (2015). A subpopulation of neurochemically-identified ventral tegmental area dopamine neurons is excited by intravenous cocaine. J Neurosci *35*, 1965-1978.

Meye, F. J., Lecca, S., Valentinova, K., and Mameli, M. (2013). Synaptic and cellular profile of neurons in the lateral habenula. Front Hum Neurosci *7*, 860.

Meye, F. J., Soiza-Reilly, M., Smit, T., Diana, M. A., Schwarz, M. K., and Mameli, M. (2016). Shifted pallidal co-release of GABA and glutamate in habenula drives cocaine withdrawal and relapse. Nat Neurosci *19*, 1019-1024.

Meye, F. J., Trusel, M., Soiza-Reilly, M., and Mameli, M. (2017). Neural circuit adaptations during drug withdrawal - Spotlight on the lateral habenula. Pharmacol Biochem Behav *162*, 87-93.

Meye, F. J., Valentinova, K., Lecca, S., Marion-Poll, L., Maroteaux, M. J., Musardo, S., Moutkine, I., Gardoni, F., Huganir, R. L., Georges, F., and Mameli, M. (2015). Cocaine-evoked negative symptoms require AMPA receptor trafficking in the lateral habenula. Nat Neurosci *18*, 376-378.

Morales, M., and Margolis, E. B. (2017). Ventral tegmental area: cellular heterogeneity, connectivity and behaviour. Nat Rev Neurosci *18*, 73-85.

Morishita, W., Connor, J. H., Xia, H., Quinlan, E. M., Shenolikar, S., and Malenka, R. C. (2001). Regulation of synaptic strength by protein phosphatase 1. Neuron *32*, 1133-1148.

Morris, J. S., Smith, K. A., Cowen, P. J., Friston, K. J., and Dolan, R. J. (1999). Covariation of activity in habenula and dorsal raphé nuclei following tryptophan depletion. Neuroimage *10*, 163-172.

Nair-Roberts, R. G., Chatelain-Badie, S. D., Benson, E., White-Cooper, H., Bolam, J. P., and Ungless, M. A. (2008). Stereological estimates of dopaminergic, GABAergic and glutamatergic neurons in the ventral tegmental area, substantia nigra and retrorubral field in the rat. Neuroscience *152*, 1024-1031.

Nestler, E. J. (2005). Is there a common molecular pathway for addiction. Nature neuroscience *8*, 1445-1449.

Neumann, P. A., Ishikawa, M., Otaka, M., Huang, Y. H., Schlüter, O. M., and Dong, Y. (2014). Increased excitability of lateral habenula neurons in adolescent rats following cocaine self-administration. Int J Neuropsychopharmacol *18*, pyu109.

Neve, R. L. (2012). Overview of gene delivery into cells using HSV-1-based vectors. Curr Protoc Neurosci *Chapter 4*, Unit 4.12.

Nicoll, R. A., and Schmitz, D. (2005). Synaptic plasticity at hippocampal mossy fibre synapses. Nat Rev Neurosci *6*, 863-876.

Nuno-Perez, A., Trusel, M., Lalive, A. L., Congiu, M., Gastaldo, D., Tchenio, A., Lecca, S., Soiza-Reilly, M., Bagni, C., and Mameli, M. (2021). Stress undermines reward-guided cognitive performance through synaptic depression in the lateral habenula. Neuron *109*, 947-956.e5.

Olivier, B., Mos, J., van Oorschot, R., and Hen, R. (1995). Serotonin receptors and animal models of aggressive behavior. Pharmacopsychiatry *28 Suppl 2*, 80-90.

Omelchenko, N., Bell, R., and Sesack, S. R. (2009). Lateral habenula projections to dopamine and GABA neurons in the rat ventral tegmental area. Eur J Neurosci *30*, 1239-1250.

Pacifici, R., di Carlo, S., Bacosi, A., Pichini, S., and Zuccaro, P. (2000). Pharmacokinetics and cytokine production in heroin and morphine-treated mice. Int J Immunopharmacol *22*, 603-614.

Paliwal, P., Hyman, S. M., and Sinha, R. (2008). Craving predicts time to cocaine relapse: further validation of the Now and Brief versions of the cocaine craving questionnaire. Drug Alcohol Depend *93*, 252-259.

Pan, B., Hillard, C. J., and Liu, Q. S. (2008). Endocannabinoid signaling mediates cocaine-induced inhibitory synaptic plasticity in midbrain dopamine neurons. J Neurosci *28*, 1385-1397.

Papathanou, M., Creed, M., Dorst, M. C., Bimpisidis, Z., Dumas, S., Pettersson, H., Bellone, C., Silberberg, G., Lüscher, C., and Wallén-Mackenzie, Å. (2018). Targeting VGLUT2 in Mature Dopamine Neurons Decreases Mesoaccumbal Glutamatergic Transmission and Identifies a Role for Glutamate Co-release in Synaptic Plasticity by Increasing Baseline AMPA/NMDA Ratio. Front Neural Circuits *12*, 64.

Pascoli, V., Besnard, A., Hervé, D., Pagès, C., Heck, N., Girault, J. A., Caboche, J., and Vanhoutte, P. (2011). Cyclic adenosine monophosphate-independent tyrosine phosphorylation of NR2B mediates cocaine-induced extracellular signal-regulated kinase activation. Biol Psychiatry *69*, 218-227.

Pascoli, V., Hiver, A., Van Zessen, R., Loureiro, M., Achargui, R., Harada, M., Flakowski, J., and Lüscher, C. (2018). Stochastic synaptic plasticity underlying compulsion in a model of addiction. Nature *564*, 366-371.

Pascoli, V., Terrier, J., Espallergues, J., Valjent, E., O'Connor, E. C., and Lüscher, C. (2014). Contrasting forms of cocaine-evoked plasticity control components of relapse. Nature *509*, 459-464.

Pascoli, V., Terrier, J., Hiver, A., and Lüscher, C. (2015). Sufficiency of Mesolimbic Dopamine Neuron Stimulation for the Progression to Addiction. Neuron *88*, 1054-1066.

Paterson, N. E., Balfour, D. J., and Markou, A. (2007). Chronic bupropion attenuated the anhedonic component of nicotine withdrawal in rats via inhibition of dopamine reuptake in the nucleus accumbens shell. Eur J Neurosci *25*, 3099-3108.

Pergolizzi, J. V., Raffa, R. B., and Rosenblatt, M. H. (2020). Opioid withdrawal symptoms, a consequence of chronic opioid use and opioid use disorder: Current understanding and approaches to management. J Clin Pharm Ther *45*, 892-903.

Piazza, P. V., and Deroche-Gamonet, V. (2013). A multistep general theory of transition to addiction. Psychopharmacology (Berl) *229*, 387-413.

Piazza, P. V., Rougé-Pont, F., Deminière, J. M., Kharoubi, M., Le Moal, M., and Simon, H. (1991). Dopaminergic activity is reduced in the prefrontal cortex and increased in the nucleus accumbens of rats predisposed to develop amphetamine self-administration. Brain Res *567*, 169-174.

Pilcher, W. H., and Joseph, S. A. (1984). Co-localization of CRF-ir perikarya and ACTH-ir fibers in rat brain. Brain Res *299*, 91-102.

Pleil, K. E., Rinker, J. A., Lowery-Gionta, E. G., Mazzone, C. M., McCall, N. M., Kendra, A. M., Olson, D. P., Lowell, B. B., Grant, K. A., Thiele, T. E., and Kash, T. L. (2015). NPY signaling inhibits extended amygdala CRF neurons to suppress binge alcohol drinking. Nat Neurosci *18*, 545-552.

Pollak Dorocic, I., Fürth, D., Xuan, Y., Johansson, Y., Pozzi, L., Silberberg, G., Carlén, M., and Meletis, K. (2014). A whole-brain atlas of inputs to serotonergic neurons of the dorsal and median raphe nuclei. Neuron *83*, 663-678.

Powell, J. E., and Taylor, D. (1992). Anger, depression, and anxiety following heroin withdrawal. Int J Addict *27*, 25-35.

Pribiag, H., Shin, S., Wang, E. H., Sun, F., Datta, P., Okamoto, A., Guss, H., Jain, A., Wang, X. Y., De Freitas, B., Honma, P., Pate, S., Lilascharoen, V., Li, Y., and Lim, B. K. (2021). Ventral

pallidum DRD3 potentiates a pallido-habenular circuit driving accumbal dopamine release and cocaine seeking. Neuron *109*, 2165-2182.e10.

Pribiag, H., and Stellwagen, D. (2013). TNF-α downregulates inhibitory neurotransmission through protein phosphatase 1-dependent trafficking of GABA(A) receptors. J Neurosci *33*, 15879-15893.

Price, R. W., Rubenstein, R., Joh, T. H., and Reis, D. J. (1981). Tyrosine hydroxylase activity in the superior cervical ganglion during herpes simplex virus infection: correlation with viral titers and viral antigen. Brain Res *214*, 357-370.

Pu, L., Liu, Q. S., and Poo, M. M. (2006). BDNF-dependent synaptic sensitization in midbrain dopamine neurons after cocaine withdrawal. Nat Neurosci *9*, 605-607.

Purvis, E. M., Klein, A. K., and Ettenberg, A. (2018). Lateral habenular norepinephrine contributes to states of arousal and anxiety in male rats. Behav Brain Res *347*, 108-115.

Qi, J., Zhang, S., Wang, H. L., Barker, D. J., Miranda-Barrientos, J., and Morales, M. (2016). VTA glutamatergic inputs to nucleus accumbens drive aversion by acting on GABAergic interneurons. Nat Neurosci *19*, 725-733.

Quadros, I. M., Takahashi, A., and Miczek, K. A. (2010). Serotonin and aggression. Handbook of Behavioral Neuroscience *21*, 687-713.

Rinker, J. A., Marshall, S. A., Mazzone, C. M., Lowery-Gionta, E. G., Gulati, V., Pleil, K. E., Kash, T. L., Navarro, M., and Thiele, T. E. (2017). Extended Amygdala to Ventral Tegmental Area Corticotropin-Releasing Factor Circuit Controls Binge Ethanol Intake. Biol Psychiatry *81*, 930-940.

Ritz, M. C., Cone, E. J., and Kuhar, M. J. (1990). Cocaine inhibition of ligand binding at dopamine, norepinephrine and serotonin transporters: a structure-activity study. Life Sci *46*, 635-645.

Robbe, D., Alonso, G., Chaumont, S., Bockaert, J., and Manzoni, O. J. (2002). Role of p/q-Ca2+ channels in metabotropic glutamate receptor 2/3-dependent presynaptic long-term depression at nucleus accumbens synapses. J Neurosci *22*, 4346-4356.

Robinson, J. D., Li, L., Chen, M., Lerman, C., Tyndale, R. F., Schnoll, R. A., Hawk, L. W., George, T. P., Benowitz, N. L., and Cinciripini, P. M. (2019). Evaluating the temporal relationships between withdrawal symptoms and smoking relapse. Psychol Addict Behav *33*, 105-116.

Robledo, P., Maldonado-Lopez, R., and Koob, G. F. (1992). Role of dopamine receptors in the nucleus accumbens in the rewarding properties of cocaine. Ann N Y Acad Sci *654*, 509-512.

Root, D. H., Barker, D. J., Estrin, D. J., Miranda-Barrientos, J. A., Liu, B., Zhang, S., Wang, H. L., Vautier, F., Ramakrishnan, C., Kim, Y. S., Fenno, L., Deisseroth, K., and Morales, M. (2020). Distinct Signaling by Ventral Tegmental Area Glutamate, GABA, and Combinatorial Glutamate-GABA Neurons in Motivated Behavior. Cell Rep *32*, 108094.

Root, D. H., Fabbricatore, A. T., Pawlak, A. P., Barker, D. J., Ma, S., and West, M. O. (2012). Slow phasic and tonic activity of ventral pallidal neurons during cocaine self-administration. Synapse *66*, 106-127.

Root, D. H., Hoffman, A. F., Good, C. H., Zhang, S., Gigante, E., Lupica, C. R., and Morales, M. (2015). Norepinephrine activates dopamine D4 receptors in the rat lateral habenula. J Neurosci *35*, 3460-3469.

Root, D. H., Mejias-Aponte, C. A., Zhang, S., Wang, H. L., Hoffman, A. F., Lupica, C. R., and Morales, M. (2014). Single rodent mesohabenular axons release glutamate and GABA. Nat Neurosci *17*, 1543-1551.

Rougé-Pont, F., Piazza, P. V., Kharouby, M., and Moal…, M. L. (1993). Higher and longer stress-induced increase in dopamine concentrations in the nucleus accumbens of animals predisposed to amphetamine self-administration. A …. Brain research *602*, 169-174.

Salamone, J. D., Correa, M., Mingote, S., and Weber, S. M. (2003). Nucleus accumbens dopamine and the regulation of effort in food-seeking behavior: implications for studies of natural motivation, psychiatry, and drug abuse. J Pharmacol Exp Ther *305*, 1-8.

Sartorius, A., Kiening, K. L., Kirsch, P., and Gall…, C. C. V. (2010). Remission of major depression under deep brain stimulation of the lateral habenula in a therapy-refractory patient. Biological Psychiatry *67*, e9-e11.

Savell, K. E., Tuscher, J. J., Zipperly, M. E., Duke, C. G., Phillips, R. A., Bauman, A. J., Thukral, S., Sultan, F. A., Goska, N. A., Ianov, L., and Day, J. J. (2020). A dopamine-induced gene expression signature regulates neuronal function and cocaine response. Sci Adv *6*, eaba4221.

Schildt, S., Endres, T., Lessmann, V., and Edelmann, E. (2013). Acute and chronic interference with BDNF/TrkB-signaling impair LTP selectively at mossy fiber synapses in the CA3 region of mouse hippocampus. Neuropharmacology *71*, 247-254.

Schultz, W., Dayan, P., and Montague, P. R. (1997). A neural substrate of prediction and reward. Science *275*, 1593-1599.

Shabel, S. J., Proulx, C. D., Piriz, J., and Malinow, R. (2014). Mood regulation. GABA/glutamate co-release controls habenula output and is modified by antidepressant treatment. Science *345*, 1494-1498.

Shabel, S. J., Wang, C., Monk, B., Aronson, S., and Malinow, R. (2019). Stress transforms lateral habenula reward responses into punishment signals. Proc Natl Acad Sci U S A *116*, 12488-12493.

Shi, S., Hayashi, Y., Esteban, J. A., and Malinow, R. (2001). Subunit-specific rules governing AMPA receptor trafficking to synapses in hippocampal pyramidal neurons. Cell *105*, 331-343.

Silberman, Y., and Winder, D. G. (2013). Emerging role for corticotropin releasing factor signaling in the bed nucleus of the stria terminalis at the intersection of stress and reward. Front Psychiatry *4*, 42.

Simpson, D. D., Joe, G. W., Fletcher, B. W., Hubbard, R. L., and Anglin, M. D. (1999). A national evaluation of treatment outcomes for cocaine dependence. Arch Gen Psychiatry *56*, 507-514.

Sinha, R. (2001). How does stress increase risk of drug abuse and relapse. Psychopharmacology (Berl) *158*, 343-359.

Skinner, B. F. (1938). The Behavior of Organisms. Massachusetts: BF Skinner Foundation *457*,

Skinner, B. F. (1984). The evolution of behavior. Journal of the experimental analysis of behavior *41*, 217.

Skinner, B. F. (2014). Contingencies of reinforcement: A theoretical analysis (Vol. 3). BF Skinner Foundation

Stamatakis, A. M., Jennings, J. H., Ung, R. L., Blair, G. A., Weinberg, R. J., Neve, R. L., Boyce, F., Mattis, J., Ramakrishnan, C., Deisseroth, K., and Stuber, G. D. (2013). A unique population of ventral tegmental area neurons inhibits the lateral habenula to promote reward. Neuron *80*, 1039-1053.

Stamatakis, A. M., and Stuber, G. D. (2012). Activation of lateral habenula inputs to the ventral midbrain promotes behavioral avoidance. Nat Neurosci *15*, 1105-1107.

Staub, D. R., Lunden, J. W., Cathel, A. M., Dolben, E. L., and Kirby, L. G. (2012). Morphine history sensitizes postsynaptic GABA receptors on dorsal raphe serotonin neurons in a stress-induced relapse model in rats. Psychoneuroendocrinology *37*, 859-870.

Stellwagen, D., Beattie, E. C., Seo, J. Y., and Malenka, R. C. (2005). Differential regulation of AMPA receptor and GABA receptor trafficking by tumor necrosis factor-alpha. J Neurosci *25*, 3219-3228.

Sánchez-Soto, M., Bonifazi, A., Cai, N. S., Ellenberger, M. P., Newman, A. H., Ferré, S., and Yano, H. (2016). Evidence for Noncanonical Neurotransmitter Activation: Norepinephrine as a Dopamine D2-Like Receptor Agonist. Mol Pharmacol *89*, 457-466.

Stewart, J., and Wit, H. D. (1987). Reinstatement of drug-taking behavior as a method of assessing incentive motivational properties of drugs. Methods of assessing the reinforcing properties of abused drugs 211-227.

Stobbe, M. (2021). US overdose deaths hit record 93,000 in pandemic last year. APA News. Source:https://apnews.com/article/overdose-deaths-record-covid-pandemic-fd43b5d91a81179def5ac596253b0304

Stuber, G. D., Stamatakis, A. M., and Kantak, P. A. (2015). Considerations when using cre-driver rodent lines for studying ventral tegmental area circuitry. Neuron *85*, 439-445.

Szőnyi, A., Zichó, K., Barth, A. M., Gönczi, R. T., Schlingloff, D., Török, B., Sipos, E., Major, A., Bardóczi, Z., Sos, K. E., Gulyás, A. I., Varga, V., Zelena, D., Freund, T. F., and Nyiri, G. (2019). Median raphe controls acquisition of negative experience in the mouse. Science *366*, eaay8746.

Tan, D., Nuno-Perez, A., Mameli, M., and Meye, F. J. (2019). Cocaine withdrawal reduces $GABA_B$ R transmission at entopeduncular nucleus - lateral habenula synapses. Eur J Neurosci *50*, 2124-2133.

Tan, K. R., Brown, M., Labouèbe, G., Yvon, C., Creton, C., Fritschy, J. M., Rudolph, U., and Lüscher, C. (2010). Neural bases for addictive properties of benzodiazepines. Nature *463*, 769-774.

Tan, K. R., Yvon, C., Turiault, M., Mirzabekov, J. J., Doehner, J., Labouèbe, G., Deisseroth, K., Tye, K. M., and Lüscher, C. (2012). GABA neurons of the VTA drive conditioned place aversion. Neuron *73*, 1173-1183.

Tchenio, A., Lecca, S., Valentinova, K., and Mameli, M. (2017). Limiting habenular hyperactivity ameliorates maternal separation-driven depressive-like symptoms. Nat Commun *8*, 1135.

Thomas, M. J., Beurrier, C., Bonci, A., and Malenka, R. C. (2001). Long-term depression in the nucleus accumbens: a neural correlate of behavioral sensitization to cocaine. Nat Neurosci *4*, 1217-1223.

Tian, J., and Uchida, N. (2015). Habenula Lesions Reveal that Multiple Mechanisms Underlie Dopamine Prediction Errors. Neuron *87*, 1304-1316.

Torres, G. E., Gainetdinov, R. R., and Caron, M. G. (2003). Plasma membrane monoamine transporters: structure, regulation and function. Nat Rev Neurosci *4*, 13-25.

Trusel, M., Nuno-Perez, A., Lecca, S., Harada, H., Lalive, A. L., Congiu, M., Takemoto, K., Takahashi, T., Ferraguti, F., and Mameli, M. (2019). Punishment-Predictive Cues Guide Avoidance through Potentiation of Hypothalamus-to-Habenula Synapses. Neuron *102*, 120-127.e4.

Tzounopoulos, T., Janz, R., Südhof, T. C., Nicoll, R. A., and Malenka, R. C. (1998). A role for cAMP in long-term depression at hippocampal mossy fiber synapses. Neuron *21*, 837-845.

Ungless, M. A., Whistler, J. L., Malenka, R. C., and Bonci, A. (2001). Single cocaine exposure in vivo induces long-term potentiation in dopamine neurons. Nature *411*, 583-587.

Labor, U. N. O. O. D. A. (2021). World Drug Report 2020 (set of 6 booklets). UN

Valentinova, K., Tchenio, A., Trusel, M., Clerke, J. A., Lalive, A. L., Tzanoulinou, S., Matera, A., Moutkine, I., Maroteaux, L., Paolicelli, R. C., Volterra, A., Bellone, C., and Mameli, M. (2019).

Morphine withdrawal recruits lateral habenula cytokine signaling to reduce synaptic excitation and sociability. Nat Neurosci *22*, 1053-1056.

Valjent, E., Bertran-Gonzalez, J., Aubier, B., Greengard, P., Hervé, D., and Girault, J. A. (2010). Mechanisms of locomotor sensitization to drugs of abuse in a two-injection protocol. Neuropsychopharmacology *35*, 401-415.

van Kerkhof, L. W., Damsteegt, R., Trezza, V., Voorn, P., and Vanderschuren, L. J. (2013). Functional integrity of the habenula is necessary for social play behaviour in rats. Eur J Neurosci *38*, 3465-3475.

Vander Weele, C. M., Siciliano, C. A., Matthews, G. A., Namburi, P., Izadmehr, E. M., Espinel, I. C., Nieh, E. H., Schut, E. H. S., Padilla-Coreano, N., Burgos-Robles, A., Chang, C. J., Kimchi, E. Y., Beyeler, A., Wichmann, R., Wildes, C. P., and Tye, K. M. (2018). Dopamine enhances signal-to-noise ratio in cortical-brainstem encoding of aversive stimuli. Nature *563*, 397-401.

Vanderschuren, L. J., Di Ciano, P., and Everitt, B. J. (2005). Involvement of the dorsal striatum in cue-controlled cocaine seeking. J Neurosci *25*, 8665-8670.

Volkow, N. D., Wang, G. J., Fowler, J. S., Hitzemann, R., Angrist, B., Gatley, S. J., Logan, J., Ding, Y. S., and Pappas, N. (1999). Association of methylphenidate-induced craving with changes in right striato-orbitofrontal metabolism in cocaine abusers: implications in addiction. Am J Psychiatry *156*, 19-26.

Vollstädt-Klein, S., Wichert, S., Rabinstein, J., Bühler, M., Klein, O., Ende, G., Hermann, D., and Mann, K. (2010). Initial, habitual and compulsive alcohol use is characterized by a shift of cue processing from ventral to dorsal striatum. Addiction *105*, 1741-1749.

Wang, D., Li, Y., Feng, Q., Guo, Q., Zhou, J., and Luo, M. (2017). Learning shapes the aversion and reward responses of lateral habenula neurons. Elife *6*, e23045.

Wang, H., Treadway, T., Covey, D. P., Cheer, J. F., and Lupica, C. R. (2015). Cocaine-Induced Endocannabinoid Mobilization in the Ventral Tegmental Area. Cell Rep *12*, 1997-2008.

Wang, H. L., Qi, J., Zhang, S., Wang, H., and Morales, M. (2015). Rewarding Effects of Optical Stimulation of Ventral Tegmental Area Glutamatergic Neurons. J Neurosci *35*, 15948-15954.

Wang, H. L., Zhang, S., Qi, J., Wang, H., Cachope, R., Mejias-Aponte, C. A., Gomez, J. A., Mateo-Semidey, G. E., Beaudoin, G. M. J., Paladini, C. A., Cheer, J. F., and Morales, M. (2019). Dorsal Raphe Dual Serotonin-Glutamate Neurons Drive Reward by Establishing Excitatory Synapses on VTA Mesoaccumbens Dopamine Neurons. Cell Rep *26*, 1128-1142.e7.

Wang, R., Hausknecht, K. A., Gancarz-Kausch, A. M., Oubraim, S., Shen, R. Y., and Haj-Dahmane, S. (2020). Cocaine self-administration abolishes endocannabinoid-mediated long-term depression of glutamatergic synapses in the ventral tegmental area. Eur J Neurosci *52*, 4517-4524.

Waung, M, Maanum, K, Driscoll, J, O'Brien, C, Bryant, S, Mansourian, K, Morales, M, Barker, D, and Margolis, E. (2020). A diencephalic circuit for opioid analgesia but not positive reinforcement. bioRxiv doi:10.1101/2020.12.15.422931.

Webster, J. F., Vroman, R., Balueva, K., Wulff, P., Sakata, S., and Wozny, C. (2020). Disentangling neuronal inhibition and inhibitory pathways in the lateral habenula. Sci Rep *10*, 8490.

Weiss, T., and Veh, R. W. (2011). Morphological and electrophysiological characteristics of neurons within identified subnuclei of the lateral habenula in rat brain slices. Neuroscience *172*, 74-93.

West, R., and Gossop, M. (1994). Overview: a comparison of withdrawal symptoms from different drug classes. Addiction *89*, 1483-1489.

Wexler, B. E., Gottschalk, C. H., Fulbright, R. K., Prohovnik, I., Lacadie, C. M., Rounsaville, B. J., and Gore, J. C. (2001). Functional magnetic resonance imaging of cocaine craving. Am J Psychiatry *158*, 86-95.

Whelan, P. J., and Remski, K. (2012). Buprenorphine vs methadone treatment: A review of evidence in both developed and developing worlds. J Neurosci Rural Pract *3*, 45-50.

Whitton, A. E., Treadway, M. T., and Pizzagalli, D. A. (2015). Reward processing dysfunction in major depression, bipolar disorder and schizophrenia. Curr Opin Psychiatry *28*, 7-12.

Williams, J. M., and Steketee, J. D. (2005). Time-dependent effects of repeated cocaine administration on dopamine transmission in the medial prefrontal cortex. Neuropharmacology *48*, 51-61.

Wise, R. A. (2004). Dopamine, learning and motivation. Nat Rev Neurosci *5*, 483-494.

Wise, R. A. (2008). Dopamine and reward: the anhedonia hypothesis 30 years on. Neurotox Res *14*, 169-183.

Yamaguchi, T., Wang, H. L., Li, X., Ng, T. H., and Morales, M. (2011). Mesocorticolimbic glutamatergic pathway. J Neurosci *31*, 8476-8490.

Yang, Y., and Calakos, N. (2013). Presynaptic long-term plasticity. Front Synaptic Neurosci *5*, 8.

Yang, Y., Cui, Y., Sang, K., Dong, Y., Ni, Z., Ma, S., and Hu, H. (2018). Ketamine blocks bursting in the lateral habenula to rapidly relieve depression. Nature *554*, 317-322.

Yin, H. H., Knowlton, B. J., and Balleine, B. W. (2004). Lesions of dorsolateral striatum preserve outcome expectancy but disrupt habit formation in instrumental learning. Eur J Neurosci *19*, 181-189.

Yin, H. H., Ostlund, S. B., Knowlton, B. J., and Balleine, B. W. (2005). The role of the dorsomedial striatum in instrumental conditioning. Eur J Neurosci *22*, 513-523.

Yoo, J. H., Zell, V., Gutierrez-Reed, N., Wu, J., Ressler, R., Shenasa, M. A., Johnson, A. B., Fife, K. H., Faget, L., and Hnasko, T. S. (2016). Ventral tegmental area glutamate neurons co-release GABA and promote positive reinforcement. Nat Commun *7*, 13697.

Young, S. N., and Leyton, M. (2002). The role of serotonin in human mood and social interaction. Insight from altered tryptophan levels. Pharmacol Biochem Behav *71*, 857-865.

Yu, X., Li, W., Ma, Y., Tossell, K., Harris, J. J., Harding, E. C., Ba, W., Miracca, G., Wang, D., Li, L., Guo, J., Chen, M., Li, Y., Yustos, R., Vyssotski, A. L., Burdakov, D., Yang, Q., Dong, H., Franks, N. P., and Wisden, W. (2019). GABA and glutamate neurons in the VTA regulate sleep and wakefulness. Nat Neurosci *22*, 106-119.

Zalutsky, R. A., and Nicoll, R. A. (1990). Comparison of two forms of long-term potentiation in single hippocampal neurons. Science *248*, 1619-1624.

Zapata, A., and Lupica, C. R. (2021). Lateral habenula cannabinoid CB1 receptor involvement in drug-associated impulsive behavior. Neuropharmacology *192*, 108604.

Zapata, A., Minney, V. L., and Shippenberg, T. S. (2010). Shift from goal-directed to habitual cocaine seeking after prolonged experience in rats. J Neurosci *30*, 15457-15463.

Zell, V., Steinkellner, T., Hollon, N. G., Warlow, S. M., Souter, E., Faget, L., Hunker, A. C., Jin, X., Zweifel, L. S., and Hnasko, T. S. (2020). VTA Glutamate Neuron Activity Drives Positive Reinforcement Absent Dopamine Co-release. Neuron *107*, 864-873.e4.

Zhang, F., Zhou, W., Liu, H., Zhu, H., Tang, S., Lai, M., and Yang, G. (2005). Increased c-Fos expression in the medial part of the lateral habenula during cue-evoked heroin-seeking in rats. Neurosci Lett *386*, 133-137.

Zhang, G. W., Shen, L., Zhong, W., Xiong, Y., Zhang, L. I., and Tao, H. W. (2018a). Transforming Sensory Cues into Aversive Emotion via Septal-Habenular Pathway. Neuron *99*, 1016-1028.e5.

Zhang, L., Hernández, V. S., Vázquez-Juárez, E., Chay, F. K., and Barrio, R. A. (2016). Thirst Is Associated with Suppression of Habenula Output and Active Stress Coping: Is there a Role for a Non-canonical Vasopressin-Glutamate Pathway. Front Neural Circuits *10*, 13.

Zhang, L., Hernández, V. S., Swinny, J. D., Verma, A. K., Giesecke, T., Emery, A. C., Mutig, K., Garcia-Segura, L. M., and Eiden, L. E. (2018b). A GABAergic cell type in the lateral habenula links hypothalamic homeostatic and midbrain motivation circuits with sex steroid signaling. Transl Psychiatry *8*, 50.

Zhao, Y. W., Pan, Y. Q., Tang, M. M., and Lin, W. J. (2018). Blocking p38 Signaling Reduces the Activation of Pro-inflammatory Cytokines and the Phosphorylation of p38 in the Habenula and Reverses Depressive-Like Behaviors Induced by Neuroinflammation. Front Pharmacol *9*, 511.

Zipperly, M. E., Sultan, F. A., Graham, G. E., Brane, A. C., Simpkins, N. A., Carullo, N. V. N., Ianov, L., and Day, J. J. (2021). Regulation of dopamine-dependent transcription and cocaine action by Gadd45b. Neuropsychopharmacology *46*, 709-720.

Zuo, W., Chen, L., Wang, L., and Ye, J. H. (2013). Cocaine facilitates glutamatergic transmission and activates lateral habenular neurons. Neuropharmacology *70*, 180-189.